TECHNICAL REPORT STANDARD TITLE PAGE

1. Report No.	2. Government Accession No.	3. Recipient's Catalog No.
FHWA/TX-91/1213-1F		

4. Title and Subtitle	5. Report Date
A STUDY OF BRIDGE APPROACH ROUGHNESS	November 1990 December 1991/Revised
	6. Performing Organization Code

7. Author(s)	8. Performing Organization Report No.
Ray W. James, Heping Zhang, Dan G. Zollinger, Louis J. Thompson, Robert F. Bruner, Dapeng Xin	Research Report 1213-1F

9. Performing Organization Name and Address	10. Work Unit No.
Texas Transportation Institute The Texas A&M University System College Station, TX 77843	11. Contract or Grant No. Study No. 2-5-89/0-1213

12. Sponsoring Agency Name and Address	13. Type of Report and Period Covered
Texas Department of Transportation Transportation Planning Division P. O. Box 5051 Austin, TX 78763	Final - September 1988 November 1990
	14. Sponsoring Agency Code

15. Supplementary Notes

Research performed in cooperation with DOT, FHWA.
Study Title: A Study of Bridge Approach Roughness

16. Abstract

Field studies of highway bridge approach roughness, including visual inspection, measurement of approach profiles by surveying techniques and by driver evaluation, soil borings, and concrete pavement corings were conducted to determine the most important causes of approach roughness at Texas bridge sites. A literature survey identified many previously identified causes, most of which are also thought to be applicable to some of the problems observed at the Texas study sites. During the studies, repeated observations of severe cracking and dislocation of the backwalls of reinforced concrete abutments led to a detailed investigation of the causes of this damage mechanism. The observed distress is correlated to the presence of adjacent reinforced concrete pavements, and the cause is attributed to the longitudinal growth of the concrete pavements. A finite element model of a representative abutment is used to study the expected stress distributions caused by several hyopothesized mechanisms which might contribute to the observed damage. Methods to prevent future damage are discussed.

A model of reinforced concrete pavement is developed and evaluated. The model can be used to evaluate pavement cracking, pavement lug effectiveness, and design requirements for isolation joints to protect bridge approach slabs and abutments from pressures applied by concrete pavements.

17. Key Words	18. Distribution Statement
continuous reinforced concrete pavements (CRCP), pavement lugs, thermal loading, one-dimensional motion, bridge approach roughness, abutment, soil properties, soil borings, measured approach profiles	No restrictions. This document is available to the public through National Technical Information Service 5285 Port Royal Road Springfield, Virginia 22161

19. Security Classif. (of this report)	20. Security Classif. (of this page)	21. No. of Pages	22. Price
Unclassified	Unclassified	116	

Form DOT F 1700.7 (8-69)

A STUDY OF BRIDGE APPROACH ROUGHNESS

by

Ray W. James

Heping Zhang

Dan G. Zollinger

Louis J. Thompson

Robert F. Bruner

Dapeng Xin

Research Report 1213-1F
Research Study Number 2-5-89/0-1213

Sponsored by

Texas Department of Transportation

in cooperation with

U. S. Department of Transportation, Federal Highway Administration

December 1991

TEXAS TRANSPORTATION INSTITUTE
The Texas A&M University System
College Station, Texas 77843-3135

TABLE OF CONTENTS

SUMMARY

Field studies of highway bridge approach roughness, including visual inspection, measurement of approach profiles by surveying techniques and by driver evaluation, soil borings, and concrete pavement corings were conducted to determine the most important causes of approach roughness at Texas bridge sites. A literature survey identified many previously identified causes, most of which are also thought to be applicable to some of the problems observed at the Texas study sites. During the studies, repeated observations of severe cracking and dislocation of the backwalls of reinforced concrete abutments led to a detailed investigation of the causes of this damage mechanism. The observed distress is correlated to the presence of adjacent reinforced concrete pavements, and the cause is attributed to the longitudinal growth of the concrete pavements. A finite element model of a representative abutment is used to study the expected stress distributions caused by several hypothesized mechanisms which might contribute to the observed damage. Methods to prevent future damage are discussed.

SUMMARY STATEMENT ON RESEARCH IMPLEMENTATION

Several design details have been identified as needing improvement. In the case of the concrete pavement sites, the recommendation is for isolation of pavement from approach slab and bridge in line with practice in other states. One representative design detail is a 3-ft long bituminous joint which will allow longitudinal pavement motion without abutment or approach slab distress requiring, instead, maintenance of the surface of the bituminous joint. Another detail which needs improvement is the pavement lug used to anchor the ends of continuous concrete pavements. In some of the study sites these lugs are not performing their intended function. While redesign of the anchor lugs may not be required if the recommended isolation joints are incorporated, the failure of the lugs may cause performance problems with the actual concrete pavement. A study of these potential problems is beyond the scope of this study, and it is recommended that such a study be incorporated into existing research studies being conducted jointly by TTI and CTR.

ACKNOWLEDGEMENTS

The work described here was funded by the Texas Department of Transportation and the U. S. Department of Transportation, Federal Highway Administration, for which support the authors are appreciative. Considerable assistance and cooperation by others was most helpful and valuable during the course of this study. Roger Bligh, Bob Bruner and Louis Thompson assisted with various tasks both in the field and in the office. Research support was provided by research assistants Scott Armstrong and Asif Qureshy. Capable TxDOT District maintenance personnel, too numerous to mention individually, provided effective traffic control and safe working conditions for the field work when required. The cooperation of district personnel in selecting study sites and providing design drawings is also appreciated. The assistance and advice of the Technical Coordinator, George Odom, and Technical Advisors, Bill Isenhower and Harold Albers, are gratefully acknowledged and appreciated.

DISCLAIMER

The contents of this report reflect the views of the authors, who are responsible for the facts and accuracy of the data presented herein. The contents do not necessarily reflect the official views or policies of the Federal Highway Administration or the Texas Department of Transportation. This report does not constitute a standard, specification, or regulation and is not intended for construction, bidding or permit purposes. This report has been prepared by Ray W. James, P.E., Texas license number 42034.

LIST OF FIGURES

LIST OF TABLES

A STUDY OF BRIDGE APPROACH ROUGHNESS

INTRODUCTION

A field study of the bridge approach roughness at bridge sites in Texas was accomplished. The methodology of the field survey included visual observation, driver evaluation, elevation profile survey, and concrete and soil coring and testing; however, not all methods were used at all sites. The field study included surveys of approximately 165 bridges and was accomplished with the intention of quantifying the bridge approach roughness. The survey sites were not selected randomly; district engineers in five of Texas' 24 districts were first requested to identify sites with a history of required approach roadway maintenance to maintain ride quality. From the responses, a set of 34 bridges was selected for initial inspection and study. In a later phase of the study, a second, randomly selected set of approximately 131 bridges was also examined.

Literature Review

The Nebraska Department of Roads is currently sponsoring a study of bridge abutment and approach slab settlement. An interim report (Tadros and Benak 1989) includes a thorough literature review, the results of a survey and the results of field inspections of bridges in eastern Nebraska. The key observations of the literature survey are summarized here. The literature review describes the findings by an earlier Nebraska study (Cheney 1975) that bridge approach settlement in Nebraska is primarily caused by consolidation of the foundation soils and not by displacement of improperly compacted embankment material beneath the pavement. Tadros and Benal also reviewed a report of a Wisconsin study (Dunn, et al. 1983) which showed dramatically different results for roughness at approaches where flexible pavements were used, compared to approaches where rigid pavements were used, with flexible pavements exhibiting much worse performance. Voids were reported under approach slabs in the Wisconsin study. Also reviewed were 1961 and 1975 Ohio surveys (Grover 1978) of settlements of abutments and approaches. Most of these abutments settled more than 2.5 in. and 10 percent settled more than 4 in., although most of these abutments were founded on spread footings in the embankment, contrary to Texas practice. Based on this study, a reported change in design procedures required pile foundations footed below the embankment, as is currently practiced in Texas. The Ohio report, summarized by Tadros and Benak, indicates that even though less differential settlement was observed at abutments on shallow spread footings, pile-supported abutments are necessary to prevent structural damage. Also reviewed by Tadros and Benak is a series of studies by the Kentucky Department of Highways (Hopkins and Deen 1969, Hopkins 1969, Hopkins and Scott 1970, Hopkins 1973, and Hopkins 1985) which included field surveys and detailed investigations. The Kentucky studies introduced a definition of an approach fault, which was defined to be present when a bump was evident when an automobile passed onto or off of the bridge deck. One observation from the Kentucky studies was that current practice in 1964 was not sufficient to obtain smooth surfaces; further, flexible pavement approaches did not perform as well as rigid pavement approaches. It was also concluded that primary and secondary consolidation within the embankment can contribute to approach roughness, improper compaction may contribute, lateral movements (creep) due to shear strain can contribute when the factor

of safety of the slope is small, erosion of materials behind and around the embankment can contribute to settlement of the pavement, and bridge approach slabs do not eliminate differential settlement but can provide a smoother transition. A California research study (Stewart 1985) discussed below was also reviewed. Wyoming has also attempted to solve the problem of bridge approach roughness with an experimental study of geosynthetic reinforced walls behind bridge abutments. The installations include compacted granular fill with embedded layers of geotextiles which increase the stiffness of the fill. These installations are still under study although early reports indicate good performance. An Oklahoma study in progress (Laguros 1986) and a Maryland study (Wolde-Tinsae, et al. 1987), both described below, are also reviewed. The survey of Nebraska bridges, also conducted by Tadros and Benak, indicated that nearly 80% of the bridges surveyed had required maintenance because of approach problems, mostly related to settlement problems. A study was initiated to determine possible tolerable settlement criteria. Initial measurements of roughness parameters at several bridges are reported, but final conclusions are not yet reported. There is not an obvious correlation between qualitative ratings of the severity of the bumps and the quantitative measurements. The recommendations resulting from the Nebraska study include a call for geotechnical investigations of the approach whenever the proposed fill exceeds 5 ft or when the slopes exceed 1 in 4. Also recommended is a minimum factor of safety of 2.0-2.5 against slope failure as determined by total stress analysis. Select granular backfill is recommended behind the abutments, and 1.5-2 in. precamber of the approach pavement is recommended for new construction.

The Oklahoma DOT is sponsoring a four-year, $400,000 study of the problem of approach roughness. At the time of this report, the only progress report available from that study is the first annual report (Laguros, et al. 1986) which consists of a detailed literature review. Laguros offers the following conclusions (among others):

- The causes of settlement of approach foundations cannot be generalized for all sites and/or states.
- Some factors influencing the settlement of approach foundations are
  a) Subsoil properties,
    i) Coefficient of permeability,
    ii) Coefficient of consolidation,
    iii) Plasticity index,
    iv) Compression index,
  b) Depth of drainage layer,
  c) Height of embankment,
  d) Compression index, and
  e) Construction history, i.e., loading rate.
- Settlement of embankment foundation, type of embankment material, and technique and quality of embankment construction are the most significant causes.
- Pavement type usually does not have a significant effect on the magnitude of long term settlement; however, it may influence the rate of settlement.

- Approach slabs shift the location of the settlement-induced problem.
- The effects of stabilization are not studied by most researchers.
- Both primary and secondary consolidation may be factors.

Laguros also made several recommendations, including:

- It is important for designers to estimate the total and the rate of settlement. Equations have been developed and proven useful, although somewhat inaccurate (Hopkins, et al. 1985).
- Secondary compression or creep can contribute.
- Development of more accurate prediction methods, perhaps based on finite element methods, will be valuable.
- A quantitative definition of a "bump" is needed.

The second phase of the study is completed (Laguros 1990), but reports have not yet been reviewed. The second phase reportedly included a survey of 760 approaches with a statistical analysis of the results, a selection of 25 sites for soil borings. Observations included the absence of preparation of the sites beneath the fill, the effect of geology (Ox-bow lakes), and poor construction practices including inadequate drainage and construction. The third phase will include completion of the soil borings at the 25 selected sites.

A California study is reported by Stewart (1985) in which a specially instrumented vehicle was used to measure approach roughness during transit at 50 mph. The vehicle measured relative displacement of the body and rear axle. Each 1/8 in. of vertical movement represents one unit on the defined roughness rating scale with a rating of 12 (1.5 in.) considered serious enough to warrant repair. The findings in the California survey indicated that reinforced concrete approach slabs provided considerably smoother transitions than asphalt approaches. No difference was observed between shallow and deep embankment fills. A monitored field study of 60 experimental approach slabs led to the conclusion that the primary causes of approach slab settlement are original ground settlement and fill settlement. Research continues (Stewart 1989) to study the concept of select backfill in the first 150 ft behind the abutment with a specially designed 30 ft approach slab.

Hopkins and Deen (1970) report a field survey of 335 bridge approaches in 1964 and 211 in 1968 in Kentucky. The degree of significant settlement is studied as a function of pavement type, abutment type, embankment type, type of backfill material, and physiographic region. Observing that between 40 percent and 90 percent of the surveyed approaches required maintenance to mitigate a "bump," the researchers conclude that "it is evident that present design and construction procedures are not sufficient to guarantee smooth bridge approaches." In addition they observed that the approach settlements appeared to be confined to within 100 ft of the end of the bridge, and settlement seldom exceeded 6 in. Three types of abutments were commonly used in Kentucky at the time of the study: stub (closed end), pile-end-bent (open end), and open column (open end). The stub abutments required maintenance slightly less frequently than the other types, but this may have been because the stub abutments were more commonly used with lower average embankment heights and lower average foundation thicknesses. The review leads to the conclusion that the causes of approach settlement may not be easily generalized across the country.

A recent study conducted for the Maryland DOT (Wolde-Tinsae, et al. 1989) consists of a state-of-the-art and a state-of-practice study including a literature review and a survey of state highway agencies on design and construction practices used at bridge approaches. The causative factors identified are classified into the following three areas:

1. Differential settlement between the highway pavement and the bridge deck,
2. Rotation and/or lateral movement of the abutment, and
3. Poor design of structural components.

Differential settlement problems may be related to consolidation of embankment foundation, volume change within the embankment, lateral movements of the embankment, and subsurface erosion of embankment fill. Rotation or lateral movement of the abutment may be associated with slope failure, seepage, thermal forces, and deep foundation settlement. Poor structural design has reportedly contributed to "attenuation *(sic)* of a bump at the ends of a bridge due to excessive camber or sag in the first span of the bridge, gaps forming between the backwall and roadway fill, additional stresses on the approach pavement, cracking of the backwalls, and cracking of the wingwalls." Factors which affect the development of bridge approach roughness include the abutment type, the construction methods and structural details. Significant differential settlements are reportedly more common for pile-supported abutments, presumably because the deep foundations do not experience much vertical motion, so that any vertical motion of the embankment is manifested as differential motion. The type and geometry of the abutment may influence the ease with which the backfill can be compacted, contributing to local settlements under the approach slab. Structural details which reportedly must be considered include the joint treatment between the approach slab and the pavement which must transfer traffic loads to the abutment, seal out surface water, and permit expansion as necessary to prevent abutment damage. The recommendations in the Maryland study interim report included further study of drainage system design methods, effect of type of soil and degree of compaction on settlement of approach fill, reinforcing embankment material with geotextiles, and development of better design details for reinforced concrete slabs.

A related FHWA study reported by Moulton (1986) provides some guidance for tolerable movements of highway bridges with respect to serviceability or ride quality. Limited data is available and conclusions are limited to maximum allowable angular distortions at approaches (0.004-0.005 radians) and maximum allowable horizontal movements of abutments (1.5 in.).

DESCRIPTION OF THE FIELD STUDIES

The field study sites visited during this study fall into two categories; sites designated by district personnel when maintenance intensive sites were solicited by the researchers and sites selected randomly by the researchers for brief inspections. Visits to these sites are discussed in the following sections.

Study of Sites Designated by District Personnel

District personnel in six districts were requested to provide five or six sites where "instability of the bridge approach has degraded riding quality...or led to reduced maintenance intervals..." As a result of this request, districts 9, 12, 13, 17, and 20 responded with a total of 31 sites suggested for study. These sites were visited, along with a few other adjacent sites selected in the field, making a total of approximately 34 sites. The visits to these sites consisted of a brief, 1/2 to 1 hr inspection of the roadway, including approach pavement, approach slab, bridge deck and joints, substructure, abutment, rip-rap, wingwalls, and, in general, an observation of any visual clues as to the reported poor performance of the structures. A brief summary of the observations made at these sites is tabulated in Appendix A. Of these 34 sites, concrete pavements were heavily represented with at least 14 of the sites being located adjacent to concrete pavements. It was noted early in the study that one form of distress was heavily represented in the sample group--cracking of the abutment backwall. It was also noted that this form of damage, especially when in advanced stages, closely correlated with the presence of concrete pavements. Of the 14 sites associated with concrete pavements, nine exhibited some significant distress to the backwall. The observed backwall damage is discussed in detail in a following section. Other types of distress, including relative displacement of pavement/approach slab and approach slab/deck interfaces, cracked approach slabs, flexible pavement distress such as rutting and alligator cracking, rotation of abutments, etc., were also noted as contributing to the pavement roughness; but the abutment damage, when present, was noteworthy in that it eventually requires a more significant repair effort--replacement or rehabilitation of the abutment. The damaged abutment contributes to approach roughness in several ways, not the least of which is by allowing more rapid erosion of material from beneath the approach slab by allowing more water into the embankment.

Soil Borings

Based on the observations made at the time of the initial visits to these sites, soil investigations, including borings, were planned at several sites. The boring logs for this portion of the study are presented in Appendix B. It has been suggested that the fills were mostly clay, and the observed problems were the result of the swelling clay fill. In an effort to determine if this was true, two bridges were surveyed and studied at El Campo and Wharton on Hwy 59. Both abutments were studied at each site. In El Campo the bridge crossed the railroad and Hwy 222. At Wharton the bridge crossed Hwy 60.

At all four abutments the three distress conditions mentioned were found, plus the void under the approach apron had not been grouted and was filled with water. As vehicles crossed the broken pavement, water was being pumped out of the void carrying fine material. This was happening behind the pavement lug cast into the approach apron. It was also observed that the pavement back from bridges in both direction was buckled about every 1000 to 1300 feet and in many cases the pavement section had been broken out and repoured. Otherwise the pavement was broken transversely at a spacing of 3 to 4 feet. Even with the cracks , the pavement was smooth and the riding surface good. It was also observed that all of the expansion joints across these bridges of many spans were closed.

The pavement did not exhibit the classic system of heaving subgrade (Lytton, Bogess & Spotts 1976). Usually pavements on heaving soil are quite irregular with both transverse and longitudinal undulations so that a vehicle rocks and pitches as it is driven down the road. Another classic system of heaving subgrade is soft paved shoulder with cracks and sometimes with longitudinal ruts.

If there is a curb section along the pavement on heaving soil, usually the curb will rotate backwards. The gutter lifts as the subgrade swells. Typically it is the cut section of a highway that experiences most heave, not the fill section. At the cut section there may be a source of water from the cut bank and the surrounding soil. Some of the worst heave is seen where the subgrade elevation is below the depth of the adjacent drainage ditch. In the case of a bridge abutment fill the drainage is excellent and if soil conditions are fairly uniform the only source of water for the soil to suck up is the crack infiltration water, water from dew and atmospheric moisture.

At the El Campo and Wharton site, the fills seemed to be made of soil that could be visually classified as CL material and marginally expansive at best. The unit weight of the soil seemed to be fairly high, the soil was stiff and not saturated. The ground the fills were built on was also well drained and not saturated.

The riprap on the abutment fill was pushed up from the fill and in many places did not touch the soil. With the good fill drainage and smooth pavement it seemed unlikely the bridge abutment distress was being caused by expansive soil.

In an effort to determine more carefully if heaving of the fill was causing the bridge abutment distress, soil boring were made at next four sites studied. The sites where the borings were made were:

1. The south end of the east lane of the overpass bridge on Hwy 96 over Lucas Dr in Beaumont--2 borings.
2. The south end of the east lane of the bridge on IH 610 crossing the Houston, Texas Ship Channel--1 boring.
3. The east end of the north lane of the bridge on FM 270 over Clear Cr near League City--1 boring.
4. The south end of the west lane of the overpass bridge on the SH 6 east by-pass over Tabor Rd in Bryan, Texas--1 boring.

The boring logs and laboratory test data (Appendix B) for each layer of soil gives the moisture content, the dry unit weight called dry density, the liquid limit (LL), the plastic limit (PL), and the plasticity index (PI). Also the

shear strength of each layer is given on the boring logs as determined by a pocket pentrometer. The number tabulated is the unconfined compressive strength, σ_{uc}, expressed in tons per square foot (tsf). The unconfined compressive strength, σ_{uc}, is twice the cohesive shear strength, c. Therefore the value tabulated multiplied by 1000 is the cohesive shear strength, c, of the soil, expressed in psf.

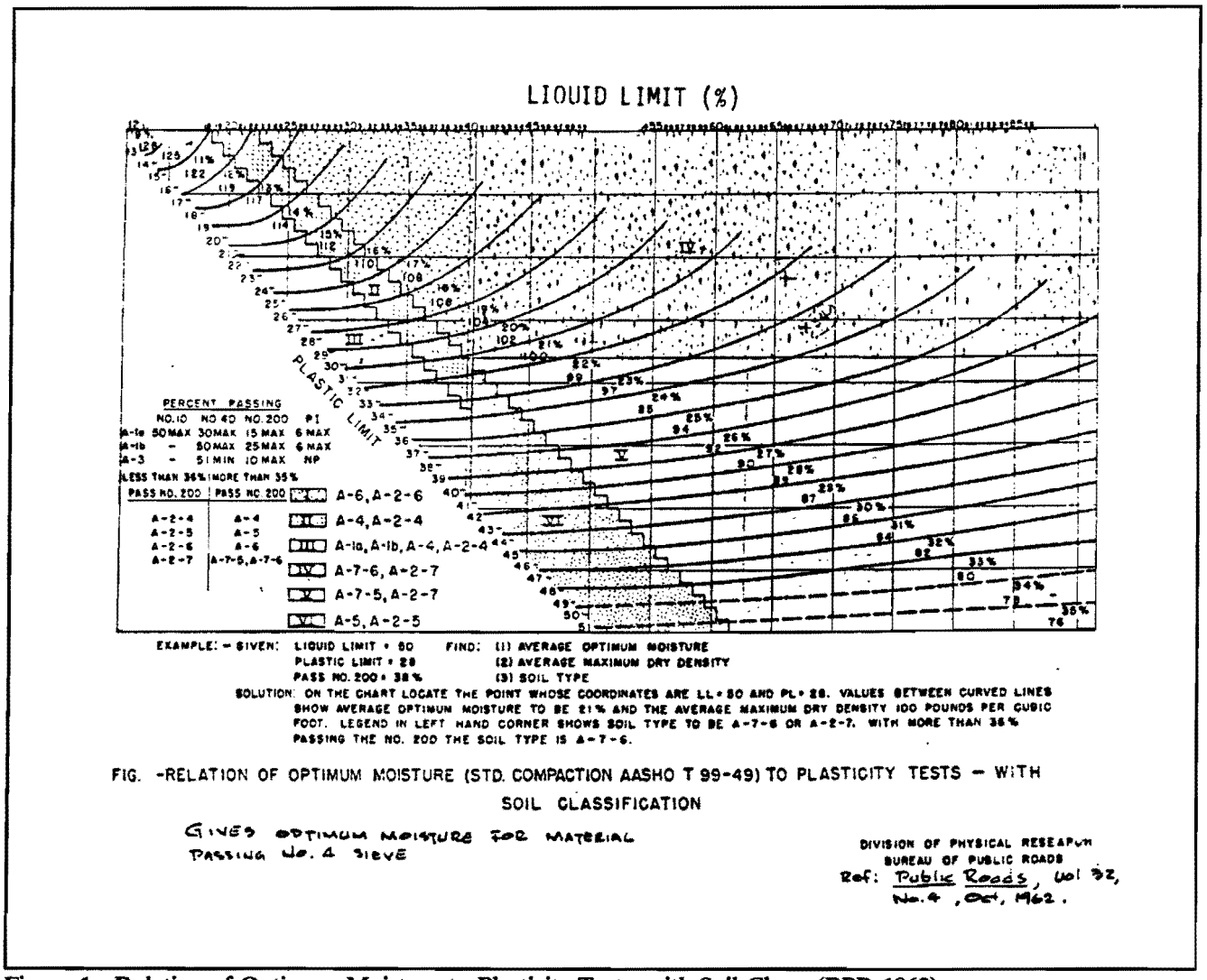

FIG. -RELATION OF OPTIMUM MOISTURE (STD. COMPACTION AASHO T 99-49) TO PLASTICITY TESTS – WITH SOIL CLASSIFICATION

Figure 1.--Relation of Optimum Moisture to Plasticity Tests--with Soil Class. (BPR 1962)

Since it was impossible to determine the compaction data from the core samples, the standard proctor test optimum moisture content and the maximum dry density were estimated using the U.S. Bureau of Public Roads Method. The U.S. Bureau of Public Roads Chart for this method is attached as Figure 1. It utilizes the soil's LL and PL to empirically determine the standard Proctor optimum moisture content and maximum dry density. In Table 1 through Table 5 these estimated values are superimposed on the laboratory test values so that the soil's insitu moisture content and dry density could be compared to the standard Proctor optimum moisture content and maximum dry density. The standard Proctor test ASTM D698-78 for the moisture-density relationship of compacted

soil and also the AASHO T99-49 test each use 12,400 ft-lb of energy per cubic foot of compacted soil. These tests are commonly called the standard Proctor test to distinguish them from the modified Proctor test ASTM D-1557-78 which uses 56,000 ft-lb/ft^3 energy input. The Texas test method Tex-113-E (1966) for the determination of moisture-density relations of soil and base materials (with 50 blows per layer) uses 22,918 ft-lb/ft^3 energy input. Thus the maximum dry density and the optimum moisture content from the Texas 113-E test and from the standard Proctor tests may not be the same. The analysis here is based on the standard Proctor (12,400 ft-lb/ft^3); the current TxDOT specification procedure uses a different compactive effort.

The liquidity index (LI) was computed and tabulated. The LI is given by

$$LI = \frac{w-PL}{PI} \tag{1}$$

where LI = the liquidity index,

w = the natural moisture content, and

PI = LL-PL, the plasticity index.

The percent saturation was also computed and tabulated. The percent saturation is given by

$$S = \frac{w}{[\frac{\gamma_0}{\gamma_D} - \frac{1}{G_S}]} \tag{2}$$

where S = percent saturation,

w = moisture content, expressed as a percentage,

γ_0 = unit weight of water,

γ_D = dry unit weight, and

G_S = specific gravity of soil, estimated to be about 2.74.

The percent compaction was also estimated but not tabulated since most values were about 95%. The percent compaction is given by

$$C = \frac{\gamma_D}{\gamma_{max}} \times 100 \tag{3}$$

where C = percent compaction,

γ_D = dry unit weight, and

γ_{max} = standard Proctor dry density.

Table 1. Measured and Calculated Soil Properties; Boring Site 1

SUMMARY OF LABORATORY TEST DATA

PROJECT: TEXAS TRANSPORTATION INSTITUTE
Approach Slab Investigation, Project No. 1213, Beaumont Site

PROJECT NO: 891082 DATE: August 28, 1989

BORING NO.	DEPTH IN FEET	SAMPLE NO.	TYPE OF MATERIAL	MOISTURE CONTENT %	DRY DENSITY pcf	ATTERBERG LIMITS LL	PL	PI	COMPUTED VALUES: 1 OPTIMUM % MOISTURE CONT.	2 STAND. MAX. DRY DEN. (PCF)	MOISTURE CONT. -OPT. MOIS. CNT.	DRY DENSITY - STAN. MAX. DEN.	LIQUIDITY INDEX	PERCENT SATURATION	OTHER TESTS: PERCENT PASSING THE NO. 200 SIEVE
CB-1	0-2	1672	Tan and gray fat clay with sand *(CH)	24	100	51	15	36	18	106	6	-6	0.25	93	76% finer
	2-4	1673	Tan and gray lean clay with sand *(CL)	24	99	49	15	34	18	106	6	-7	0.18	91	81% finer
	4-6	1674	Tan and gray lean clay with sand *(CL)	22	106	48	13	35	17	108	5	-2	0.26	98	85% finer
	6-8	1675	Tan and dark gray lean clay with sand (CL)	19	104	42	15	27	17	108	2	-4	0.15	81	76% finer
	8-10	1676	Tan and dark gray lean clay (CL)	21	104	40	17	23	17	108	4	-4	0.17	89	86% finer
	10-12	1677	Tan and dark gray lean clay (CL)	20	106	43	16	27	17	108	3	-2	0.15	89	87% finer
	12-14	1678	Tan and dark gray lean clay (CL)	24	99	40	18	22	17	108	7	-9	0.27	90	93% finer
	14-16	1679	Tan lean clay (CL)	19	108	38	16	22	16	110	3	-2	0.14	89	87% finer
	16-18	1680	Tan and gray lean clay with sand and shells (CL)	19	106	38	18	20	16	110	3	-4	0.05	85	85% finer
	18-20	1681	Tan and gray sandy lean clay (CL)	19	107	34	15	19	15	112	3	-5	0.21	87	69% finer
	20-22	1682	Tan and gray lean clay (CL)	30	93	46	17	29	18	106	12	-13	0.45	98	96% finer
	22-24	1683	Tan and gray lean clay (CL)	20	106	47	17	30	18	106	2	0	0.10	89	97% finer

1 and 2 taken from U.S. Bureau of Public Roads. Public Roads Vol. 32, No. 4, October 1962. Based on LL and PL.

Table 2. Measured and Calculated Soil Properties; Boring Site 2

SUMMARY OF LABORATORY TEST DATA

PROJECT: TEXAS TRANSPORTATION INSTITUTE
Approach Slab Investigation, Project No. 1213, Beaumont Site
PROJECT NO: 891082 DATE: August 28, 1989

BORING NO.	DEPTH IN FEET	SAMPLE NO.	TYPE OF MATERIAL	MOISTURE CONTENT %	DRY DENSITY pcf	ATTERBERG LIMITS LL	PL	PI	COMPUTED VALUES: 1 OPTIMUM % MOISTURE CONT.	2 STAND. MAX. DRY DEN. (PCF)	MOISTURE CONT. -OPT. MOIS. CNT.	DRY DENSITY - STAN. MAX. DEN.	LIQUIDITY INDEX	PERCENT SATURATION	OTHER TESTS PERCENT PASSING THE NO. 200 SIEVE
CB-2	0-2	1684	Tan and gray lean clay with sand (CL)	24	98	47	17	30	18	106	6	--8	0.23	88	77% finer
	2-4	1685	Tan and gray lean clay with sand and shells (CL)	21	104	44	16	28	17	108	4	--4	0.18	89	75% finer
	4-6	1686	Tan and gray sandy lean clay (CL)	24	96	41	17	24	17	108	7	-12	0.29	84	65% finer
	6-8	1687	Tan and gray sandy lean clay with shells (CL)	18	110	27	14	13	13	117	5	-7	0.31	89	57% finer
	8-10	1688	Tan and dark gray lean clay (CL)	21	103	37	15	22	16	110	5	-7	0.27	87	91% finer
	10-12	1689	Tan and dark gray lean clay with sand (CL)	15	111	25	14	11	13	117	2	-6	0.09	76	84% finer
	12-14	1690	Tan lean clay (CL)	20	102	37	13	24	15	112	5	-10	0.29	81	86% finer
	14-16	1691	Tan and dark gray lean clay with sand (CL)	17	107	27	14	13	13	117	4	-10	0.23	78	80% finer
	16-18	1692	Tan and gray lean clay (CL)	18	108	36	16	20	16	110	2	-2	0.10	85	87% finer
	18-20	1693	Tan and gray lean clay (CL)	22	101	36	16	20	16	110	6	-9	0.30	87	86% finer
	20-22	1694	Tan and gray fat clay (CH)	22	103	50	17	33	18	106	4	-3	0.15	91	92% finer
	22-24	1695	Tan and gray fat clay (CH)	21	106	51	19	32	19	104	2	+2	0.06	94	96% finer

1 and 2 taken from U.S. Bureau of Public Roads. Public Roads Vol. 32, No. 4, October 1962. Based on LL and PL.

2

Table 3. Measured and Calculated Soil Properties; Boring Site 3

SUMMARY OF LABORATORY TEST DATA

PROJECT: TEXAS TRANSPORTATION INSTITUTE
Approach Slab Investigation, Project No. 1213, Houston Site

PROJECT NO: 891082 DATE: August 28, 1989

BORING NO.	DEPTH IN FEET	SAMPLE NO.	TYPE OF MATERIAL	MOISTURE CONTENT %	DRY DENSITY pcf	ATTERBERG LIMITS LL	PL	PI	COMPUTED VALUES 1 OPTIMUM % MOISTURE CONT. STAN. MAX. DRY DEN. (PCF)	2 MOISTURE CONT. -OPT. MOIS. CNT	DRY DEN. - STAN. MAX. DEN.	LIQUIDITY INDEX	PERCENT SATURATION	OTHER TESTS PERCENT PASSING THE NO. 200 SIEVE
CB-3	6½-8	1705	Dark gray lean clay with sand and shells (CL)	22		39	13	26	16 110	---	---	0.35	--	75% finer
	8-10	1706	Tan and gray sandy lean clay with shells (CL)	16	113	32	15	17	15 112	-1	-1	0.06	86	68% finer
	10-12	1707	Tan and gray lean clay* (CL)	21	105	49	19	30	19 104	2	-1	0.07	92	86% finer
	12-14	1708	Tan and dark gray lean clay with sand and shells * (CL)	21	104	48	15	33	18 106	3	-2	0.18	89	77% finer
	14-16	1709	Tan and dark gray lean clay with sand (CL)	26	96	46	15	31	17 108	9	+12	0.36	91	76% finer
	16-18	1710	Tan and dark gray lean clay with brick and sand (CL)	26	98	36	13	23	15 112	11	-14	0.57	96	74% finer
	18-20	1711	Tan and dark gray lean clay with shells and sand (CL)	21	102	42	14	28	17 108	4	-6	0.25	85	80% finer
	20-22	1712	Tan and gray lean clay with sand (CL)	19	109	40	15	25	16 110	3	-1	0.16	92	73% finer
	22-24	1713	Tan and gray sandy lean clay (CL)	18	109	45	17	28	18 106	0	3	0.04	87	64% finer
	24-26	1714	Dark gray lean clay with shells, sand and nodules (CL)	20	109	39	13	26	16 110	4	-1	0.27	96	73% finer
	26-28	1715	Dark gray fat clay with shells * (CH)	22	101	53	16	37	19 104	3	-3	0.16	87	82% finer
	28-30	1716	Dark gray sandy lean clay with shells and brick (CL)	19	107	40	14	26	16 110	+3	-3	0.19	87	64% finer
	30-32	1717	Tan and dark gray fat clay * (CH)	25	98	55	23	32	1 and 2 taken from U.S. Bureaus of Public Roads, Public Roads Vol. 32, No. 4, Oct. 1962, Based on LL and PL					94% finer

Table 4. Measured and Calculated Soil Properties; Boring Site 4

SUMMARY OF LABORATORY TEST DATA

PROJECT: TEXAS TRANSPORTATION INSTITUTE
Approach Slab Investigation, Project No. 1213, League City Site
PROJECT NO: 891082 DATE: August 28, 1989

BORING NO.	DEPTH IN FEET	SAMPLE NO.	TYPE OF MATERIAL	MOISTURE CONTENT %	DRY DENSITY pcf	ATTERBERG LIMITS LL	PL	PI	COMPUTED VALUES 1 OPTIMUM % MOISTURE CONT.	2 STAND. MAX. DRY DEN. (PCF)	MOISTURE CONT. -OPT. MOIS. CNT.	DRY DENSITY - STAN. MAX. DEN.	LIQUIDITY INDEX	PERCENT SATURATION	OTHER TESTS PERCENT PASSING THE NO. 200 SIEVE
CB-4	3½-4	1719	Tan and gray lean clay with sand (CL)	17	113	36	15	21	15	112	2	1	0.10	91	78% finer
	4-6	1720	Tan and gray lean clay with sand (CL)	17	113	35	15	20	15	112	2	1	0.10	91	73% finer
	6-8	1721	Tan and gray lean clay with sand (CL)	19	109	41	15	26	16	110	3	-1	0.15	92	84% finer
	8-10	1722	Tan and gray lean clay (CL)	20	108	43	15	28	17	108	3	0	0.18	94	87% finer
	10-12	1723	Tan and gray lean clay (CL)	19	104	46	18	28	18	108	1	-4	0.04	81	86% finer
	12-14	1724	Tan and gray lean clay with sand and nodules (CL)	16	114	35	17	18	16	110	0	4	-0.06	88	76% finer
	14-16	1725	Tan and gray lean clay with sand (CL)	20	107	45	17	28	17	108	3	1	0.17	92	82% finer
	16-18	1726	Tan and gray fat clay* (CH)	24	99	54	19	35	19	104	5	-5	0.14	90	89% finer
	18-20	1727	Tan and gray lean clay with sand (CL)	20	108	48	15	33	18	106	2	2	0.15	94	80% finer
	20-22	1728	Tan and gray fat clay with sand (CH)	26	98	61	18	43	20	102	6	-4	0.19	96	83% finer
	22-23½	1729	Tan silty fine sand (SM)	23		Non-Plastic									
	24-25½	1730	Gray sandy silt (ML)	23		20	18	2							57% finer
	28½-30	1731	Gray silty, clayey sand (SC-SM)	24		18	14	4	1 and 2 taken from U.S. Bureau of Public Roads. Public Roads Vol. 32, No. 4, October 1962. Based on LL and PI.						39% finer
	33½-35	1732	Gray sandy, silty clay (CL-ML)	28		24	17	7							66% finer

Table 5. Measured and Calculated Soil Properties; Boring Site 5

SUMMARY OF LABORATORY TEST DATA

PROJECT: TEXAS TRANSPORTATION INSTITUTE
Approach Slab Investigation, Project No. 1213, Bryan Site
PROJECT NO: 891082 DATE: August 28, 1989

BORING NO.	DEPTH IN FEET	SAMPLE NO.	TYPE OF MATERIAL	MOISTURE CONTENT %	DRY DENSITY pcf	ATTERBERG LIMITS LL	PL	PI	COMPUTED VALUES: 1 OPTIMUM % MOISTURE CONT.	2 STAND. MAX. DRY DEN. (PCF)	MOISTURE CONT. -OPT. MOIS. CNT.	DRY DENSITY - STAN. MAX. DEN.	LIQUIDITY INDEX	PERCENT SATURATION	OTHER TESTS PERCENT PASSING THE NO. 200 SIEVE
CB-5	2-4	1734	Tan and gray sandy lean clay (CL)	24	100	42	21	21	18	106	6	-6	0.14	93	62% finer
	4-6	1735	Tan fat clay *(CH)	30	91	54	24	30	20	102	10	-11	0.20	94	87% finer
	6-8	1736	Gray clayey sand *(SC)	21	104	49	17	32	18	106	3	-2	0.13	89	47% finer
	8-10	1737	Dark gray sandy lean clay (CL)	22	104	45	18	27	18	106	4	-2	0.15	94	64% finer
	10-12	1738	Tan and dark gray sandy lean clay *(CL)	23	103	48	17	31	18	106	5	-3	0.20	96	63% finer
	12-14	1739	Dark gray fat clay with sand *(CH)	24	101	54	18	36	19	104	5	-3	0.17	95	73% finer
	14-16	1740	Dark gray fat clay with sand *(CH)	25	102	51	18	33	19	104	6	-2	0.21	(101)	75% finer
	16-18	1741	Gray fat clay *(CH)	27	92	60	19	41	20	102	7	-10	0.20	86	93% finer
	18-20	1742	Dark gray lean clay with sand (CL)	25	100	33	16	17	15	115	10	-12	0.53	97	83% finer
	20-22	1743	Gray fat clay with sand *(CH)	22	105	54	17	37	19	104	3	1	0.14	96	76% finer
	22-24	1744	Gray sandy lean clay (CL)	23	103	35	19	16	16	110	7	-7	0.25	96	51% finer
	24-26	1745	Gray clayey sand (SC)	23	105	33	17	16	15	112	8	-7	0.38	100	49% finer
	26-28	1746	Tan and gray lean clay with sand (CL)	25	101	39	20	19							78% finer

1 and 2 taken from U.S. Bureau of Public Roads. Public Roads Vol. 32, No. 4, October 1962. Based on LL and PL.

5

Generally when a soil has LL less than 50 and PI less than 25, it is usually not considered to be expansive, and normal construction practices can be used (Patrick 1977). This is not always true, however, and some soils with a PI of 15 have been known to swell. They must be dry before a structure is built over them in order to develop the suction necessary to pull in sufficient water to swell. The potential swell for soil with LL less than 50 and PI less than 25 is usually thought to be less than 0.5 percent. The potential swell for soil with LL between 50 and 60 and PI between 25 and 35 is usually thought to be between 0.5 percent and 1.5 percent.

The soils at the four sites that fall into last category are labeled with an asterisk (*) in Table 1 through Table 5 in the column listing the type of material. These are called marginally expansive soil. At the Beaumont site, the data from borehole CB-1 indicated that the top 6 feet was marginally expansive. At the same site the data from the second borehole CB-2 indicated that the top 2 feet and that the layer between 20-24 deep was marginally expansive. At the League City Site data from Borehole CB-4 indicated that the soil between the depths of 16 to 18 feet was marginally expansive. At the Houston Ship Channel site data from borehole CB-3 indicated that the soil from depth 10-14 feet and from 26-32 feet was marginally expansive. At the Bryan site data from Borehole CB-5 indicated that the soil from 4 to 8 ft, from 10-18 feet and from 20-22 feet was marginally expansive.

In order for any clay to swell its suction must be higher than that of the adjacent soil or other source of water. Clays with high suctions usually have a low moisture content (generally 15 percent or less), a high dry density (generally 110 pcf or more), and a high cohesive strength (generally 3000 psf or more). After the clay has absorbed water and swelled, the moisture content will be high (as much as 30 percent), the dry density will be low (generally 85 pcf or less), and the cohesive strength will be low (generally 500 psf or less). A good measure of the relative moisture content is the LI. A soil in the dry or high suction state may have a LI as low as -0.5, and in the very wet or low suction state as high as 0.5 (McNeill & Poormoayed 1980). The LI for each layer sampled is tabulated. The tabulated LI data shows that the LIs for all layers are positive (in the range of 0.04 to 0.57), that is the moisture content is always above the PL. The average value for all layers in the four fills is about 0.15. The layers that have the high LI are deep and probably below the natural grade on which the fill was placed.

If any clay soil is compacted with a moisture content 2 percent to 5 percent above optimum moisture content to a dry unit weight less than 90 percent of standard Proctor dry unit weight, its potential to swell is severely limited (Thompson & Thomas 1964). It is believed that the Texas Highway Department has made this a standard practice for many years. This procedure is described in Texas Standard test method Tex 114-E(1965) compaction ratio method for selection of density of soils and base materials in place. Usually this practice will produce fills with a cohesive strength of 1000 to 1500 psf or more with little potential to swell regardless of its LL and PL.

Table 1 though Table 5 show the existing moisture content and the dry density for each soil layer. Also shown are the calculated standard Proctor optimum moisture content and the two dry densities. It can be seen that the existing dry density is quite high (91 to 109 pcf), but somewhat less than the standard Proctor maximum dry density. Typically the existing dry density is about 95 percent of standard Proctor maximum dry density. The existing moisture content is typically about 5 percent more than the standard Proctor optimum moisture content. This is what

would be expected in a clay fill engineered by the Texas Highway Department. These data lead to the conclusion that there has been no significant swelling of the soil in the bridge approach fills sampled.

A further indication that there has been no swell of the subgrade is that the moisture content is fairly uniform with depth. Typically in swollen subgrades the moisture content is quite high directly under the pavement and diminishes to a uniformly lower moisture content in a distance of 6 to 8 ft. Also, after a soil has swelled its degree of saturation is usually 100 percent. None of the soils at the four sites were saturated, except for 2 deep layers at the Bryan site.

The fill at the east end of the bridge over Clear Creek on FM 270 near League City has settled about 8 in. with respect to the bridge. Bituminous concrete has been used to fill the gap between bridge and pavement. There is no indication that the soil fill is consolidating, because the soil in the fill has a high dry density and is not saturated. The settlement is occurring because of deep-seated consolidation of layers of soil underneath the fill. It should be noted that Clear Creek is really a marsh on the south side of Galveston Bay.

When a soil subgrade swells it tends to lift the pavement nonuniformly because of the inhomogeneity in the soil, the amount of drying it experienced, and distance to the source of available water. Unless the soil is very close to an unsupported edge, the heave is one-dimensionaly upward. From the Rankine soil failure condition, it can be seen that

$$\sigma_H = \sigma_V \tan^2(45° + \frac{\phi}{2}) + 2c \tan (45° + \frac{\phi}{2}) \qquad (4)$$

where σ_H = horizontal normal stress,

σ_V = vertical normal stress equal to the overburden stress,

ϕ = the angle of internal friction, and

c = the cohesive strength of the soil.

If there is 8 in. of concrete pavement, the σ_V = 113 psf, approximately. If ϕ = 0, and c = 1500 psf, which is typical of the clay fill where the strength was measured, then

$$\sigma_H = \sigma_V + 2\times1500 psf = \sigma_V + 3000\ psf \qquad (5)$$

This indicates that the resistance to horizontal swell is always much higher than resistance to vertical swell.

The clay fill at the bridge abutments is paved with concrete riprap. It was observed that the riprap under the bridge was broken and lifted off the soil fill as much as 3 or 4 in. It has been speculated that this was caused by either the clay fill settling or swelling. Settlement is indicated by the fact that the riprap seems to be 3 or 4 inches lower than point where it was placed, relative to the side of the abutment. Had settlement caused the broken riprap, however, the soil would be expecte to remain in contact with the riprap, which was not the case as several sites. If there had been settlement in fills it had to be deep-seated, because the fill soil has high density, high cohesive strength, and is not saturated.

Swelling fill is indicated by the buckling nature of some of the riprap failures. Had swelling fill caused the broken riprap under the bridge the soil would have still been in contact with the riprap, and the same effect would have occurred on the sides of the bridge. For the soil in a clay fill adjacent to a slope to swell it must have been compacted very dry, or it must have shrunk during drying. In such a case the soil would be desiccated and maybe even cracked. Secondly the soil must have sufficient clay in it, usually more that 20%, and this clay must be active. In order to develop the suction to pull water into it. Third there must be a source of water in the adjacent soil or in the atmosphere. If the source of water is in the adjacent soil, it must have a higher moisture content than the soil on the slope so that a suction gradient can develop.

If the clay soil had a LL in the range 50-60 and a PI in the range 25-35, then the potential swell would be between 0.5 percent and 1.5 percent. Typically the distance over which the swell acts is 5 to 6 ft. The average swell over this distance will be roughly half these values. If the fill had been placed with a low moisture content of 10 percent to 15 percent or dried to these values and subsequently swollen until the moisture reached 20 to 25 percent, then the heave δ_h would be expected to be between the lower limit given by

$$\delta_h = (6\ ft)\ (0.005 \times \frac{1}{2})\ (\frac{12\ in.}{ft}) = 0.18\ in. \tag{6}$$

and the upper limit given by

$$\delta_h = (6\ ft)\ (0.015 \times \frac{1}{2})\ (\frac{12in.}{ft}) = 0.54\ in. \tag{7}$$

Since the borings analyses presented earlier are based on the BPR empirical relationship between the optimum moisture content and the liquid limit and plastic limit, and because the specified compactive effort in the embankments was different from that used in the standard Proctor tests, it is not possible to say with confidence that the embankments were originally constructed at the proper moisture content. It is clear that the current *in-situ* moisture content/density in the embankments are at levels which may be considered indicative of good construction, --that is, there should be no future approach roughness due to expansive soil actions. It is believed, though, that this moisture content/density relationship resulted from proper specification and construction, and has not contributed significantly to any past approach instabilities. It is considered unlikely that swelling clay caused the observed riprap movement of 3 in. to 4 in., when the potential heave is between 0.18 to 0.54 in. Also deep-seated settlement is highly unlikely at bridges in El Campo, Wharton and Bryan. All of these structures are founded on unsaturated soil of high density.

In conclusion the broken and lifted riprap under the bridges and the differential movement between the wing walls and the side riprap can be explained by movement of the pile cap that supports the end of the bridge. If the

pile cap has been pushed forward, the riprap would have been lifted and broken, the wing walls broken off and the wing wall--riprap separation occurred. It is highly likely that pavement elongation could have done this by pushing on the approach slab which in turn pushed the pile cap forward to do the riprap damage. At the same time it could have closed all the expansion cracks in the approach pavement and pushed the pavement lugs forward to form the observed voids under the pavement.

Measured Approach Profiles

At selected sites, profile measurements were made with surveying techniques. The measured approach profiles are presented in Figure 2 through Figure 12. These figures illustrate various types of irregularities contributing to approach roughness including pavement roughness, discontinuities at approach slab interfaces, rotation of approach slab, and distortion of approach slab. The two figures depicting the SH 6 over FM 974 overpass illustrate significant pavement roughness. The rigid pavement is distorted into a sinusoidal profile with wavelength approximately 75-125 ft and double amplitude approximately 0.05-0.09 ft adjacent to the approach slabs on either end of the structure. The approach slabs are distorted, also. At both ends of the bridge the approach slabs indicate a "hogging" profile, that is, the ends have settled relative to the central portion. Typically, the rigid pavement is higher than the approach slab at the interface creating a vertical discontinuity of 0.04 ft, as identified in the two figures. This implies that the "sleeper" ledge supporting the pavement has settled, or debris has been introduced between the sleeper ledge and the end of the rigid pavement. The observed pavement longitudinal growth at this site may be contributing in an unknown manner to the observed vertical pavement profile and discontinuities.

The five figures depicting approach roughness on US 59 sites do not exhibit the large sinusoidal profile of the rigid pavement as was observed at the SH 6 site. Where the rigid pavements on US 59 do exhibit roughness, it is less significant and typically varies across the width of the roadway, while the SH 6 site pavements were uniformly distorted across the width of the roadway. Distortion of the approach slabs is not as significant at these sites either, although the approach slabs exhibit the same general type of distress, high central portions and low ends. The vertical discontinuities at the ends of the approach slabs are more significant at the US 59 sites with vertical discontinuities up to 0.08 ft commonly observed.

At the US 69 overpass over Lucas Dr., considerable evidence of pavement and approach slab maintenance was observed. The most significant aspects of the observed approach profiles are the vertical discontinuities at the ends of the approach slabs which were measured to be 0.07 ft on the north approach. Evidence of pressure grouting was observed on both approaches. The joint between the bridge deck and the north approach slab was observed to be open, indicating that longitudinal growth of the continuous concrete pavements is probably not a significant factor at this site.

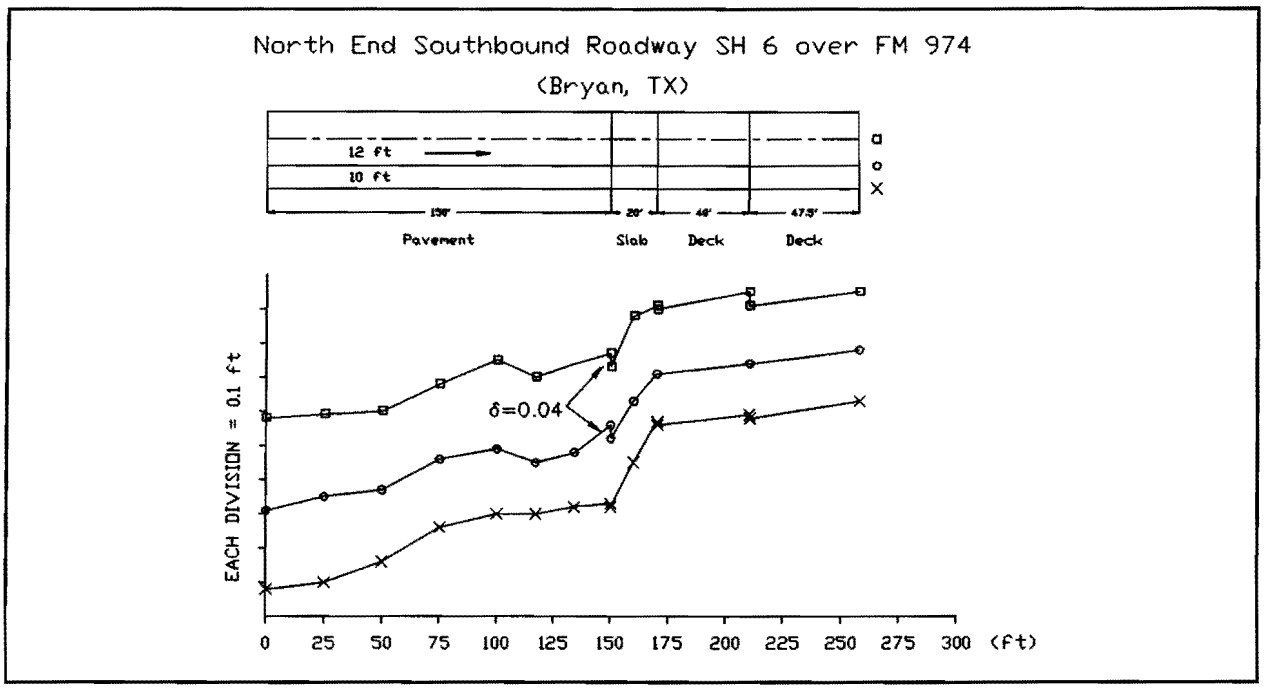

Figure 2.--Approach Profile; North End, Southbound SH 6 over FM 974

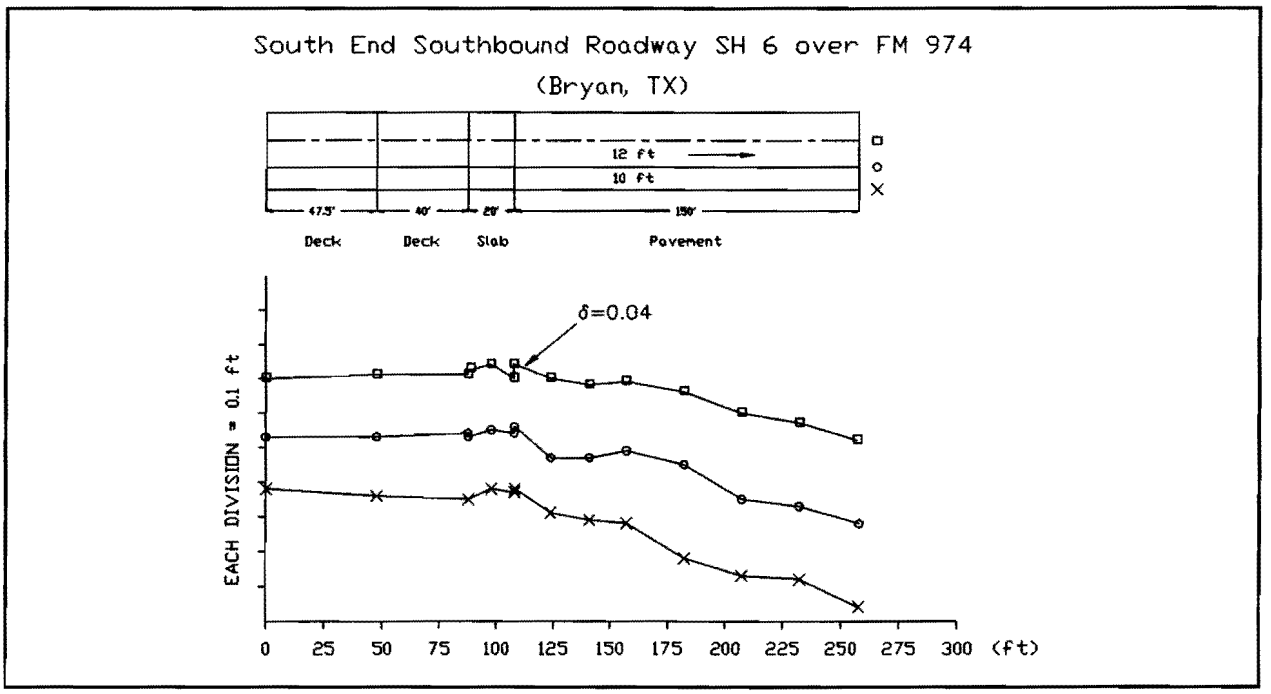

Figure 3.--Approach Profile; South End, Southbound SH 6 over FM 974

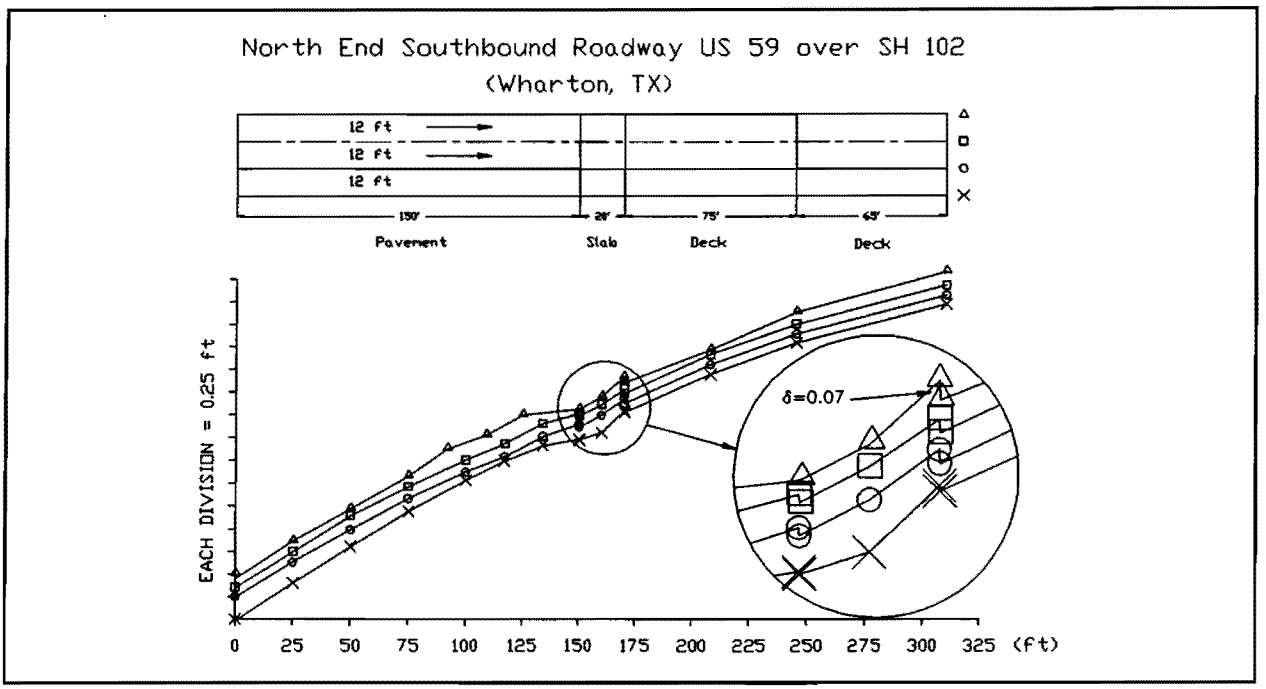

Figure 4.--Approach Profile; North End, Southbound US 59 over SH 102

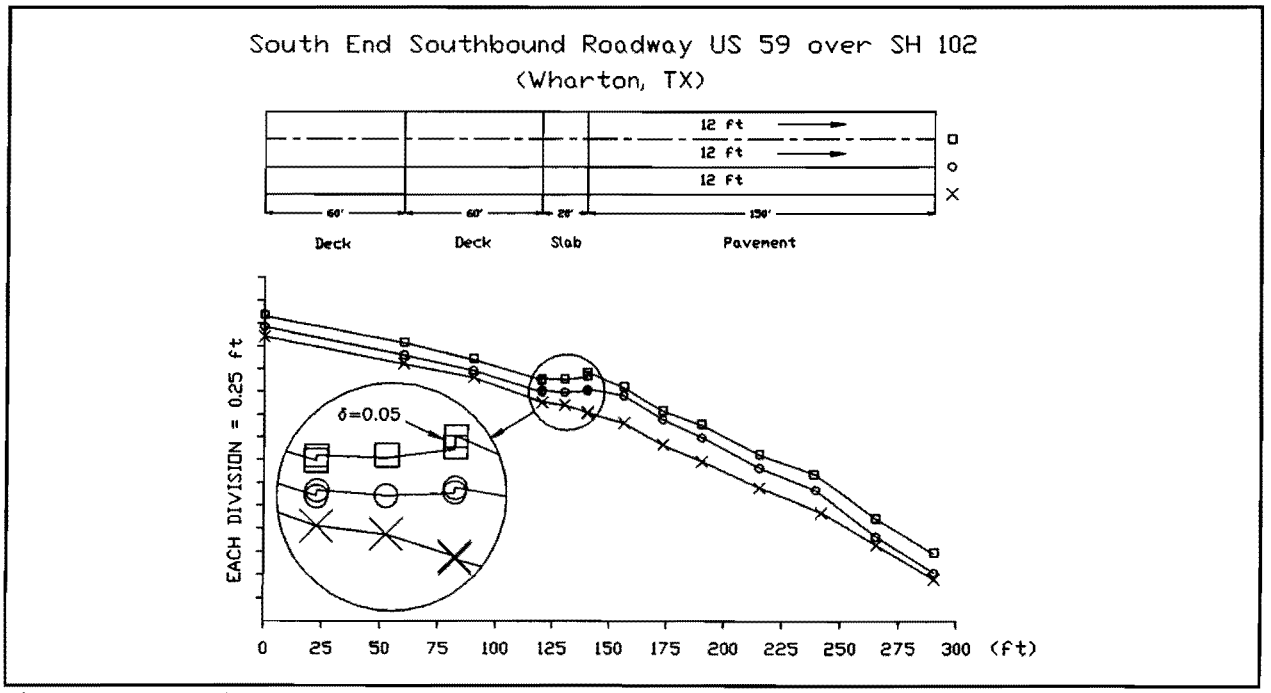

Figure 5.--Approach Profile; South End, Southbound SH 6 over SH 102

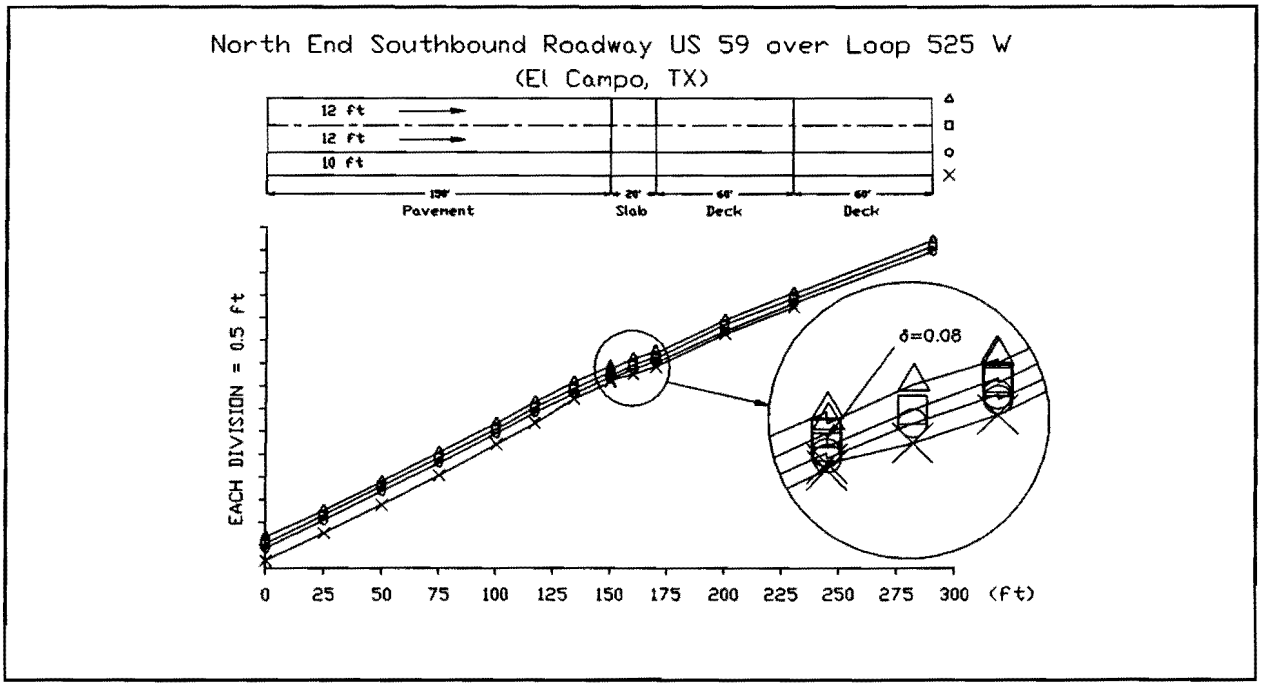

Figure 6.--Approach Profile; North End Southbound US 59 over L 525W

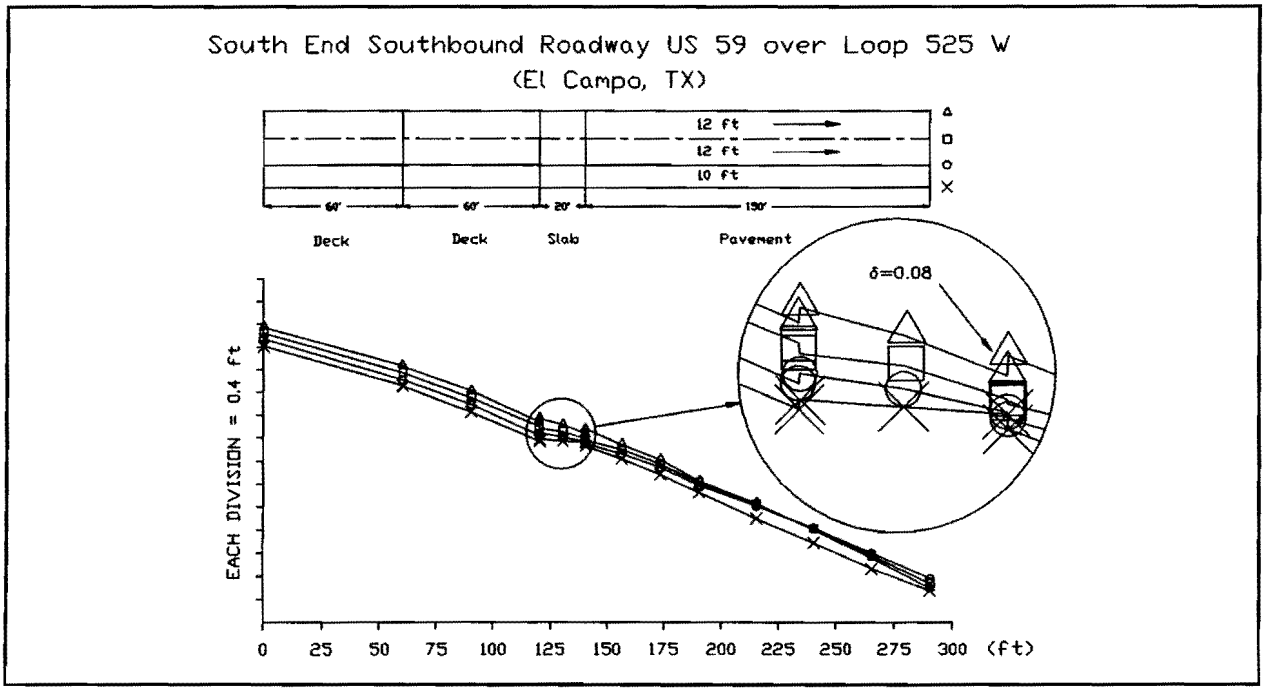

Figure 7.--Approach Profile; South End Southbound US 59 over L 525W

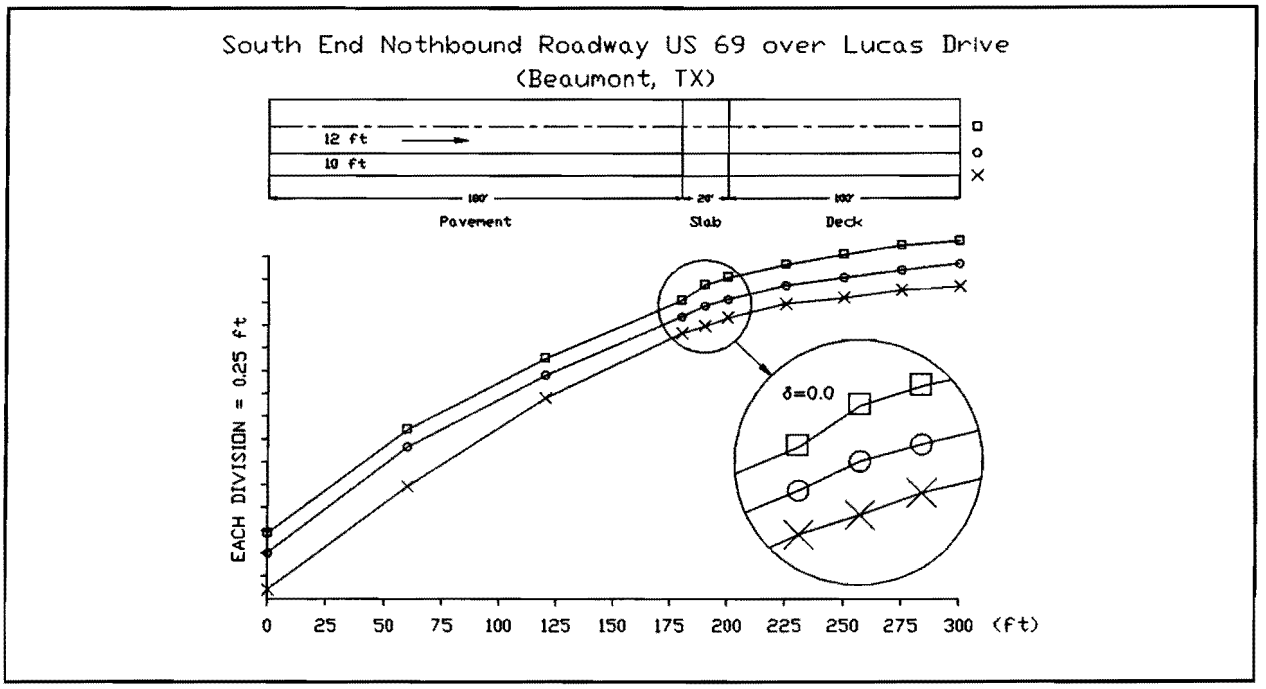

Figure 8.--Approach Profile; South End Northbound US 69 over Lucas Dr.

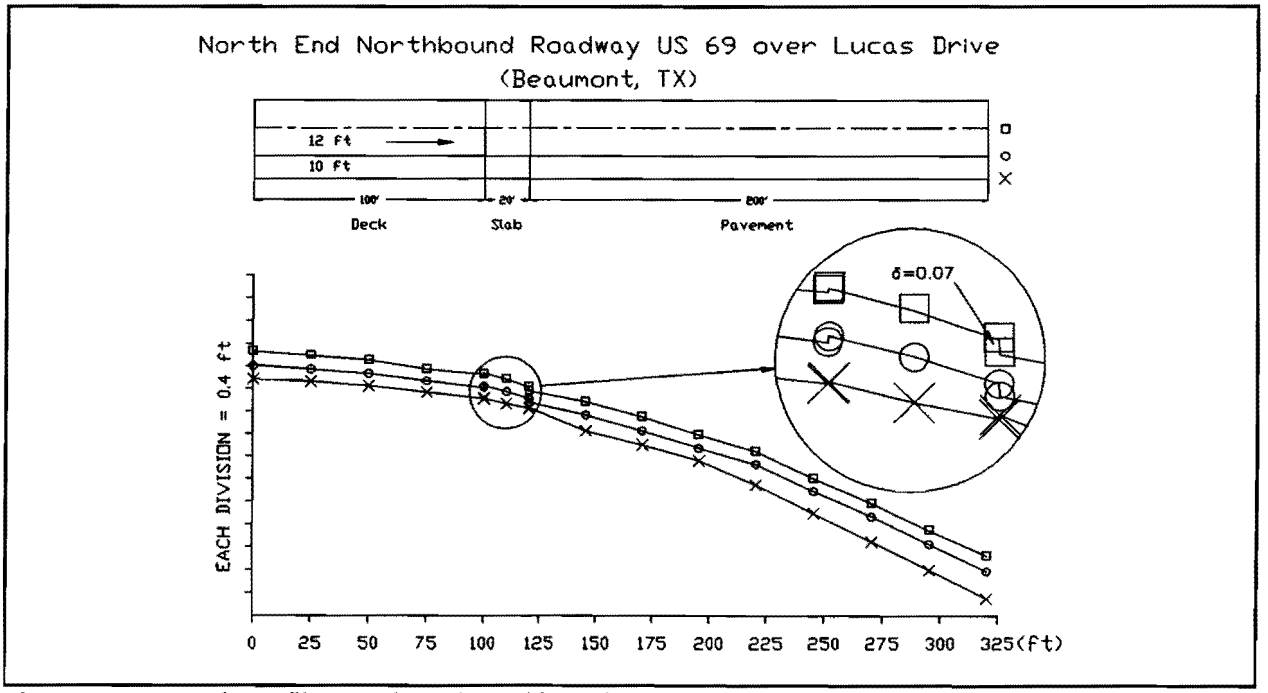

Figure 9.--Approach Profile; North End Northbound US 69 over Lucas Dr.

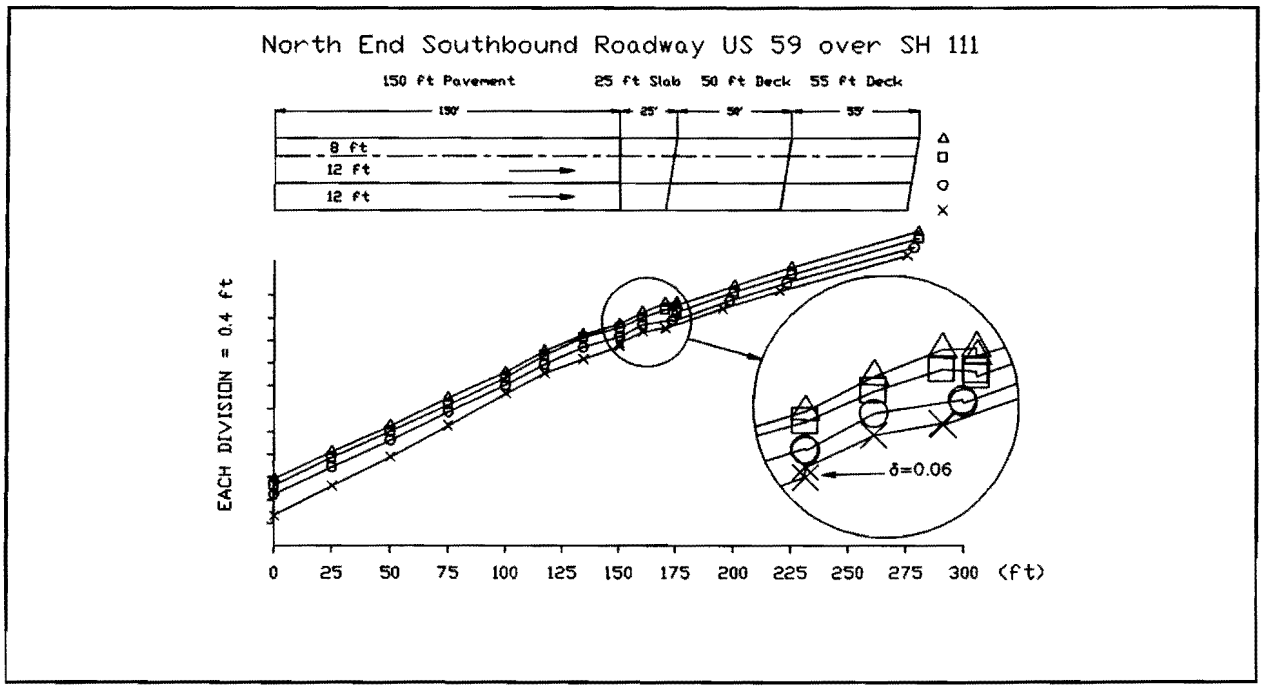

Figure 10.--Approach Profile; North End Southbound US 59 over SH 111

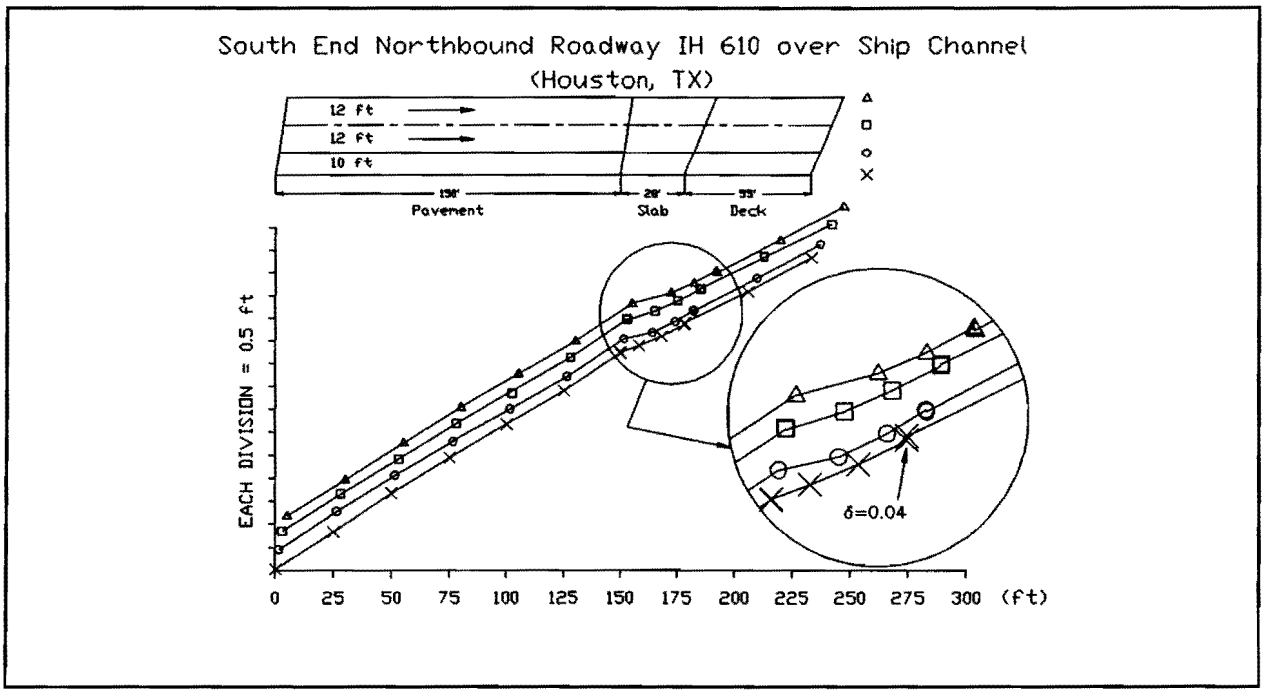

Figure 11.--Approach Profile; South End Northbound IH 610 over Ship Channel

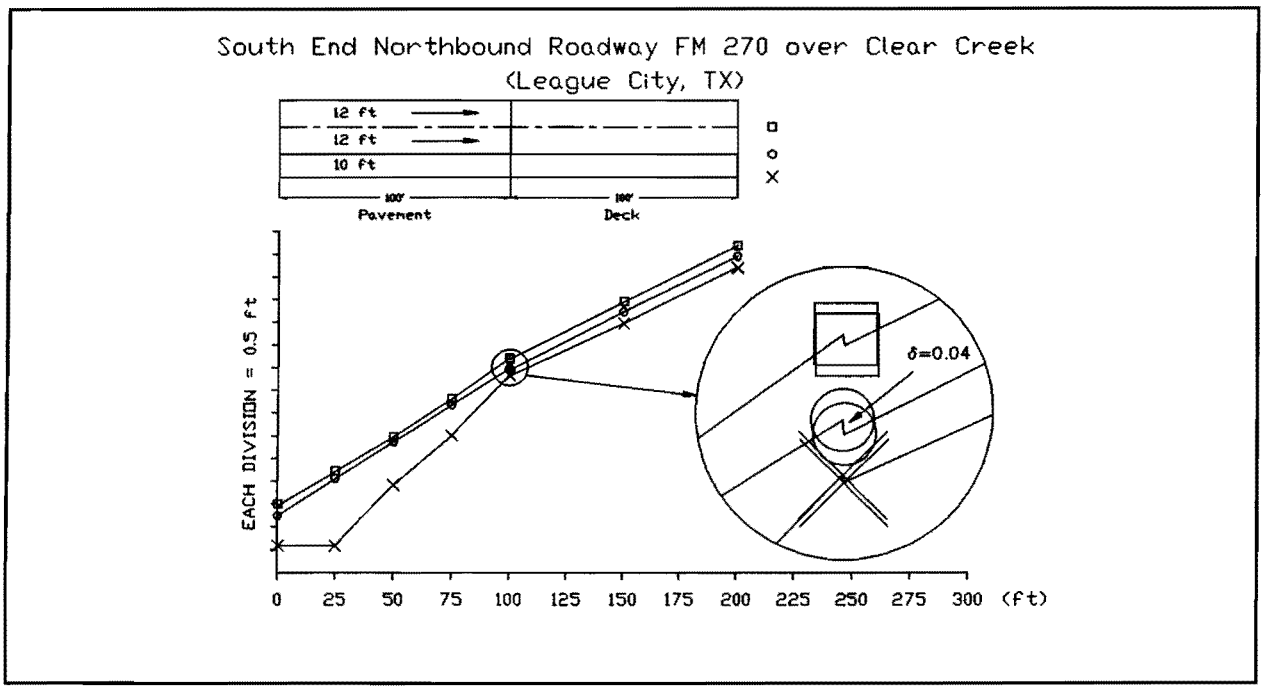

Figure 12.--Approach Profile; South End FM 270 over Clear Creek

At the IH 610 approach to the ship channel crossing, the joints at either end of the approach slab were closed, and the first few joints between the multiple approach spans were closed. Further from the approach, the joints between the simple spans were open, which was interpreted as indicating that the longitudinal motion closing the joints is from the approach moving into the bridge rather than the bridge spans moving "downhill" toward the approach. Vertical discontinuities at the ends of the approach slab were not as large as at other sites; the maximum observed vertical discontinuity was 0.04 ft. The rigid pavement at the approach was not significantly distorted either. The most significant observation, other than the closed joints, is seen in Figure 11, where the observed misalignment of the bridge deck and approach roadway appears to be resulting from a high spot at the approach slab/pavement interface. Along with the observations that the joints are closed, this may be evidence of a developing blow-up at this point caused by longitudinal motion of the concrete pavement. The present magnitude of the displacement is approximately 0.2 ft.

At the FM 270 bridge over Clear Creek, the measured approach profiles reflect considerable maintenance work including a significant area of pavement which was filled with asphalt concrete to maintain a smooth profile. Still, the profile along the outside edge of the paved shoulder indicates a large (approximately 0.5 ft) settlement in the 100 ft of roadway adjacent to the bridge deck. This large settlement is believed to be caused by consolidation of the soils beneath the embankment.

Study of Randomly Selected Sites

Because the study sample described above contained a higher fraction of bridges adjacent to concrete pavements than the overall population of bridges in the state, a second, randomly selected set of bridges was visited and surveyed. The bridges were selected in a random fashion by arbitrary choice of routes to include samples of highways of various service classes. The highway routes traveled are shown in Figure 13. The objective of this phase of the study was to provide an evaluation within a more representative group of bridges of the extent of the problem of extensive damage to abutment backwalls, to determine whether this problem was also associated with flexible pavements, and to assess the significance of approach roughness, in general, on a random sample of Texas bridges. These objectives are discussed in the following sections. A brief report summarizing the observations of one of the researchers after visiting approximately 80 bridges is presented in Appendix C.

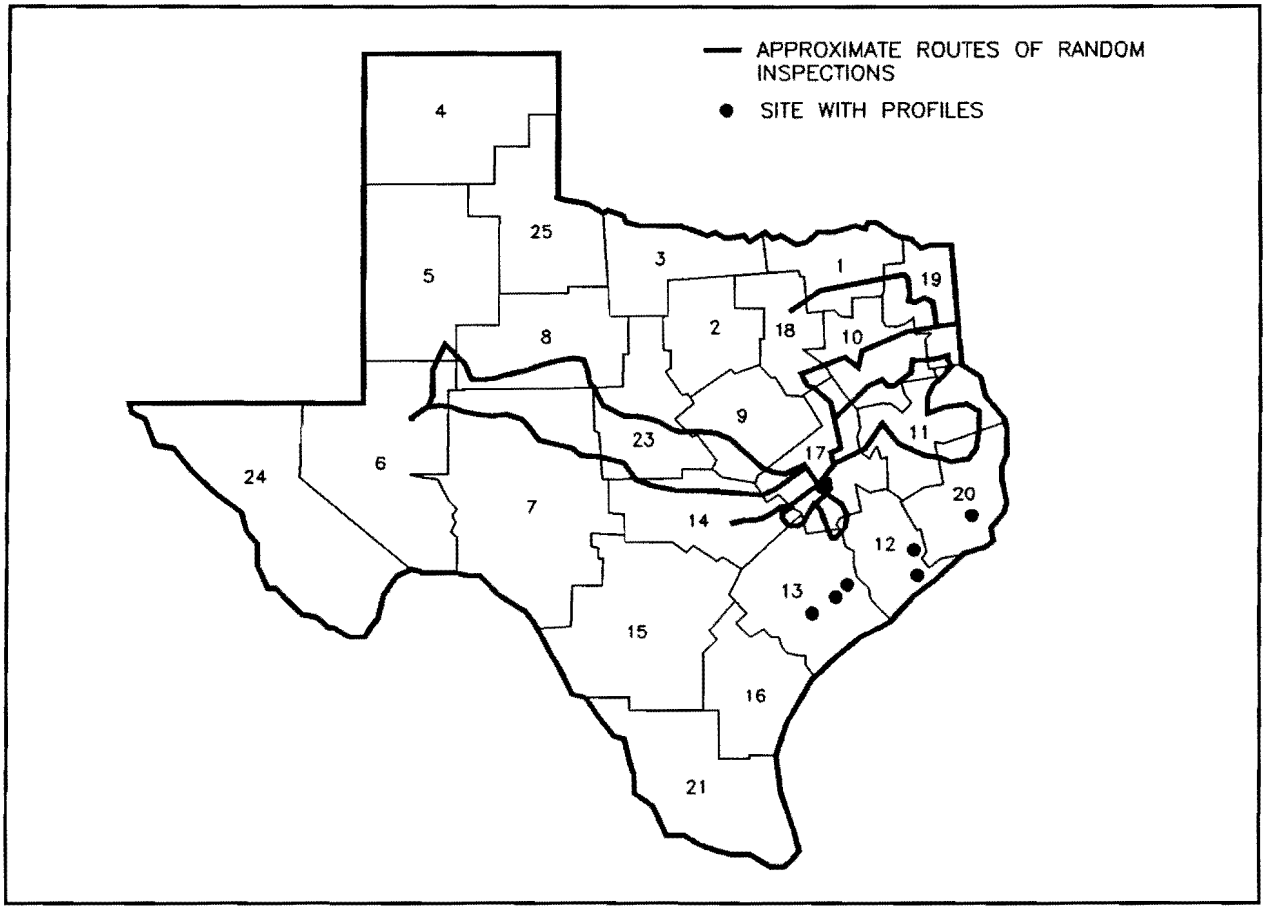

Figure 13.--Routes Travelled During Field Studies of Bridge Approach Roughness at Randomly Selected Sites

Assessment of Significance of Approach Roughness

To assess the severity of bridge approach roughness, the following scale was defined and used by the observers:

Rating	Description
0	No bump noticed
1	Audible perception only
2	Slight bump felt
3	Moderate bump felt
4	Significant jolt felt
5	Bump threatens loss of control

The rating was assigned by the driver of an automobile as the automobile passed over the bridge at approximately 50 mph or the posted speed limit, whichever was lower. Two observers were used, and no calibration of observer standards was accomplished. One observer rated 79 bridges and the other rated 52 bridges. The results of the ratings are presented in Table 6.

Table 6. Average Approach Roughness Ratings

	Observer 1			Observer 2			Totals		
	N	Avg.	σ	N	Avg.	σ	N	Avg.	σ
Flexible pvmts.	73	1.02	0.54	36	1.47	0.74	109	1.16	0.64
Rigid pvmts.	6	1.40	0.64	16	1.50	0.82	22	1.47	0.76
Totals	79	1.04	0.55	52	1.48	0.75	131	1.21	0.67

(N = number rated, Avg. = Average roughness rating, and σ = standard deviation)

From these observations it may be concluded that approaches to bridges in Texas are generally maintained to provide good riding qualities. Observers frequently commented that the roughness at the bridge approach degrades riding quality no more than pavement roughness which is randomly distributed along the roadways. While there are recognized means for measuring and quantifying pavement roughness, there are no recognized standards for severity of discrete "bumps." It may be further concluded that flexible pavement approaches to bridges exhibit less roughness on the average than do rigid pavement approaches, a conclusion that contrasts with the surveyed literature where most researchers categorized rigid pavement approaches as performing better than flexible pavement approaches. The sample size represents only 0.3 percent of the bridge population in the state but was weighted

geographically in favor of the southeast portion of the state, the region expected, because of traffic levels, climatic conditions, and soils, to represent the worst instances of approach roughness.

Description of the Observed Backwall Damage

Figure 14 shows a longitudinal section of a representative highway bridge, approach slab, and abutment, typical of current TxDOT design practice. Most commonly, the approach slab is doweled to the abutment backwall with reinforcing steel. The expansion joint at the end of the girders is usually either an open armored joint or sealed with a prefabricated neoprene joint seal. Expansion of the girders, in the case of short beams, is usually provided for with a polymeric bearing pad. Drilled shafts, typically 30 in. in diameter, are commonly used to support the abutment, with shorter and smaller drilled shafts supporting the wingwalls. This relatively deep drilled shaft foundation design has been used for many years to provide durable, stiff, and stable abutment foundations. Figure 15 shows selected design details for a typical abutment used under a two-lane structure.

Figure 16 through Figure 18 show several examples of observed backwall damage and represent three observed stages of damage development. The various instances of observed damage are usually remarkably similar. The crack pattern shown in Figure 16 from the lower outside corner of the backwall is the initial indication of distress in the backwall. This crack increases in length and becomes displaced, until the entire backwall is broken off at its base along the length of the abutment. In advanced stages considerable spalling occurs, and sometimes embankment fill material is carried out of the displaced fracture.

Correlation of Observed Backwall Damage to Concrete Pavements

Of the 34 sites visited in the initial phase of the field survey, damage to the abutment backwall was observed and noted at nine sites, all at structures adjacent to reinforced concrete pavements. At five other structures adjacent to concrete pavements, no mention was made of observed abutment damage. At eight study sites where the adjacent pavement was noted to be asphalt concrete, no damage was noted at any of the eight sites. The objective of the study was to observe approach roughness, not necessarily abutment damage or type of adjacent pavements. In some early records the type of adjacent pavement or the absence of abutment damage was not noted. Still, the strong apparent correlation of significant abutment damage with the presence of concrete pavements motivated additional study.

Since the initial study set was obtained by requesting examples of maintenance-intensive sites, the bridges and associated damage are probably not representative of the State's bridges. Because of this question, a more detailed and more random sample of 131 bridges was surveyed. The study bridges were selected by inspecting essentially all bridges on a series of randomly chosen circuitous routes on highways of various types, including farm roads, state highways, U.S. highways, and Interstate highways. Of these 131 bridges, all but 22 were adjacent to asphalt concrete pavements (ACP). Of the 109 bridges adjacent to ACP, damage to the abutment backwall was noted in only two instances. In the case of these two bridges, the observed damage was not similar to that damage as illustrated in Figure 16 through Figure 18. The observed damage in one case consisted of cracking and spalling

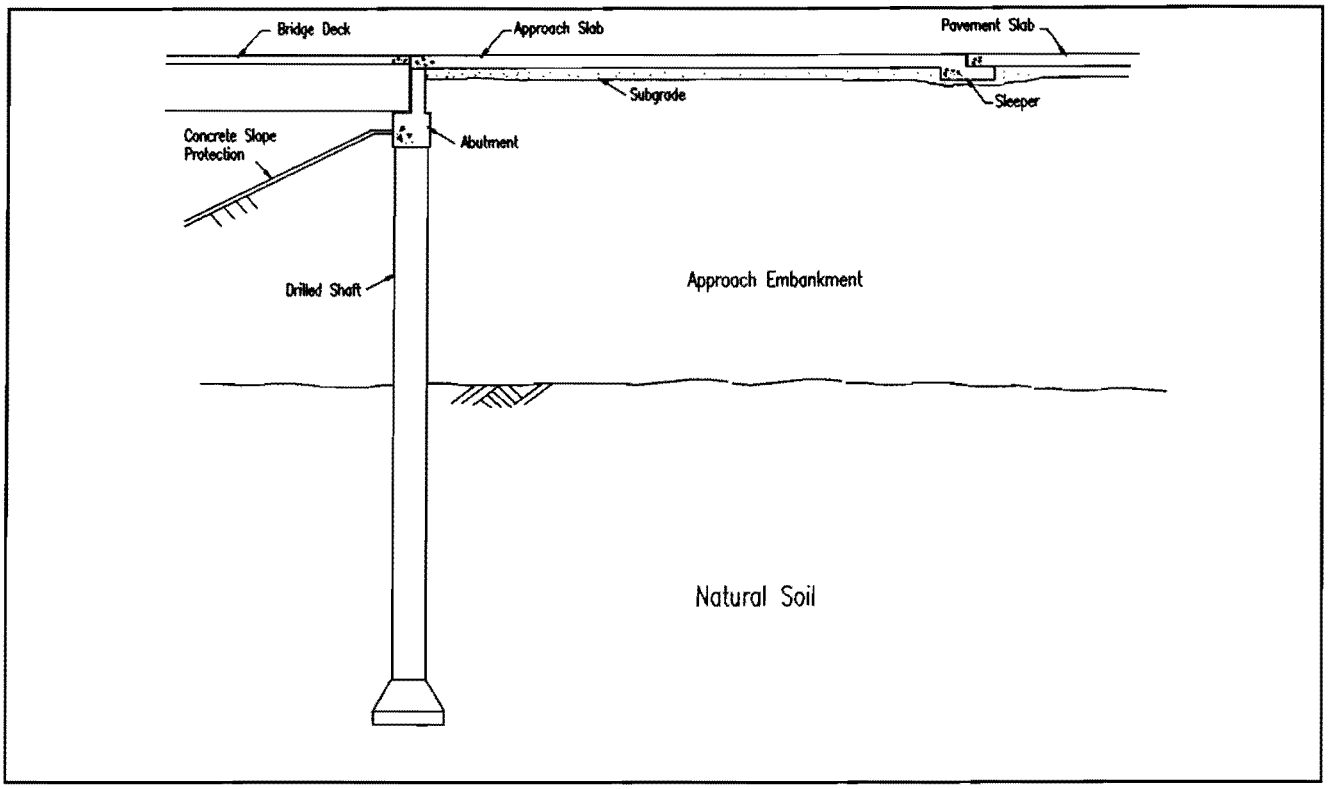

Figure 14.--Longitudinal Section Through a Typical Bridge Approach

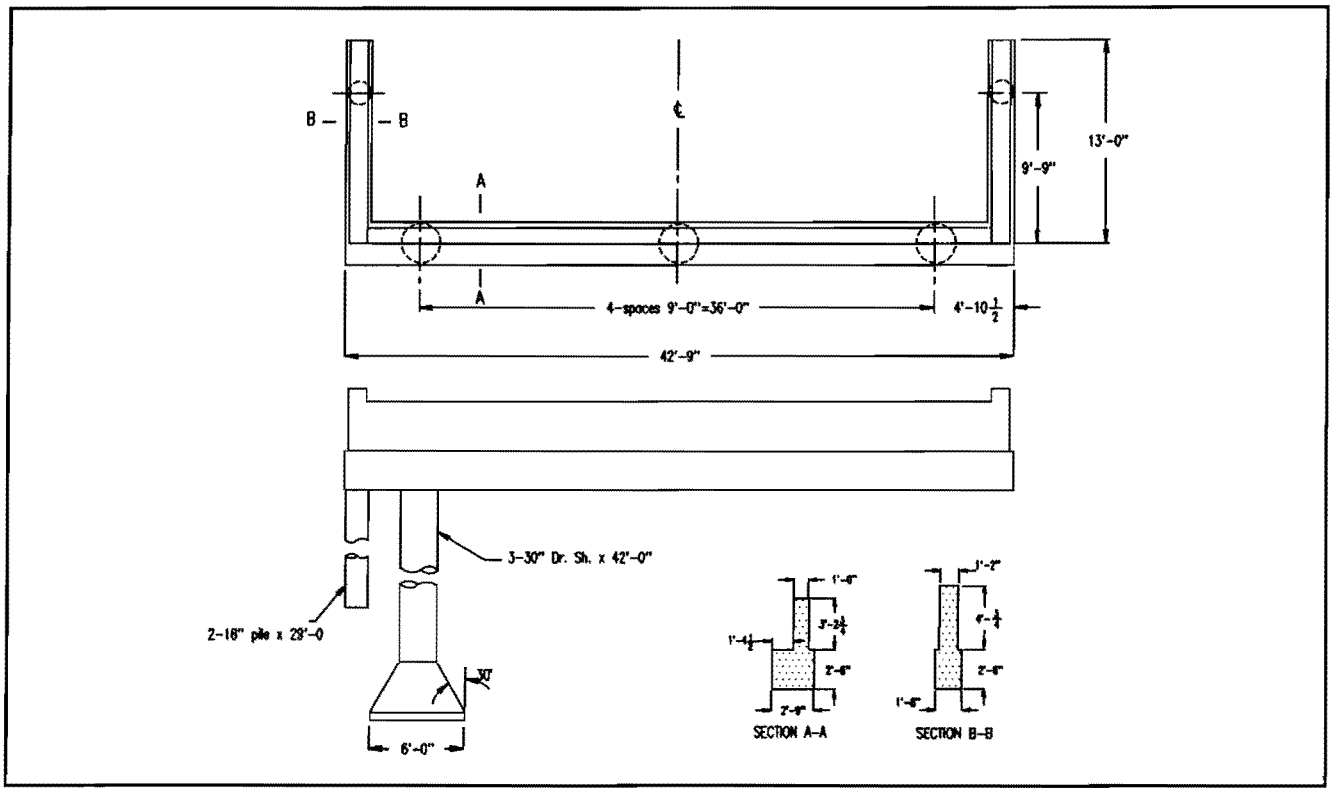

Figure 15.--Design Details for Representative Reinforced Concrete Abutment

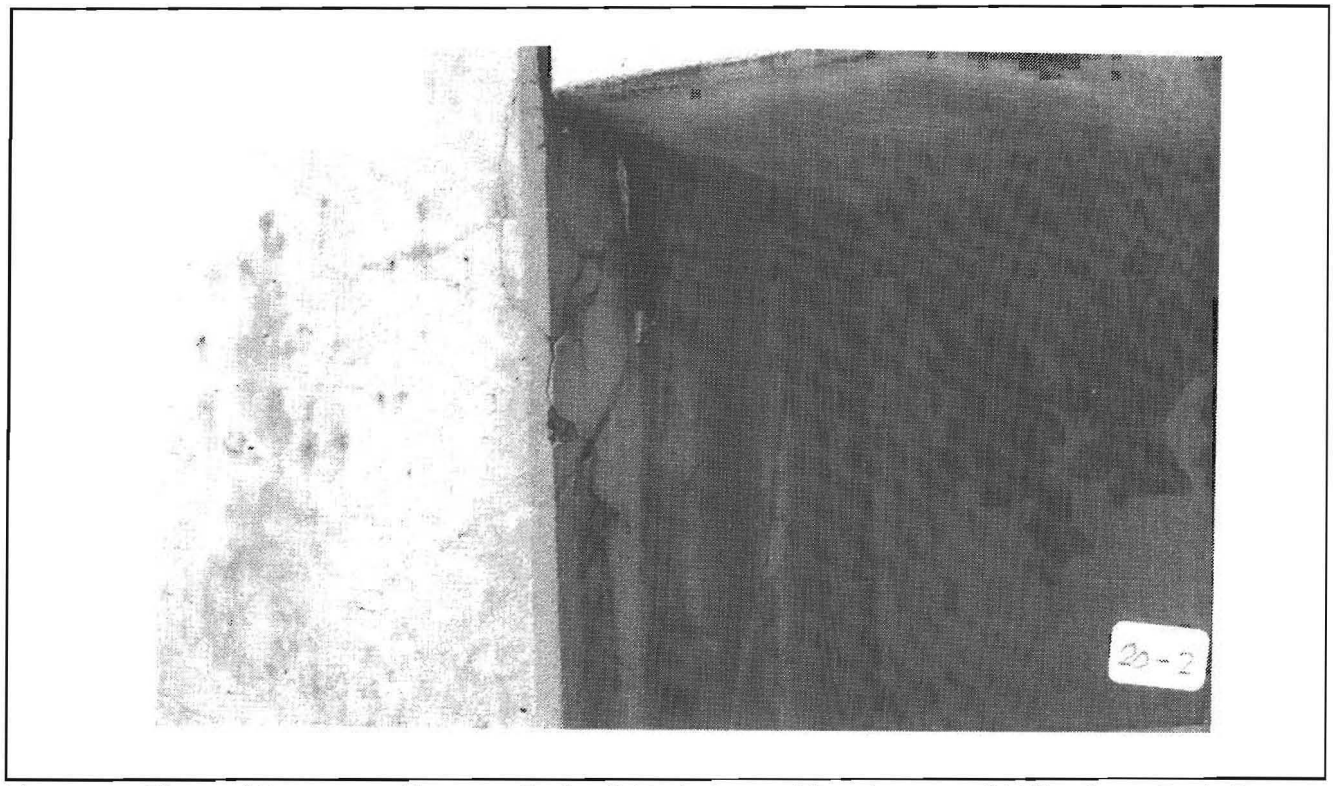

Figure 16.--Observed Damage to Abutment Backwall, Early Stage of Development (US69 at Lucas Dr. in Beaumont)

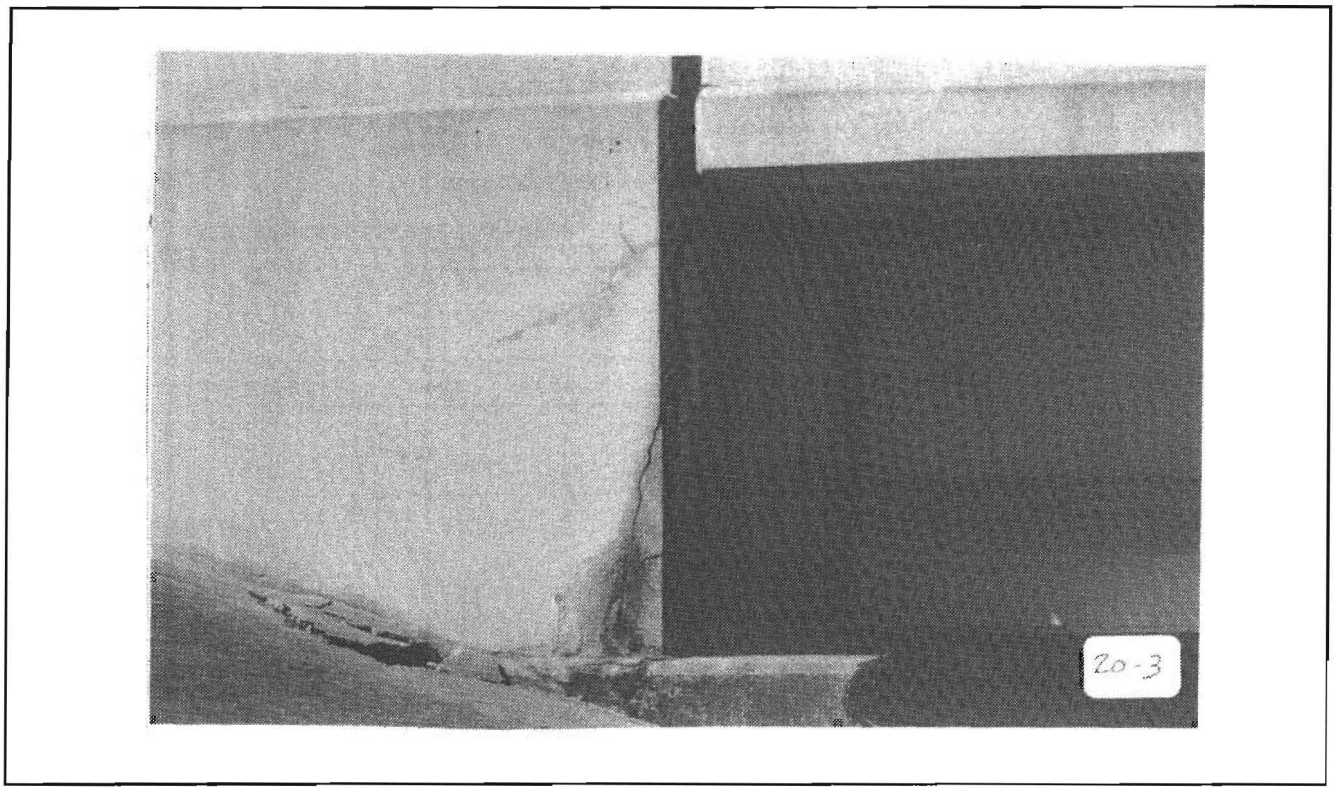

Figure 17.--Observed Abutment Backwall Damage, Intermediate Stage (US69 at Fannet, Beaumont)

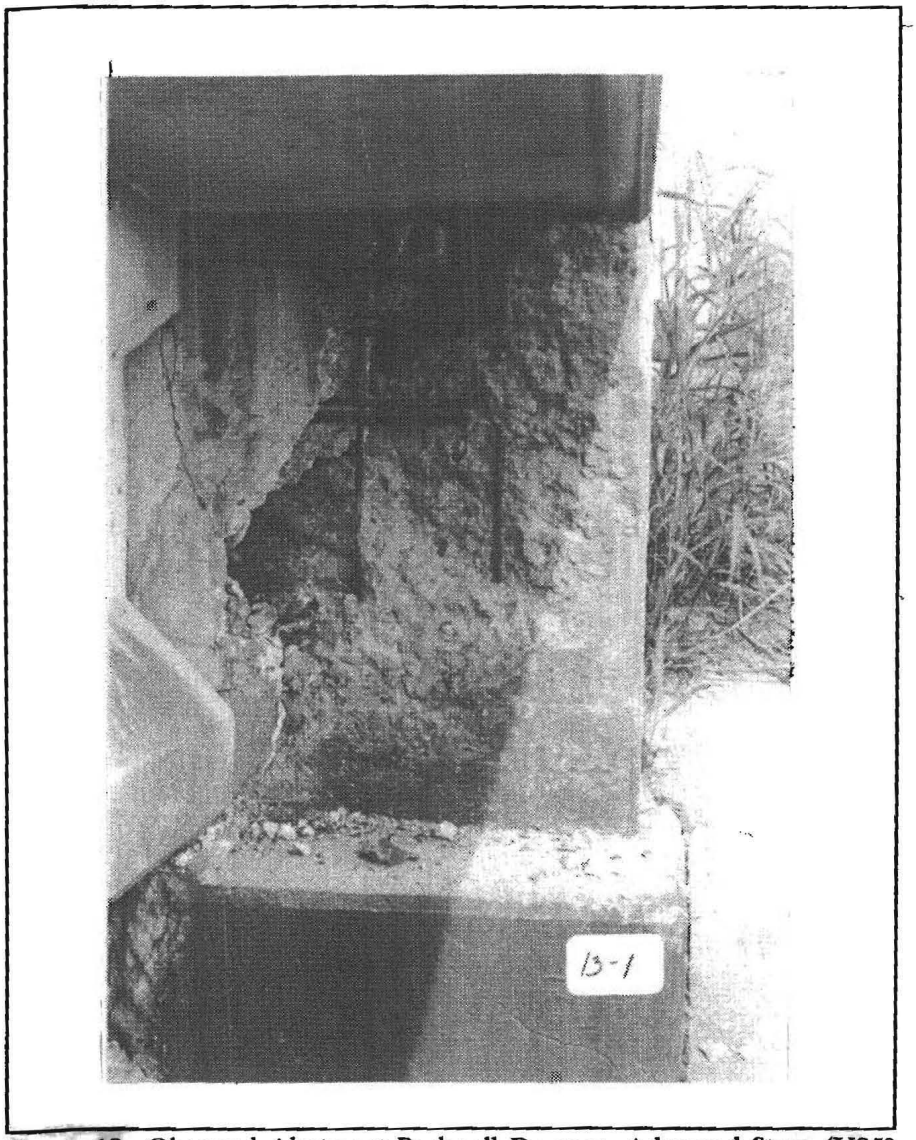

Figure 18.--Observed Abutment Backwall Damage, Advanced Stage (US59 over FM102 in Wharton Co.)

of the top of the wingwall as shown in Figure 19, apparently caused by unintended contact between the wingwall and the bridge deck. On the opposite side of the deck at that abutment, a similar unintended contact pressure has caused cracking and spalling of the edge of the bridge deck. The cause of the bridge or embankment movement resulting in this unintended contact is not known. It may be deduced only that either the embankment is moving toward the bridge carrying the abutment, or the bridge superstructure is moving toward the embankment. Localized pressure by soil or pavement against the top of the backwall is expected to cause backwall damage before the backwall contacts the girder ends. In the second instance of damage to a backwall at a site adjacent to ACP, the observed damage is generally similar to the first, as shown in Figure 20. It is not as clear in this case that the damage is caused by bearing pressure between the wingwall and the deck, as in Figure 19, but a close inspection of the abutment reveals that the damage in this instance is isolated in the wingwall with the backwall undamaged.

Another type of distress in bridge abutments adjacent to ACP was observed in the field study. The observed distress took the form of an apparently displaced approach slab, as shown in Figure 21. The cause of this displacement, however, is the gross rotation of the abutment as evidenced in Figure 22. The embankment at this site is underlain by very soft soils, and the rotation is attributed to differential settlement. Other evidence of differential settlement is also noted at this site. The mechanism causing the observed distress is therefore different from the mechanism observed at the sites adjacent to reinforced concrete pavements. It is noteworthy that no

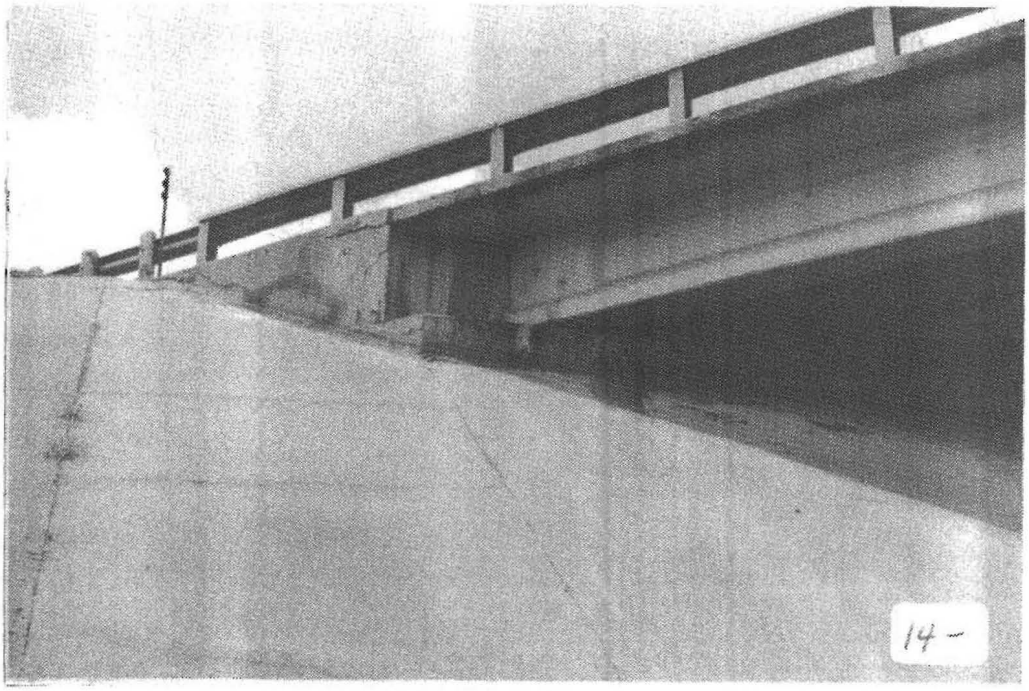

Figure 19.--Isolated Instance of Observed Damage to Abutment Backwall Adjacent to Asphalt Concrete Pavement (SH21W at US77 in Lee Co.)

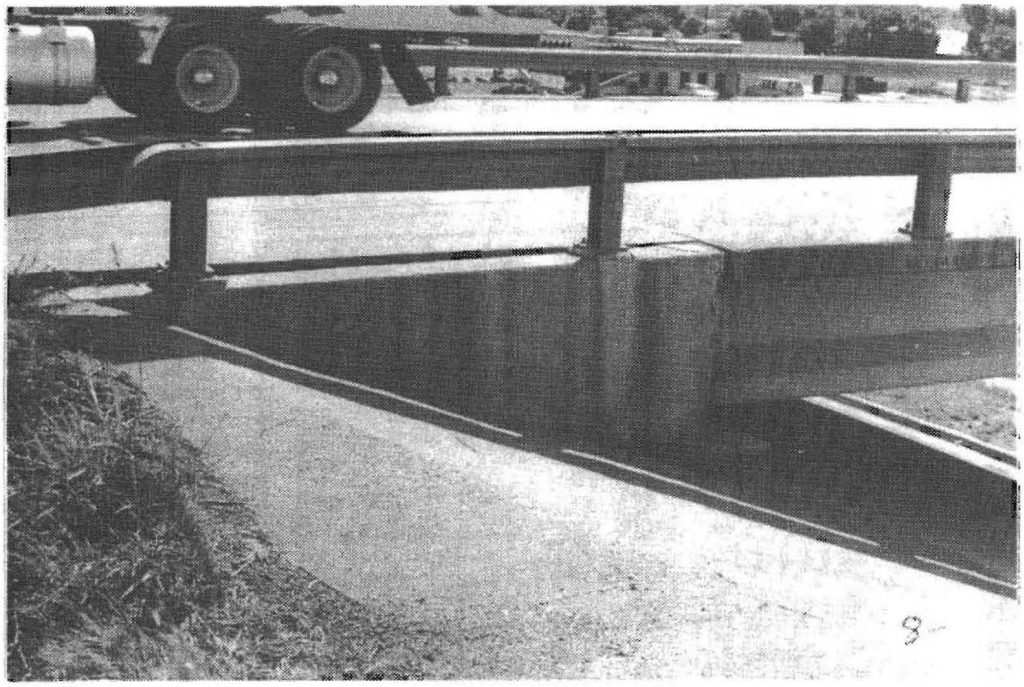

Figure 20.--Observed Damage to Abutment Wingwall at Structure Adjacent to Asphalt Concrete Pavement (US84W at US 83N in Abilene)

damage was sustained by the backwall in this instance, even though the backwall has been displaced approximately 2 in. toward the approach slab. Design drawings for this structure indicate that the approach slab is not dowelled to the abutment backwall as is commonly done in other similar structures. Because of this, the relative displacement of backwall and approach slab is not restrained and does not cause distress.

Of the 22 bridges at sites adjacent to reinforced concrete pavements, three exhibited significant abutment backwall distress, essentially identical to that illustrated in Figure 16 through Figure 18. In summary, significant backwall damage was observed in four of 22 abutments next to rigid pavements, while none of the 112 bridges next to ACP exhibited similar damage.

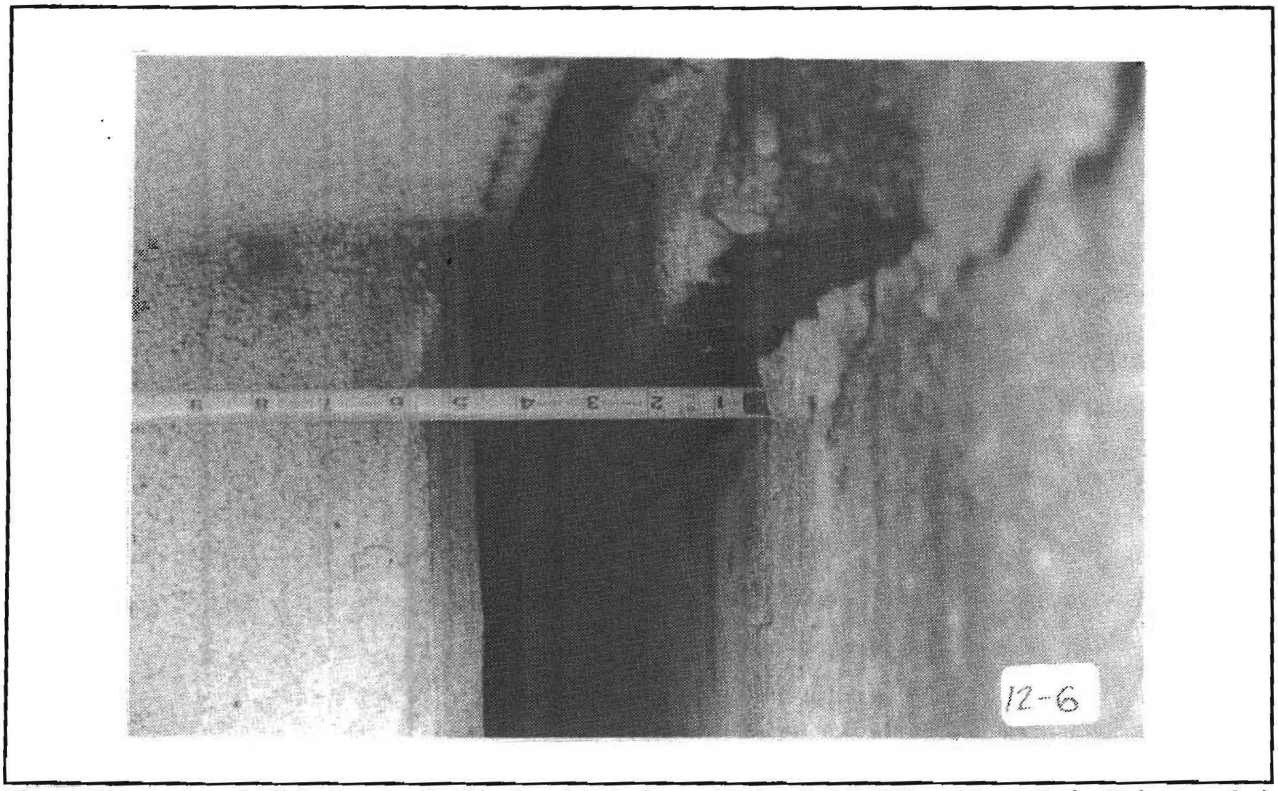

Figure 21.--Approach Slab Apparently Displaced Relative to Backwall (FM270 at Clear Cr. in Galveston Co.)

Other Observations Implicating Pavement Growth

In addition to the broken backwalls, other observations indicate longitudinal growth of the CRCP. At some sites where extensive backwall damage was observed, the shoulders adjacent to the CRCP were paved with a thin layer of hot-mix asphalt concrete. Cracks were observed in the paved shoulder emanating from the edge of the CRCP and propagating out into the paved shoulder at an angle roughly approximating 45 degrees toward the abutment. The points of intersection of these cracks with the edge of the CRCP coincided closely with the known locations of the reinforced concrete pavement lugs which are designed to anchor the pavement to the subgrade, as illustrated in the sketch in Figure 23. The presence of these cracks is evidence that the pavement lugs are being

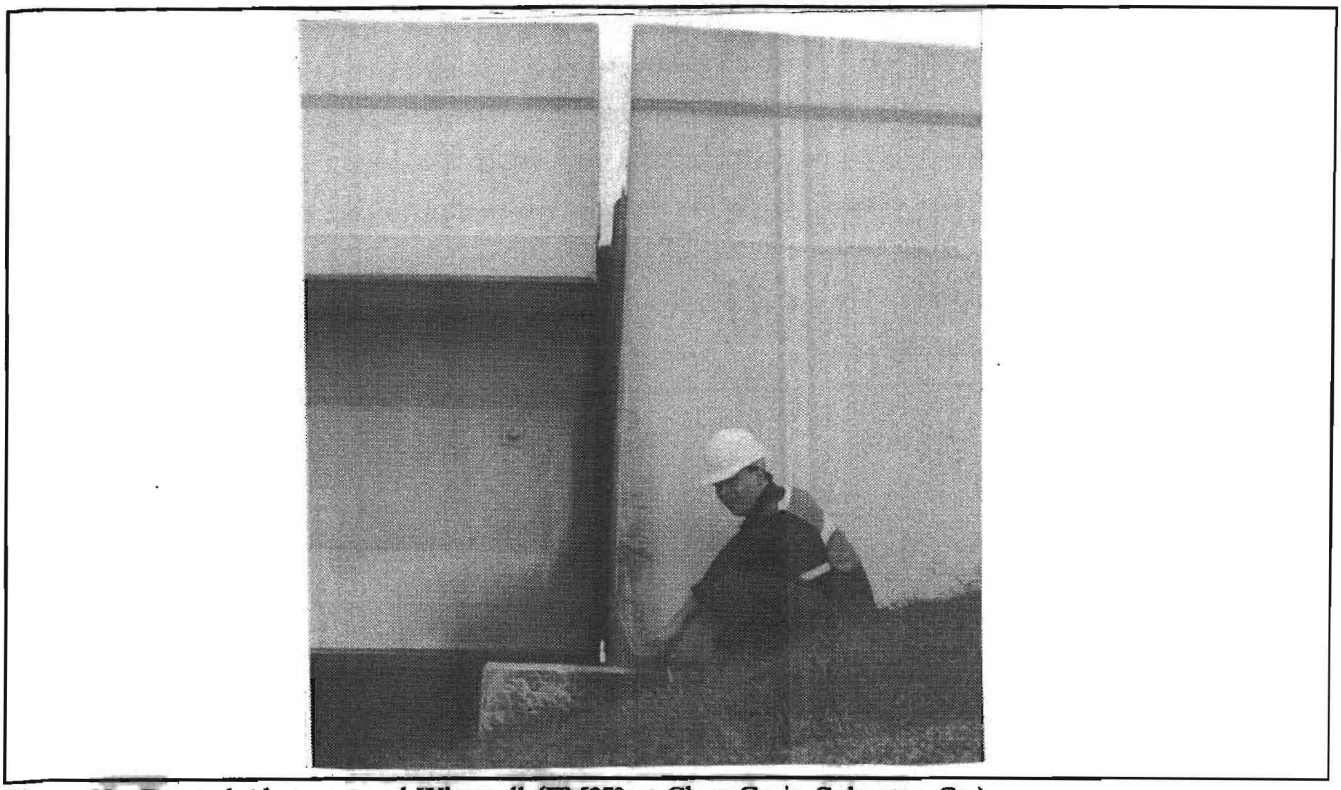

Figure 22.--Rotated Abutment and Wingwall (FM270 at Clear Cr. in Galveston Co.)

pushed through the subgrade causing soil failure planes whose intersections with the surface are manifested by the observed cracks. Excavations in the shoulder at one such site revealed a large open cavity behind the exposed pavement lug which is further evidence that the CRCP is moving toward the abutment in spite of the pavement lugs. These voids may be caused or aggravated by pumping action, as evidence of active pumping action was commonly observed at the pavement edge near the lug locations.

Also, the CRCP exhibits transverse cracks which are more or less randomly spaced except near the approach slab. Near the approach slab, transverse cracks occur only on either side of each pavement lug. These cracks, which precisely locate each of the lugs, are thought to be caused by negative moments above the lugs due to wheel loading and serve to allow expansion and contraction sufficient to prevent other cracks in the vicinity of the lugs.

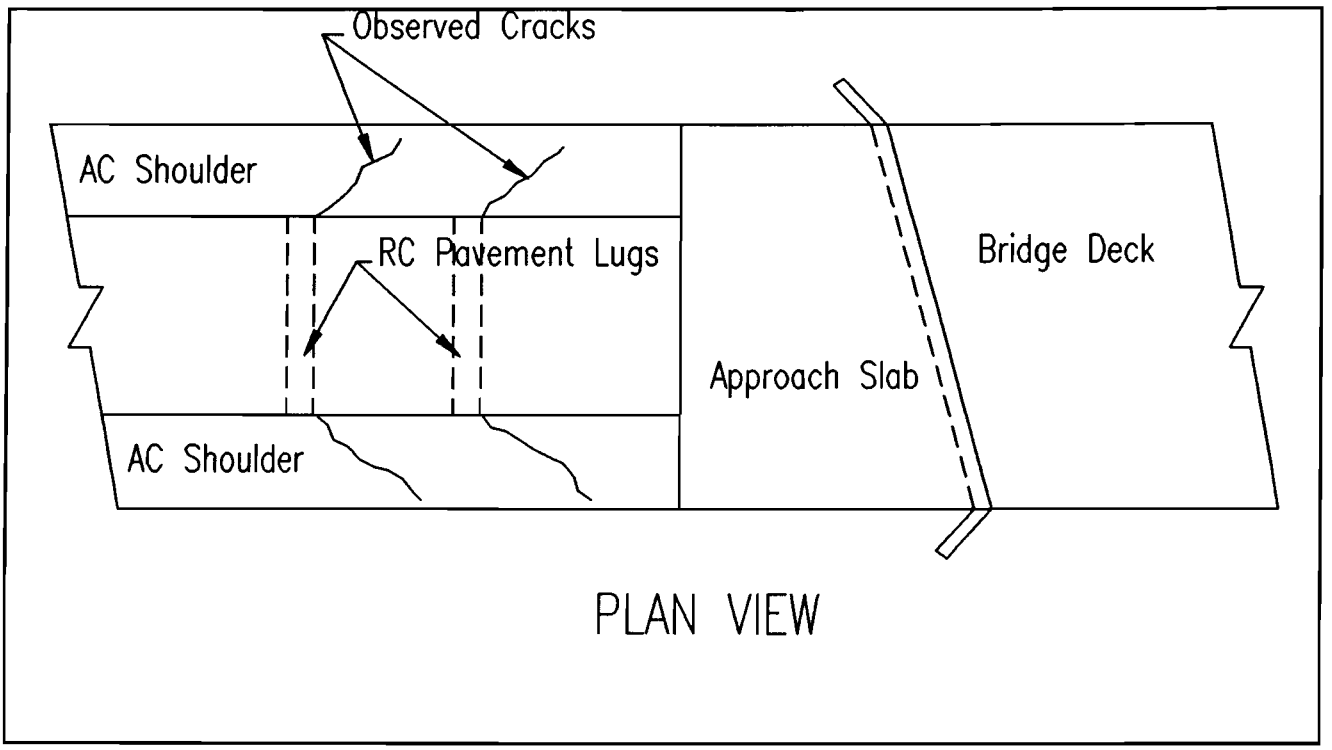

Figure 23.--Drawing of Observed Crack Patterns in ACP Shoulders Adjacent to CRCP (as observed at several locations; see Southbound SH6 at Tabor Rd. in Bryan)

MECHANISMS POTENTIALLY CAUSING LONGITUDINAL PAVEMENT MOTION

At least two mechanisms may be identified as potential causes of the longitudinal motion or growth of the CRCP and the resulting backwall damage. The first of these is a thermal ratcheting mechanism which hypothetically results in a gradual increase in length of the pavement. The second mechanism is a chemical reaction causing dilatational strain in the pavement and a resulting growth in length. This second mechanism presumably results in a monotonic growth, while the first hypothetically results in either an annual cyclic variation in length or a superposition of an annual cyclic variation and a monotonically increasing growth. These two mechanisms are discussed briefly below and in greater detail in a later section of this report and in other reports.

Thermal Ratcheting Mechanism

The thermal ratcheting mechanism proposed to explain the apparent longitudinal growth of CRCP consists of a thermal expansion of the rigid pavement during a summer season, followed during the cooler months by a thermal contraction which is restrained by ground friction on the lower surface of the rigid pavement sufficient to open transverse cracks. These cracks are partially blocked, or propped, with fine soil particles carried from the roadway into the cracks by water. Subsequently, during the next warm season, the pavement again expands and the next cool season results in another ratchet increment of growth. This mechanism is hypothetically unbounded and could certainly cause large enough longitudinal growth to close the joints between the pavement and the approach slab and between the approach slab and the deck. This same mechanism may be at work in rigid pavement blow-ups and in other phenomena indicative of a significant locked-in longitudinal compressive stress in the pavement.

Chemical Reactions in the Concrete Resulting in Dilatational Strains

A second mechanism which could be a factor in the apparent longitudinal growth of concrete pavements is a chemical reaction involving the hydroxyl ions in the pore water within the concrete and certain forms of silica in the aggregate. Such alkali-silica reactions (ASR) resulting in dilatational strains on the order of 0.01 have been reported in the literature (Carrasquillo and Snow 1987, Swamy and Al-Asali 1988b). ASR may result in extensive deterioration in reinforced concrete, due to resulting large strains in the cementatious matrix. Many reported studies of the volume change of portland cement concrete roads are found in the literature. The reported studies deal with both physical events and chemical reactions, some of which result in improvement in performance but many of which result in unacceptable distress.

It is often difficult, if not practically impossible, to separate and quantify the combined effects of length and volume changes in concrete pavements. Generally speaking, it is the increase in length and/or volume of a given concrete pavement and the associated distress that calls attention to the problem. Pavement blow-ups, for example, may be caused by a combination of improper joint maintenance (for jointed pavements) and/or volume changes in

the concrete mass due to, say, alkali-aggregate reactivity. Even continuous reinforced concrete pavements may suffer similar distress with both types of pavements requiring extended periods of time for the distress to become critical. Although blow-ups are common and quite extensive in those parts of the United States subjected to high temperatures and high solar flux, this is not the only distress that takes place. The subject study is concerned with distress that has been widely observed in bridge structures in the specific areas of bents, caps and support piers. Damages of these types may be caused by volume-length changes in the abutting pavement. End anchors for continuously reenforced concrete pavements do not always function as designed or may not be constructed as designed. For jointed pavements, the joints may not be properly maintained.

It is, however, the volume changes in concrete pavements brought about by alkali-aggregate activity that is the subject of this segment of this report. A review of the literature on alkali-aggregate reactivity seems appropriate. Among the noteworthy early researchers of the adverse effects of alkali-aggregate reactivity was Stanton (1941). His conclusions from this early study are:

> "1. Certain mineral constituents in concrete aggregates contribute to expansion of concrete and sometimes develop stresses of such magnitude as to cause failure.
> 2. Some shales expand excessively when saturated with water or when they are alternately wet and dry and, therefore, the percentage of such material should be kept to a minimum. This action, however, appears to be physical and of much less intensity than a chemical reaction with other minerals.
> 3. Excessive expansion, sufficient to rupture a concrete mass, may occur when certain minerals are present. The reaction in this case is chemical, and evidence indicates that it always takes place with the siliceous magnesian lime rocks found in the aggregates from the Upper Miocene sedimentary deposits of the state [California] and frequently in the presence of some of the low-magnesia, low-lime shales and cherts.
> 4. The chemical reaction producing excessive expansion apparently occurs only when the portland cement component contains an appreciable percentage of alkali in the form of sodium and potassium oxides. It is of an intensity proportional to the percentage of such oxides, apparently being of low order as to be negligible when the alkali content is less than 0.6%."

What was not clearly understood some fifty years ago and not completely clear today is the rate at which this distressful expansion may occur. This rate factor was further evaluated by other researchers over the years following Stanton's work. Neville (1981) published a textbook on "Properties of concrete" which included the following statements:

> "The most common reaction is that between the active silica constituents of the aggregate and the alkalis in cement. The reactive forms of silica are opal (amorphous), chalcedony (cryptocrystalline fibrous), and tridymite (crystalline). These reactive materials occur in: opaline or chalcedonic cherts, siliceous limestones, rhyolites and rhylotic tuffs, dacite and dacite tuffs, andesite and andesite tuffs, and phyllites (Goldbeck 1956). The reaction starts with the attack on the siliceous minerals in the aggregate by the alkaline hydroxides derived from the alkalis (Na_2O and K_2O) in the cement. As a result, an alkali-silicate gel is formed, and alteration of the borders of the aggregate takes place. The gel is of the "unlimited swelling" type; it imbibes water with a consequent tendency to increase in volume. Since the gel is confined by the surrounding cement paste, internal pressures result and eventually lead to

expansion, cracking and disruption of the cement paste. Thus expansion appears to be due to hydraulic pressure generated through osmosis, but expansion can also be caused by the swelling pressure of the still solid products of the alkali-silica reaction (Powers and Steinour 1952). For this reason it is believed that it is the swelling of the hard aggregate particles that is most harmful to concrete. Some of the relatively soft gel is later leached out by water and deposited in the cracks already formed by the swelling of the aggregate."

According to Neville, it is not generally possible to estimate the deleterious effects of the reaction from the properties and quantities of the reactive materials. In fact, he stated,

"In exceptional cases, however, cements with an even lower alkali content have been known to cause expansion. Within limits, the expansion of concrete made with a given reactive aggregate is greater the higher the alkali content of the cement and, for a given composition of cement, the greater its fineness."

Figure 24 shows the relation between expansion of a mortar bar and the reactive silica content for a given alkali content. Surface area effects are apparent. Mindess and Young (1981) present a table listing reactive aggregates, which is reproduced here as Table 7. One of the chemical reactions which may lead to expansion according to Mindess and Young is given in Equation (8). Their explanation of the probable effects on the volume of concrete follows:

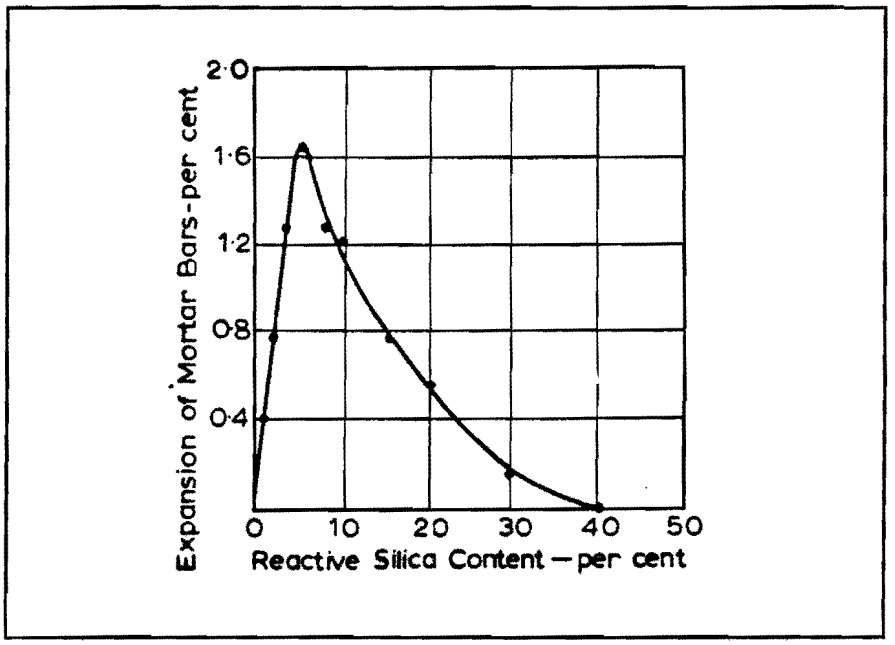

Figure 24.--Relation between expansion after 224 days and reactive silica content in the aggregate (Neville 1981, after Vivian 1950)

"Equation (8) does not involve extensive dissolution and is not expansive in itself, but it destroys the integrity of the aggregate particle. The reaction does not necessarily take place from the

$$\underset{\text{aggregate}}{S} + \underset{\text{pore fluid}}{N(K)H} \rightarrow \underset{\text{alkali-silica gel}}{N(K)-S-H} \quad * \qquad (8)$$

*Notation in this equation is symbolic, not chemical formulas.

outside inward, but may proceed throughout the reactive silica particle, depending on its structure. However, the gel has the ability to imbibe considerable amounts of water, which is accompanied by a volume expansion. If this expansion is sufficient, the resulting stress will crack the weakened aggregate and the surrounding cement paste. The final step takes place after the critical expansion has occurred, when further ingestion of water turns the solid gel into a fluid sol which escapes into the surrounding cracks and voids. Secondary reactions with calcium hydroxide in the cement paste may also take place, forming deposits of a calcium-alkali-silica gel at the periphery of the distressed aggregate."

They further state:

"This description of the alkali-aggregate reaction visualizes the localized centers of expansion at the sites of the particles of reactive silica. If the number of reactive particles is relatively small, the soluble alkali metal ions can migrate to these scattered centers to form the alkali-silicate gel and cause high, localized expansions that disrupt the matrix. If there are a large number of reactive particles, there are not enough alkali metal ions to cause complete reaction of all particles and therefore expansions are reduced. This explains the occurrence of a 'pessimum percentage,'... Small particle size encourages a rapid reaction without deleterious effects."

Table 7. Forms of Reactive Silica in Rocks that can Participate in the Alkali-Aggregate Reaction (Mindess and Young 1981)

Reactive Component	*Physical Form*	*Rock Types in Which It Is Found*	*Occurrence*
Opal	Amorphous	Siliceous (opaline) limestone, cherts, shales, flints	Widespread
Silica glass	Amorphous	Volcanic glasses (rhyolite, andesite dacite) and tuffs; synthetic glasses	Regions of volcanic origin; river gravels originating in volcanic areas; container glass
Chalcedony	Poorly crystallized quartz	Siliceous limestones and sandstones, cherts and flints	Widespread
Tridymite, cristobalite	Crystalline	Opaline rocks, fired ceramics	Uncommon
Quartz	Crystalline	Quartzite, sands, sandstones, many igneous and metamorphic rocks (e.g., granites and schists)	Common, but reactive only if microcrystalline or highly strained

Also from Mindess and Young in Table 8 is shown the effect of pH on the hydrolysis of amorphous silica in a cement paste. Note the solubility of SiO_2 in high alkali cement paste. The authors suggest approaches that may be used to control the alkali-aggregate reaction. These include (a) control of pH, (b) control of alkali concentrations, (c) control of amount of reactive silica, (d) control of moisture, and (e) alteration of alkali-silica gel.

Table 8. Effect of pH on the Hydrolysis of Amorphous Silica in a Cement Paste (Mindess and Young 1981)

Medium	*pH*	*Approximate Solubility of SiO_2 (ppm)*
Neutral water	7-8	100-150
Moderately alkaline water	10	<500
Saturated $Ca(OH)_2$	12	90,000
Low-alkali cement paste	~12.5	~500,000
High-alkali cement paste	>13.0	Infinite

Specific recommendations are made by Farbiarz and Carrasquillo (1986) in their study of the effect of fly ash additives on the reduction of damage due to alkali-aggregate reaction in concrete. In a later report (1989) the same authors concluded, as many researchers before them have, that the alkali content of the cement is the main variable affecting the reaction and, further, that replacement of part of such high alkali cements with fly ash reduces the expansion of the subject concrete, provided, of course, that the fly ash has a low alkali content.

Schumann, Carrasquillo and Farbiarz (1988) presented a state-of-the-art report on the mechanism of alkali-aggregate reaction in concrete containing fly ash. These authors point out that the chemistry and mechanisms of the chemical reactions taking place in the alkali-aggregate reactions are not, as yet, very well known. Prevention of the ill effects of the reactions has been studied world-wide, and methods and materials are suggested to minimize distress due to expansion.

Swami and Al-Asali (1988a) note that the engineering properties of concrete subject to alkali-aggregate reaction also affected the properties of compression and tensile strength, elastic modulus and pulse velocity. Their study also indicated that critical expansion limits due to this reaction would vary depending on the type and use of the structure.

These same authors (1988b) reported on the effects of alkali aggregate reactivity on concrete, whereas most previous researchers utilized mortar for their studies. The concrete under study used fly ash to replace part

of the Portland cement. The results of the study showed that the fly ash serves a dual role, controlling deformation and reducing strength loss.

Kerr (1991) reports a study of pavement blowups and the relation to thermally induced pavement growth. The study includes empirical and analytical formulations of the pavement lift-off buckling problem, including the effects of the dead weight of the pavement. The criterion of the "safe temperature increase" is presented and discussed.

In the present study, a very limited investigation was made to determine whether or not alkali-aggregate reactivity might be a contributing cause to observed roughness at the pavement/approach slab interface. Field cores were taken at the sites, one near Bryan and one near Victoria. These were analyzed for evidence of alkali-aggregate reactivity. The full report on these test results are included as Appendix D. It is evident from this report that chemical reactions may very well account for a portion of the volume (length) change in these pavements, and possibly this distress is felt at the juncture of the bridge and the pavement or the approach slab.

These particular sample sites were chosen because (a) reactive aggregates are known to exist in the deposits from which the coarse and fine aggregate were taken and (b) high-alkali cements were likely used in concrete pavements built in these areas some 15 to 25 years ago. Although hard data were not found on the long-term effects of a very slow rate of volume change in concrete (brought about by alkali-aggregate reactivity), it appears evident that such chemical reactions continue for decades. When volume changes of this type are added to pure length increases by joint and crack infiltration, it is not surprising to find distress at bridge approaches and, indeed, distress of the bridge elements.

It will not be easy or inexpensive to correct the faults built into the pavements that are contributing to the subject problem; however, future work in this area should be planned as to eliminate improper materials selection, the mix design faults and construction control aspects that are known to contribute to the problem. Where justified, pavement joint maintenance can be upgraded to relieve stresses due to joint infiltration. This alone may be sufficient to minimize or eliminate the observed bridge abutment problem, at least to a tolerable level.

While evidence of such degradation is not found in the pavements surveyed in the present study, the magnitude of the dilatational strains required to account for the observed growth is very small compared with the strains which are associated with severe deterioration. As a result, a mild reaction could cause the observed longitudinal growth without significant concrete degradation. Tests to determine the role played by alkali-aggregate reactions indicate that extensive alkali-silica reactions are not occurring, but some limited reactions are indicated by observed reaction products in accelerated testing. In short, the reactions which may be occurring are not sufficient to cause distress to the pavement but cannot be ruled out as a cause of longitudinal strains of the magnitude necessary to cause the observed distress to the adjacent abutment backwalls. Unlike the thermal ratcheting mechanism, the ASR mechanism will result in a bounded increase in strain and, therefore, limited pavement growth occurring over a limited time. The time duration and resulting magnitude of strain

depends on the details of the concrete chemistry and on the environmental conditions, particularly temperature. It is not possible to determine exactly the significance of ASR in the cases studied here. More details may be found in the letter report provided by the concrete petrographer which is provided in Appendix D.

Growth of Concrete Pavements--Background

It is common knowledge that temperature is an important factor which influences the structural response of continuously reinforced concrete (CRC) pavement. However, most of the previous research relating to the structural response of CRC pavement has been focused on the effect of temperature drop with respect to the development of the cracking pattern in CRC pavement. The present understanding of the response of CRC pavement to temperature increases is much less developed, and this problem has recently become an area of concern in the state of Texas. The present research addresses this aspect of pavement response.

Increasing and decreasing temperature will cause different structural behavior in CRC pavement. When the thermally induced tensile strain of the concrete slab due to temperature drop in addition to strain from drying shrinkage (in the presence of restraint) exceeds the strain associated with the concrete tensile strength, a crack is assumed to form in the concrete. Any further contraction will primarily lead to widening of the cracks and associated stress increase in the reinforcing steel. On the other hand, when temperature increases, concrete will expand and the crack widths, if unobstructed, will become narrower with a corresponding change in concrete and steel stress. Field observations, as discussed later, have suggested that a theory describing horizontal, longitudinal expansion of the CRC pavement due to an increase in temperature may be appropriate towards explaining a portion of the movement which has resulted in the rupture of adjacent bridge abutments and backwall failure. This section will provide a theoretical model developed at the Texas Transportation Institute (TTI) to evaluate the structural response of the CRC pavement due to a temperature increase under the restraint of the terminal lug system.

Temperature drop effects on CRC pavement behavior have been previously discussed and numerically modeled. Present models (Chiang et al. 1975, Ma et al. 1988, Vetter 1933) assume a uniform bond stress distribution between the concrete and the steel reinforcing with an average stress acting over the development length. Recently, the TTICRCP model (Palmer et al. 1988) improved upon this aspect by using a bond stress-slip function as verified by experimental results. However, the only model which may be directly applicable for the prediction of the structural response of CRC pavement under a temperature increase is PSCP-2 developed at the Center for Transportation Research at the University of Texas. This model is useful for the evaluation of the performance of prestressed concrete pavement.

Several bridge sites were considered during the field survey portion of this study. The field survey was broken into two phases consisting of an initial phase and a subsequent phase. The initial phase included 34 bridge sites located within the area bordered by Bryan-College Station, Victoria, and Houston (southeastern Texas), where nine of the bridge sites were adjacent to CRC pavement. Abutment backwall damage due to

excessive pavement growth was noted on 9 of the 14 bridge sites adjoining CRC pavement. As an added note, all of these pavements were determined preliminarily to contain river gravel aggregates as the coarse aggregate type.

Other bridge sites (some adjoining jointed concrete pavement) which were observed did not show backwall damage to the abutment; one site in particular used limestone as the coarse aggregate in the CRC pavement. No backwall damage was noted at eight bridge sites where the adjoining pavement type was noted to be asphalt concrete pavement (ACP). Preliminary information has indicated some conclusive evidence with respect to pavement performance in terms of coarse aggregate type. The authors recognize that further study is required to verify the preliminary findings and that final conclusions are unwarranted at this point in time with respect to the performance of certain aggregate types.

These observations were made as a part of the effort to study bridge approach roughness and the factors which may contribute to the development of approach roughness. Earlier studies of approach roughness did not directly address abutment damage or the type of adjoining pavement; therefore, information of this nature has not been noted. Nonetheless, an apparent strong correlation may exist between the pavement type, coarse aggregate type, and jointing method to the frequency of abutment backwall damage and has motivated additional study.

Since the initial study examined maintenance-intensive bridge sites, the bridges and associated damage are probably not representative of the typical performance of highway bridges in Texas. Consequently, a subsequent field survey was conducted based on a random sampling of bridge sites which included, at the time of this report, 73 different bridges. These bridge sites were selected from the inspection of most of the bridges on a series of randomly chosen circuitous routes on highways of various types such as farm roads, state highways, U.S. highways, and Interstate highways. All but six of the 73 bridges are on routes constructed of AC pavements. Minor damage to the abutment backwall was noted on only two of the 67 sites where the bridges were adjacent to ACP.

In the case of these two bridges, the abutment damage was determined to be unrelated to pavement growth symptoms. The observed cracking damage is manifested in the form of spalling at the top of the wingwall, caused by unintended contact between the wingwall and the bridge deck. The contact is thought to have been caused by the embankment moving toward the bridge, carrying the abutment. The cause of this movement is unknown. Localized pressure by embankment soil or the concrete pavement against the top of the backwall can be expected to cause backwall damage well before the backwall makes contact with the ends of the bridge girders. Because of the lack of restraint originally provided by the abutment backwall, the amount of pavement movement due to longitudinal thermal expansion is difficult to evaluate from field measurements. Once restraint against longitudinal movement is relaxed, a thermally induced ratcheting mechanism may tend to promote continued pavement expansion that otherwise would not occur. Further restraint is not provided until the backwall has made contact with the ends of the bridge girders.

Another example of distress in a bridge abutment adjacent to ACP was observed in the initial field study which was apparently unrelated to pavement type. The observed distress took the form of a displaced approach slab. The cause of the displacement appeared to be the gross rotation of the abutment. The embankment at the particular site was underlain by very soft soils, and the rotation is attributed to differential settlement. Other evidence of differential settlement was also noted at the site. The mechanism causing the observed distress is therefore different from the mechanism observed at the sites adjacent to CRC pavements. It is noteworthy that no damage was sustained by the backwall in this instance, even though the backwall has been displaced approximately 2 inches toward the approach slab. Design drawings for the structure indicate that the approach slab is not dowelled to the abutment backwall, as is commonly done in other similar structures. Because of this, the relative displacement of backwall and approach slab is not restrained and did not cause distress.

The six bridges at sites adjacent to reinforced concrete pavements were all on the same section of highway, and of these six, three exhibited significant abutment backwall distress. In summary, three of the six abutments next to CRC pavements were damaged, while none of the 67 bridges next to ACP exhibited similar damage.

In addition to the broken backwalls, other observations indicate longitudinal growth of the CRC pavement. At most CRC pavement sites where extensive backwall damage was observed, the bituminous shoulders were adjacent to the pavement. Cracks were observed in the paved shoulders emanating from the edge of the CRC pavement and propagating out into the paved shoulder at an angle roughly approximating 45 degrees toward the abutment. The points of intersection of these cracks with the edge of the CRC pavement coincided closely with the known locations of the reinforced concrete pavement lugs which are designed to anchor the pavement to the subgrade. The presence of these cracks is evidence that the pavement lugs are being pushed through the subgrade causing soil failure planes whose intersections with the surface are manifested by the observed cracks. Excavations in the shoulder at one such site revealed a large open cavity behind the exposed pavement lug--further evidence that the CRC pavement is moving toward the abutment in spite of the pavement lugs.

Exceptions to the typical cracking pattern exhibited by CRC pavement (transverse cracks which are more or less randomly spaced) were noted near the approach slab at the locations of the lugs. The transverse cracks occurred only on either side of the pavement lugs. These cracks, which precisely locate each of the lugs, are thought to be caused by negative moments above the lugs due to the pavement shoving, lug rotation action resulting from the thermal expansion, and live loading.

The fact that the observed damage correlates closely with the presence of adjacent CRC pavement has led to a preliminary conclusion that longitudinal growth or thermal expansion has caused damage to adjacent bridge abutments. Consequently the problem of a thermally induced, ratcheting growth mechanism occurring in the pavement was investigated.

Development of a Model of CRC Pavement Growth

Analysis of CRC pavement response under an expansive strain can be mathematically modeled depending on certain assumptions made prior to formulation of the mathematical model. These assumptions are as follows:

1. The concrete and the reinforcing steel behave in a linearly elastic manner;
2. The base material beneath the concrete slab is rigid and does not deflect under action of the horizontal friction forces;
3. All materials are homogenous (cracks are closed or filled with debris);
4. All expansion is uniformly distributed throughout the depth and the width of the CRC pavement;
5. All behavior in the slab is symmetrical about the midpoint of the slab; and
6. Since an analysis of the effects of shrinkage, and creep is beyond the scope of this study, these factors are not addressed. Instead, the movement of the pavement end resulting from a net dilatational strain is considered. This net dilatational strain is actually the superposition of the effects of shrinkage and creep as well as alkali-silica reaction, and is referred to for simplicity below as the strain due to ASR.

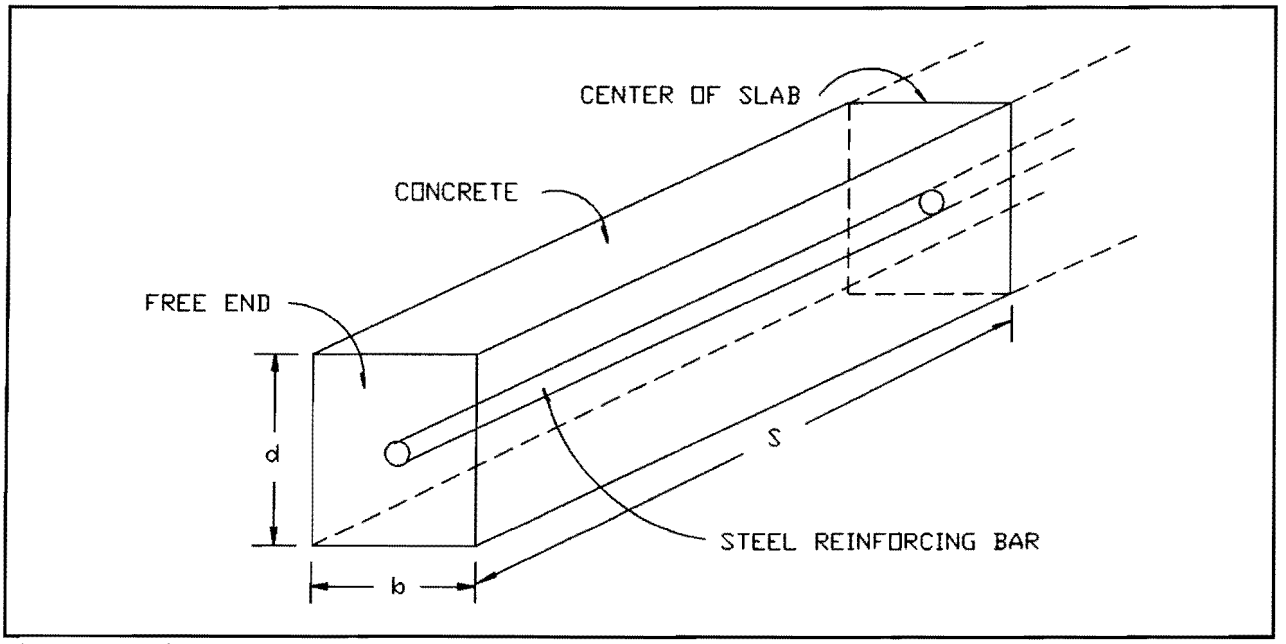

Figure 25.--Prism Used to Model the CRCP Slab.

The uniformity of the expansive strain across the depth and the width of the slab allows the mathematical model to be considered a one-dimensional, uniaxial problem, since variations in stress and strain will occur only along the length of the slab. Figure 25 shows a prism used in the model with a length equal to one-half of the length of the slab. It has thickness d, and a width b corresponding to the spacing of the steel reinforcement. There is also a cylindrical steel reinforcing bar running through the length of the slab.

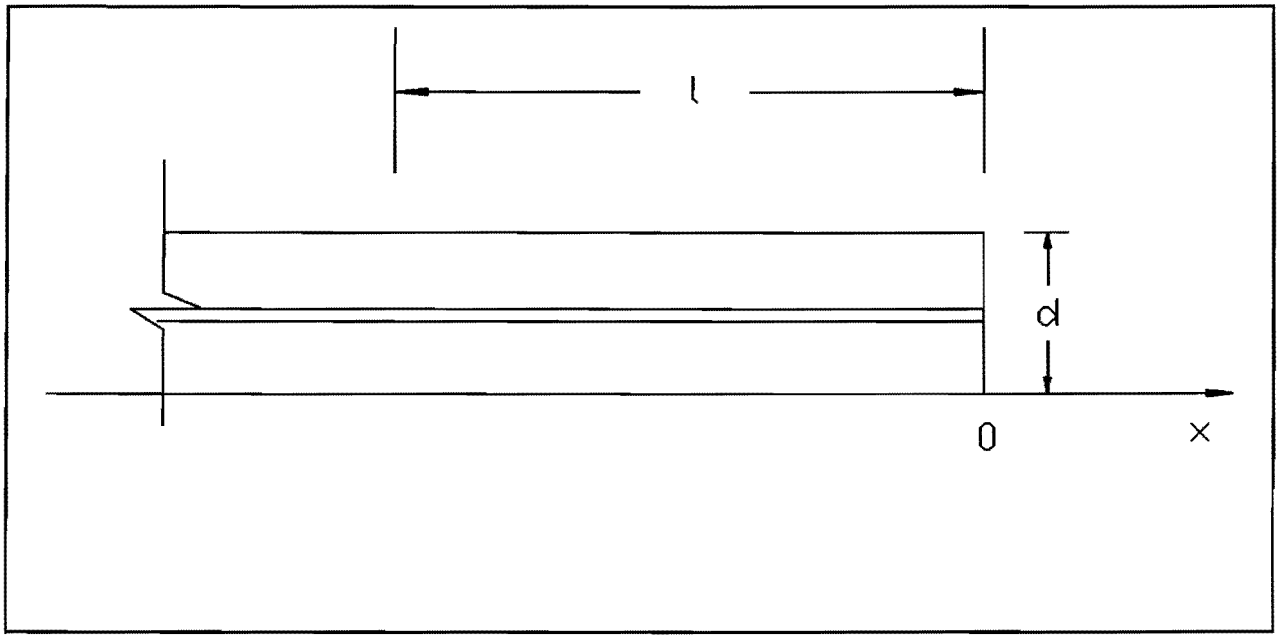

Figure 26.--Coordinate System Used in the Model.

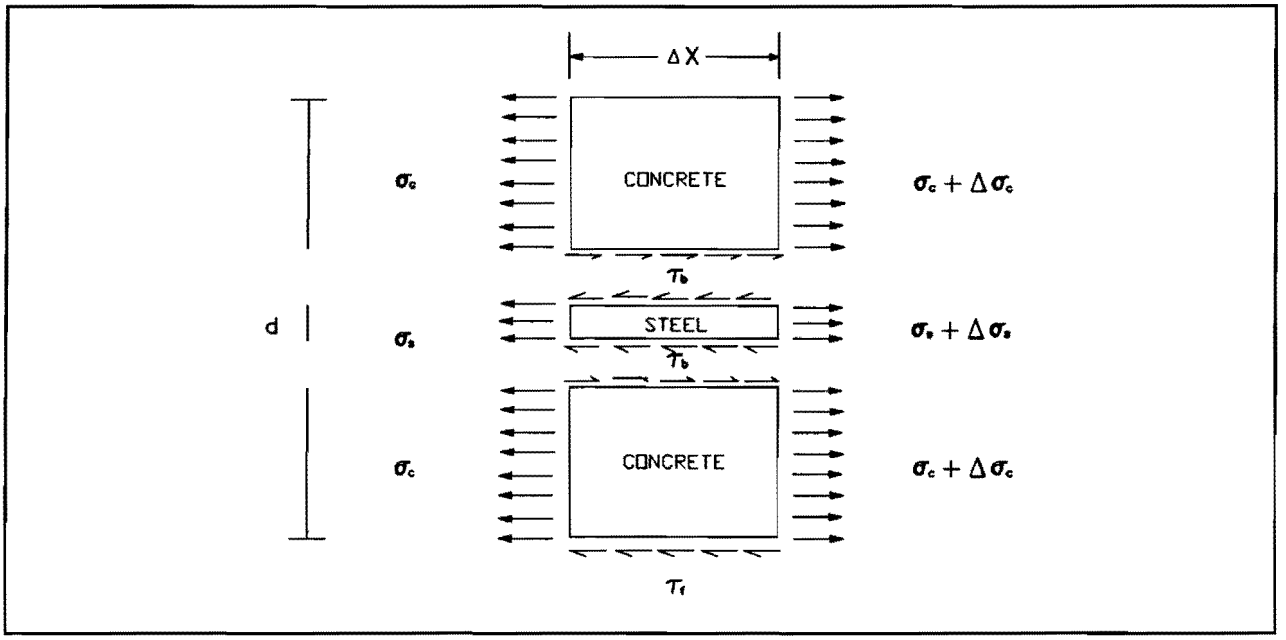

Figure 27.--Stresses Acting on an Elemental Slice of the Prism.

Before derivation of the governing equations for the model, a rectangular coordinate system is assumed as follows: The origin is at the free end of the concrete slab. The x-coordinate with the direction to the right is considered positive as is shown in Figure 26. Friction stress acting to the left is positive and bond stress acting to the left with respect to the steel is positive as Figure 27 shows.

As Figure 27 indicates, a change in the magnitude of both the concrete stress, σ_c, and the steel stress, σ_s, occurs across the width of the slice, which equals $\Delta\sigma_c$ and $\Delta\sigma_s$, respectively. A bond stress, τ_b, is present between the steel reinforcing and the concrete, and a friction stress, τ_f, is present between the concrete and the base material. The model assumes that the prism undergoes a quasistatic change in its environmental and internal system. Mathematically, the summation of forces acting upon the prism must equal zero for the prism to be at rest.

That is:

$$\sum F=(\sigma_c+\Delta\sigma_c)A_c-\sigma_c A_c+\pi d_s\tau_b\Delta x-b\tau_f\Delta x=0 \tag{9}$$

This equation can be simplified to:

$$\frac{\Delta\sigma_c}{\Delta x}+[\frac{\pi d_s}{A_c}]\tau_b-[\frac{b}{A_c}]\tau_f=0 \tag{10}$$

The same type of development is applied to the steel by setting the summation of forces equal to zero:

$$(\sigma_s+\Delta\sigma_s)A_s-\sigma_s A_s-\pi d_s\tau_b\Delta x=0 \tag{11}$$

which is simplified to:

$$\frac{\Delta\sigma_s}{\Delta x}-[\frac{\pi d_s}{A_s}]\tau_b=0 \tag{12}$$

The strain in the concrete, ϵ_c, is defined as:

$$\epsilon_c=\frac{du_c}{dx} \tag{13}$$

The stress in the concrete, σ_c, is equal to:

$$\sigma_c=E_c(\epsilon_c-\alpha_c\Delta T) \tag{14}$$

or:

$$\sigma_c = E_c\left(\frac{du_c}{dx} - \alpha_c \Delta T\right) \tag{15}$$

Differentiating (15) once yields:

$$\frac{d\sigma_c}{dx} = E_c \frac{d^2 u_c}{dx^2} \tag{16}$$

Replacing $\Delta\sigma_c/\Delta x$ in with $d\sigma_c/dx$, (10) can be rewritten as:

$$E_c \frac{d^2 u_c}{dx^2} + \left[\frac{\pi d_s}{A_c}\right]\tau_b - \left[\frac{b}{A_c}\right]\tau_f = 0 \tag{17}$$

which reduces to:

$$\frac{d^2 u_c}{dx^2} + \left[\frac{\pi d_s}{E_c A_c}\right]\tau_b - \left[\frac{b}{E_c A_c}\right]\tau_f = 0 \tag{18}$$

Similarly, for the steel:

$$\sigma_s = E_s\left(\frac{du_s}{dx} - \alpha_s \Delta T\right) \tag{19}$$

Differentiating (19) once yields:

$$\frac{d\sigma_s}{dx} = E_s \frac{d^2 u_s}{dx^2} \tag{20}$$

By performing the same substitution as was used for the concrete, (12) becomes:

$$\frac{d^2 u_s}{dx^2} - \left[\frac{\pi d_s}{E_s A_s}\right]\tau_b = 0 \tag{21}$$

Equations (18) and (21) are the general differential equations that govern the behavior of the prism. All that remains is to substitute the correct expressions for τ_b and τ_f and solve the differential equations for u_c and u_s. In this model, τ_b is modeled by a three-part linear function as:

$$\begin{aligned} \tau_b &= K_1(u_s - u_c) && \text{if } 0 < |u_s - u_c| \le \delta_b \\ \tau_b &= C_1\left[\frac{(u_s - u_c)}{|u_s - u_c|}\right] - K_2(u_s - u_c) && \text{if } \delta_b \le |u_s - u_c| \le \delta_{bl} \\ \tau_b &= 0 && \text{if } \delta_{bl} \le |u_s - u_c| \end{aligned} \tag{22}$$

and τ_f is modeled by a two-part linear function as:

$$\begin{aligned} \tau_f &= K_3 u_c && \text{if } 0 < |u_c| \le \delta_f \\ \tau_f &= C_2\left[\frac{u_c}{|u_c|}\right] && \text{if } \delta_f \le |u_c| \end{aligned} \tag{23}$$

Table 9. Combinations of Stress Functions

	Zone 1	Zone 2	Zone 3	Zone 4
Case 1	$\tau_b = K_1(u_s - u_c)$	$\tau_b = K_1(u_s - u_c)$		
	$\tau_f = K_3 u_c$	$\tau_f = C_2$		
Case 2	$\tau_b = K_1(u_s - u_c)$	$\tau_b = K_1(u_s - u_c)$	$\tau_b = C_1 - K_2(u_s - u_c)$	
	$\tau_f = K_3 u_c$	$\tau_f = C_2$	$\tau_f = C_2$	
Case 3	$\tau_b = K_1(u_s - u_c)$	$\tau_b = K_1(u_s - u_c)$	$\tau_b = C_1 - K_2(u_s - u_c)$	$\tau_b = 0$
	$\tau_f = K_3 u_c$	$\tau_f = C_2$	$\tau_f = C_2$	$\tau_f = C_2$

Both stress functions are shown in Figure 28 and Figure 29, respectively. Figure 30 and Figure 31 illustrate the definitions of the parameters defining the four zones comprising the domain of the stress functions and three of the possible cases of stress functions anticipated, respectively. These stress functions provide the basis for three of the most likely situations or cases (listed in Table 9) which are of interest with respect to one-dimensional expansion displacement (six other cases are possible but are not considered here). Each situation causes the general differential equations to have different solutions, and each depends not only on the magnitude of the strain, but also upon the coefficients of the bond stress function and the friction stress function. The

distinguishing characteristics between each case are the locations of the interfaces, indicated by the dimensions l_1, l_2, and l_3 for different combination of the displacement. The length l_1 is the distance from the free end to the point at which the relative slip between the steel reinforcing and the concrete, $(u_s - u_c)$, is equal to δ_b, which is the slip at which the maximum bond stress occurs. The length l_2 corresponds to the point at which the relative slip between the steel and the concrete is equal to δ_{bl}, the slip at which the bond stress has just decreased to zero. The length l_3 corresponds to the point at which the displacement of the concrete, u_c, is equal to δ_f, the displacement at which the maximum friction stress occurs. For purposes of illustration, the solution for the first case is subsequently developed.

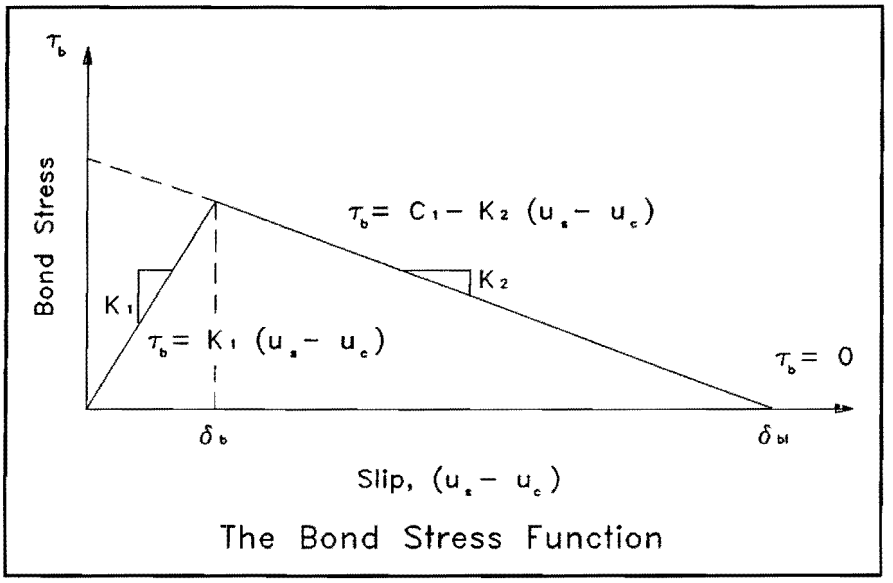

Figure 28.--The Bond Stress Function Used in the Model.

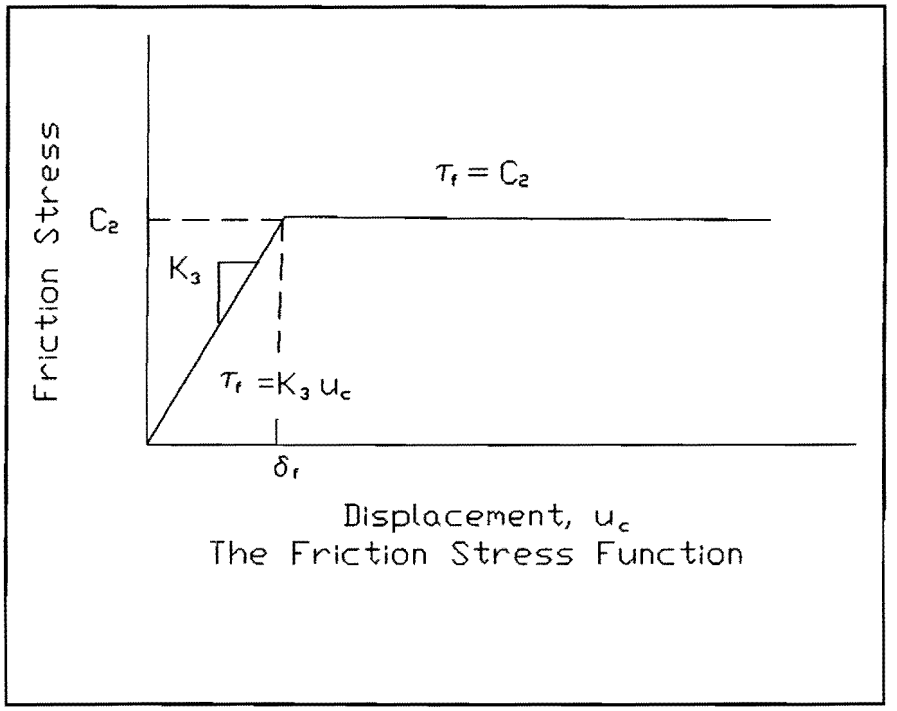

Figure 29.--The Friction Stress Function Used in the Model.

Solution Development

The solutions of this case will be presented to demonstrate the technique that was used to solve all three cases. The solutions of the displacement functions for semi-infinite length slab are derived in terms of two zones.

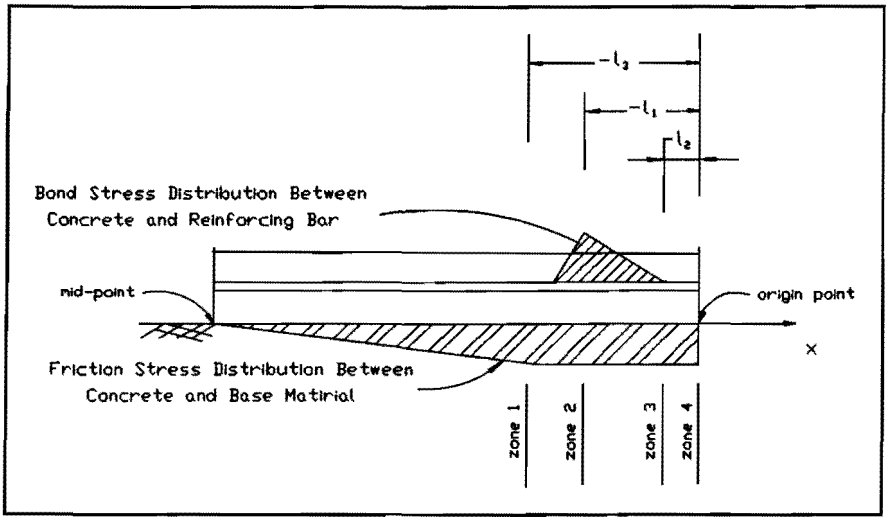

Figure 30.--Description of the Locations for Each Zone.

Consideration of Zone 1

In zone 1, the bond stress function is:

$$\tau_b = K_1(u_s - u_c) \tag{24}$$

and the friction stress function is:

$$\tau_f = K_3 u_c \tag{25}$$

Substituting the both stress functions into (18) yields:

$$\frac{d^2u_c}{dx^2} - [\frac{K_1\pi d_s + K_3 b}{E_c A_c}]u_c + [\frac{K_1\pi d_s}{E_c A_c}]u_s = 0 \tag{26}$$

Similarly, (21) becomes:

$$\frac{d^2u_s}{dx^2} + [\frac{K_1\pi d_s}{E_s A_s}]u_c - [\frac{K_1\pi d_s}{E_s A_s}]u_s = 0 \tag{27}$$

In operator form, these equations can be written as:

$$(D^2 - a_1)u_s + a_1 u_c = 0 \tag{28}$$

$$d_1 u_s + (D^2 - c_1)u_c = 0 \tag{29}$$

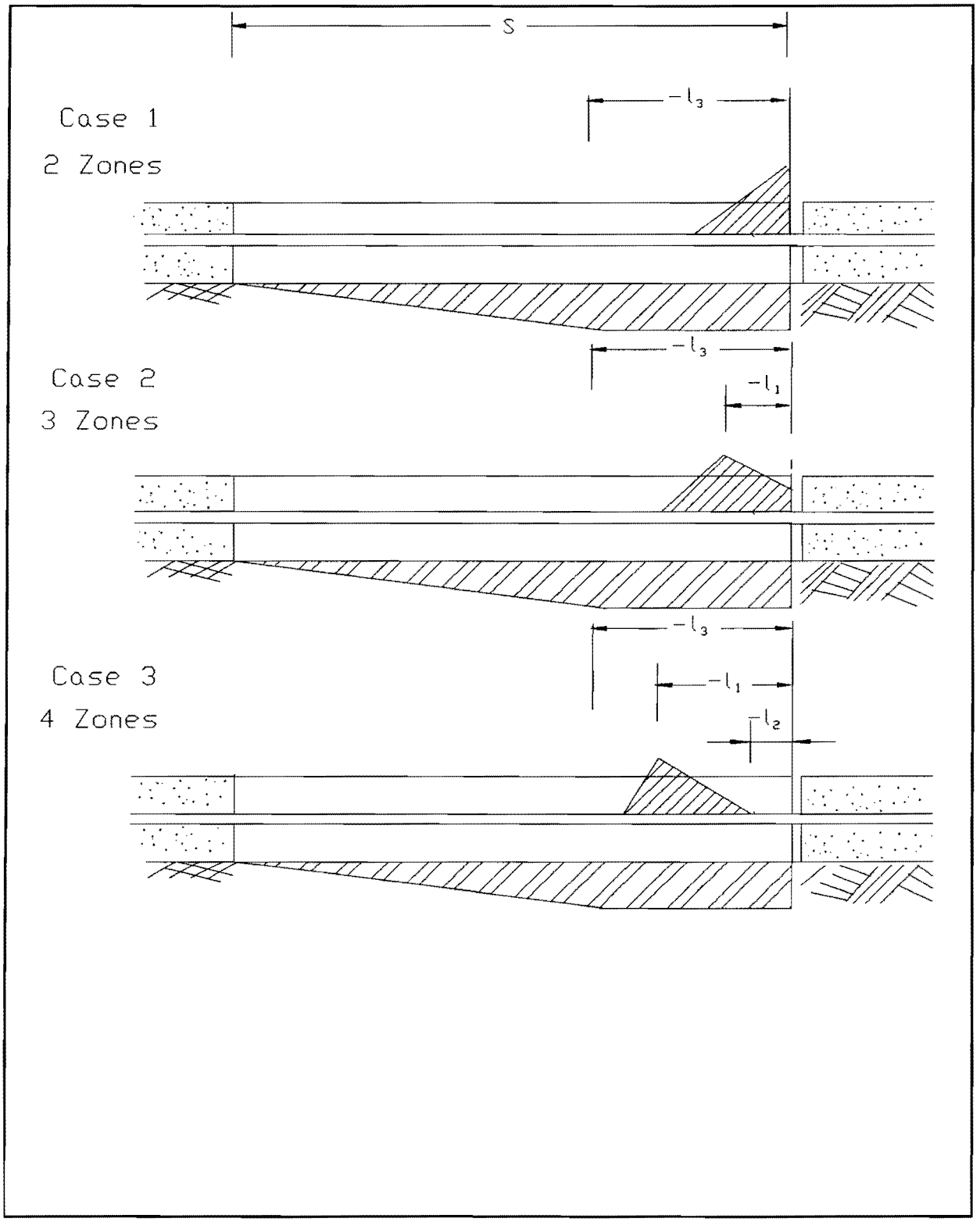

Figure 31.--Illustration of Stress Functions in Cases 1-3

where D = differential operator,

$a_1 = (K_1\pi d_s/E_sA_s)$,

$c_1 = (K_1\pi d_s + K_3 b)/E_cA_c$, and

$d_1 = (K_1\pi d_s/E_cA_c)$.

Elimination of one dependent variable is straightforward. Operating on (28) with d_1 and on (29) with $(D^2 - a_1)$ and then subtracting one from the other (Rainville 1958), yields:

$$[D^4-(a_1+c_1)D^2+(a_1c_1-a_1d_1)]u_c=0 \tag{30}$$

In a similar manner u_c may be eliminated, the resultant equation for u_s is:

$$[D^4-(a_1+c_1)D^2+(a_1c_1-a_1d_1)]u_s=0 \tag{31}$$

From (30) and (31) it follows at once that the general solutions for zone 1 are:

$$u_{c1}=A_{c1}e^{g_1x}+B_{c1}e^{-g_1x}+C_{c1}e^{h_1x}+D_{c1}e^{-h_1x} \tag{32}$$

$$u_{s1}=A_{s1}e^{g_1x}+B_{s1}e^{-g_1x}+C_{s1}e^{h_1x}+D_{s1}e^{-h_1x} \tag{33}$$

where:

$$g_1=\left(\frac{(a_1+c_1)}{2}+\frac{(a_1+c_1)}{2}\left(1-\frac{4(a_1c_1-a_1d_1)}{(a_1+c_1)^2}\right)^{\frac{1}{2}}\right)^{\frac{1}{2}}$$

$$h_1=\left(\frac{(a_1+c_1)}{2}-\frac{(a_1+c_1)}{2}\left(1-\frac{4(a_1c_1-a_1d_1)}{(a_1+c_1)^2}\right)^{\frac{1}{2}}\right)^{\frac{1}{2}}$$

Combination of (32) and (33) with (28) leads to the identity:

$$((g_1^2-a_1)A_{s1}+a_1A_{c1})e^{g_1x}+((g_1^2-a_1)B_{s1}+a_1B_{c1})e^{-g_1x}+$$
$$((h_1^2-a_1)C_{s1}+a_1C_{c1})e^{h_1x}+((h_1^2-a_1)D_{s1}+a_1D_{c1})e^{-h_1x}=0$$

For this to be true for all values of x,

$A_{s1} = r_1 A_{c1}$, $B_{s1} = r_1 B_{c1}$

$C_{s1} = s_1 C_{c1}$, $D_{s1} = s_1 D_{c1}$

where: $r_1 = [a_1/(a_1 - g_1^2)]$ and

$s_1 = [a_1/(a_1 - h_1^2)]$.

Consideration of Zone 2

In zone 2, the bond stress function is:

$$\tau_b = K_1(u_s - u_c) \tag{34}$$

and the friction function is:

$$\tau_f = C_2 \tag{35}$$

Substituting the above relations into (18) and (21) yields:

$$\frac{d^2u_c}{dx^2} - [\frac{K_1\pi d_s}{E_cA_c}]u_c + [\frac{K_1\pi d_s}{E_cA_c}]u_s = [\frac{C_2b}{E_cA_c}] \tag{36}$$

$$\frac{d^2u_s}{dx^2} - [\frac{K_1\pi d_s}{E_sA_s}]u_s + [\frac{K_1\pi d_s}{E_sA_s}]u_c = 0 \tag{37}$$

In operator form, these equations are written as:

$$(D^2 - a_2)u_s + a_2u_c = 0$$

$$b_2u_s + (D^2 - b_2)u_c = d_2$$

where: $a_2 = [K_1\pi d_s/E_sA_s]$,

$b_2 = [K_1\pi d_s/E_cA_c]$, and

$d_2 = [C_2b/E_cA_c]$.

A similar derivation with zone 1 yields the general solutions for zone 2 as:

$$u_{c2}=A_{c2}e^{g_2x}+B_{c2}e^{-g_2x}+C_{c2}+D_{c2}x+\frac{a_2d_2}{2(a_2+b_2)}x^2$$

$$u_{s2}=r_2A_{c2}e^{g_2x}+r_2B_{c2}e^{-g_2x}+C_{c2}+D_{c2}x+\frac{a_2d_2}{2(a_2+b_2)}x^2+\frac{d_2}{a_2+b_2}$$

where: $r_2 = [a_2/(a_2-g_2^2)]$, and

$g_2 = (a_2+b_2)^{1/2}$.

Boundary Conditions

If the pavement is assumed to be long enough that the midpoint does not move, then the displacements of the concrete and the steel are assumed to equal zero:

$$u_{c1}|_{x=-\infty}=0$$

$$u_{s1}|_{x=-\infty}=0$$

These conditions result in: $B_{c1} = D_{c1} = 0$. At the interfaces between zones, the displacements and the forces for the concrete and the steel are equal:

$$u_{c1}|_{x=-l_3}=u_{c2}|_{x=-l_3}$$

$$u_{s1}|_{x=-l_3}=u_{s2}|_{x=-l_3}$$

$$\frac{du_{c1}}{dx}|_{x=-l_3}=\frac{du_{c2}}{dx}|_{x=-l_3}$$

$$\frac{du_{s1}}{dx}|_{x=-l_3}=\frac{du_{s2}}{dx}|_{x=-l_3}$$

At the free end of the concrete slab, the resultants of axial forces for the concrete and the steel equal zero, respectively:

$$\sigma_c A_c|_{x=0}=0$$

$$\frac{du_{c2}}{dx}|_{x=0}=\alpha_c \Delta T$$

This results in : $A_{c2}g_2$-$B_{c2}g_2+D_{c2}=\alpha_c\Delta T$.

$$\sigma_f A_s|_{x=0}=0$$

$$\frac{du_{s2}}{dx}|_{x=0}=\alpha_s \Delta T$$

This results in: $r_2A_{c2}g_2$-$r_2B_{c2}g_2+D_{c2}=\alpha_s\Delta T$

If the coefficients of displacement functions and l_3 can be written in terms of x(i) (i=1, ... ,7) as:

$$[X(1)\ X(2)\ X(3)\ X(4)\ X(5)\ X(6)\ X(7)]^T = [A_{c1}\ C_{c1}\ A_{c2}\ B_{c2}\ C_{c2}\ D_{c2}\ l_3]^T$$

then the above boundary conditions can be expressed as:

$$\begin{aligned}
F(1)&=X(1)e^{-g_1X(7)}+X(2)e^{-h_1X(7)}-X(3)e^{-g_2X(7)}-X(4)e^{g_2X(7)}-X(5)+X(6)X(7)-0.5\frac{a_2d_2X(7)^2}{(a_2+b_2)}=0\\
F(2)&=r_1X(1)e^{-g_1X(7)}+s_1X(2)e^{-h_1X(7)}-r_2X(3)e^{-g_2X(7)}-r_2X(4)e^{g_2X(7)}-X(5)+X(6)X(7)-0.5\frac{a_2d_2X(7)^2}{(a_2+b_2)}-\frac{d_2}{(a_2+b_2)}=0\\
F(3)&=X(1)g_1e^{-g_1X(7)}+X(2)h_1e^{-h_1X(7)}-X(3)g_2e^{-g_2X(7)}+X(4)g_2e^{g_2X(7)}-X(6)+\frac{a_2d_2X(7)}{(a_2+b_2)}=0\\
F(4)&=X(1)r_1g_1e^{-g_1X(7)}+X(2)s_1h_1e^{-h_1X(7)}-X(3)r_2g_2e^{-g_2X(7)}+X(4)r_2g_2e^{g_2X(7)}-X(6)+\frac{a_2d_2X(7)}{(a_2+b_2)}=0\\
F(5)&=X(3)g_2-X(4)g_2+X(6)-\alpha_c\Delta T=0\\
F(6)&=X(3)r_2g_2-X(4)r_2g_2+X(6)-\alpha_s\Delta T=0
\end{aligned} \tag{38}$$

Solution Method

It is seen from the above equations that both the coefficients in the displacement functions and the variable l_3 upon which they depend are unknown. The following conditions can be used for determining the locations between zones according to the definition of l_3:

$$u_{c1}|_{x=-l_3}=u_{c2}|_{x=-l_3}=\delta_f$$

$$F(l_3)=\delta_f-u_{c1}|_{x=-l_3}$$
$$=\delta_f-u_{c2}|_{x=-l_3}=0$$

$$F(7)=X(1)e^{-g_1X(7)}+X(2)e^{-h_1X(7)}-\delta_F=0 \tag{39}$$

The addition of (39) to (38) results in seven equations in seven unknown variables, which requires the solution (roots) of a system of highly nonlinear equations. The determination of the roots of this system may be solved by many methods. A routine called NEQNJ from the IMSL package of mathematical software (IMSL 1987) has been used successfully in the present work on the VAX computer at Texas A&M University. This routine is based on the MINPACK subroutine HYBRDJ, which uses a modification of M. J. D. Powell's hybrid algorithm, which is a variation of Newton's method.

If the slip between the concrete and the steel is neglected, a simpler model, will be obtained. Similar derivation with this simple model gives the following formulas which can be used for determining the initial value for l_3.

$$l_3=\frac{(c_0-b_0\delta_f)}{a_0} \tag{40}$$

where $a_0=bC_2/(E_cA_c+E_sA_s)$,

$b_0=[bK_3/(E_cA_c+E_sA_s)]^{1/2}$, and

$c_0=(E_cA_c\alpha_c+E_sA_s\alpha_s)\Delta T/(E_cA_c+E_sA_s)$.

It is important to note that positive values of l_3 occur only for $c_0 > b_0\delta_f$, i.e., for large enough temperature change. Otherwise, the entire slab will have only one zone. If a positive value for l_3 is obtained from (40), the correct solution for the displacement must be in case 1, case 2, or case 3. If we assume case 1 and u_s-u_c is greater than δ_{bi}, the correct solution is in case 3. If u_s-u_c is less than δ_{bi} but greater than δ_b , the correct solution is in case 2. If u_s-u_c is less than δ_b, the correct solution is in case 1.

Model Structural Response

Analysis of the structural responses (displacement, steel and concrete stress) predicted by the slip model indicated nearly no difference between the slip model and the no slip model, as illustrated in Figure 32 and Figure 33. It is noted that the predicted slip shown in Figure 34 between the steel and the concrete is 0.000798 in. which is less than δ_b = 0.002 in., which confirms that the solution is in Case 1.

Figure 32 considers the displacement of the free end of the pavement restrained primarily by the subbase frictional forces. These responses corresponded to the observations noted in the field study, as did the displacements calculated by the PCP model (Tena-Colunga et al. 1989). Figure 35 is an enlargement of part of Figure 32 near the free end of the slab. The concrete stresses in both models change from tensile to compression at the point of x=1030 in. This appearance is due to the fact that the coefficient of steel thermal expansion is larger than that of concrete thermal expansion. The steel tends to move with the concrete. If the effect of the dilatational strains due to alkali-silica reaction is considered in this model, the concrete stress term will become:

$$\sigma_c = E_c(\epsilon_c - \alpha_c \Delta T - \epsilon_{asr})$$
$$= E_c(\frac{du_c}{dx} - \alpha_c \Delta T - \epsilon_{asr})$$

where ϵ_{asr} is the strain due to alkali-silica reaction.

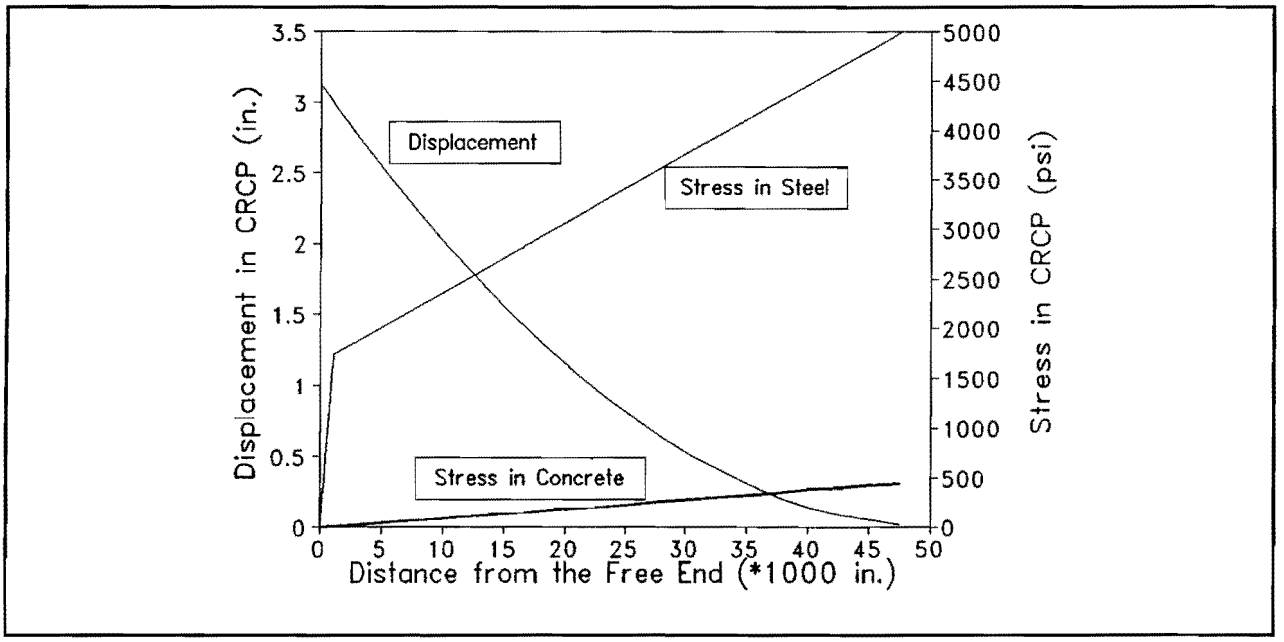

Figure 32.--Structural Responses in CRCP from Present Model.

CRC pavements typically are constructed with a lug anchor system at the pavement ends to resist the movement described previously with respect to the ruptured bridge backwalls and abutments (Mitchell 1963). The lug anchor system may vary state to state but typically consists of 3 to 6 lugs at approximately 17 ft intervals. Each lug is configured similar to a retaining wall which is integrally connected to the mainline pavement. The lugs are constructed into the pavement subgrade to a depth of 3 to 4 ft such that the force of pavement expansion and contraction is applied to the terminal lug and transferred to the support soil in the form of passive earth pressures. By this mechanism, the lug system provides restraint to the free end movement of the CRC pavement caused by temperature induced or ASR dilatational strains. As indicated previously, the bond slip

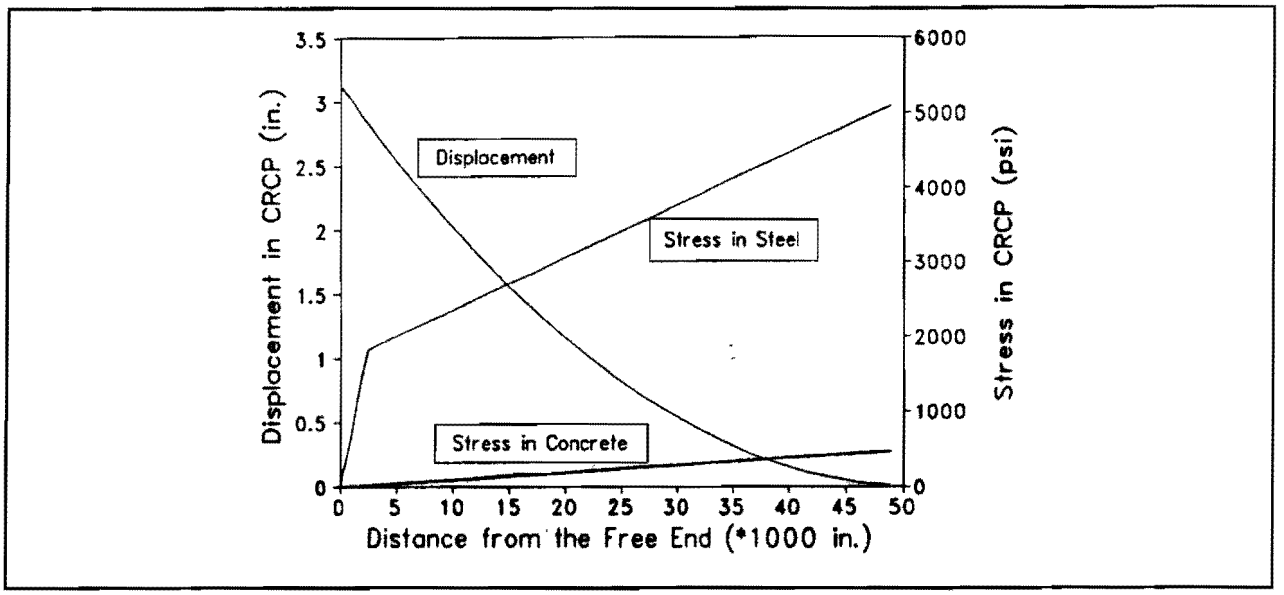

Figure 33.--Structural Responses in CRCP from No-Slip Model

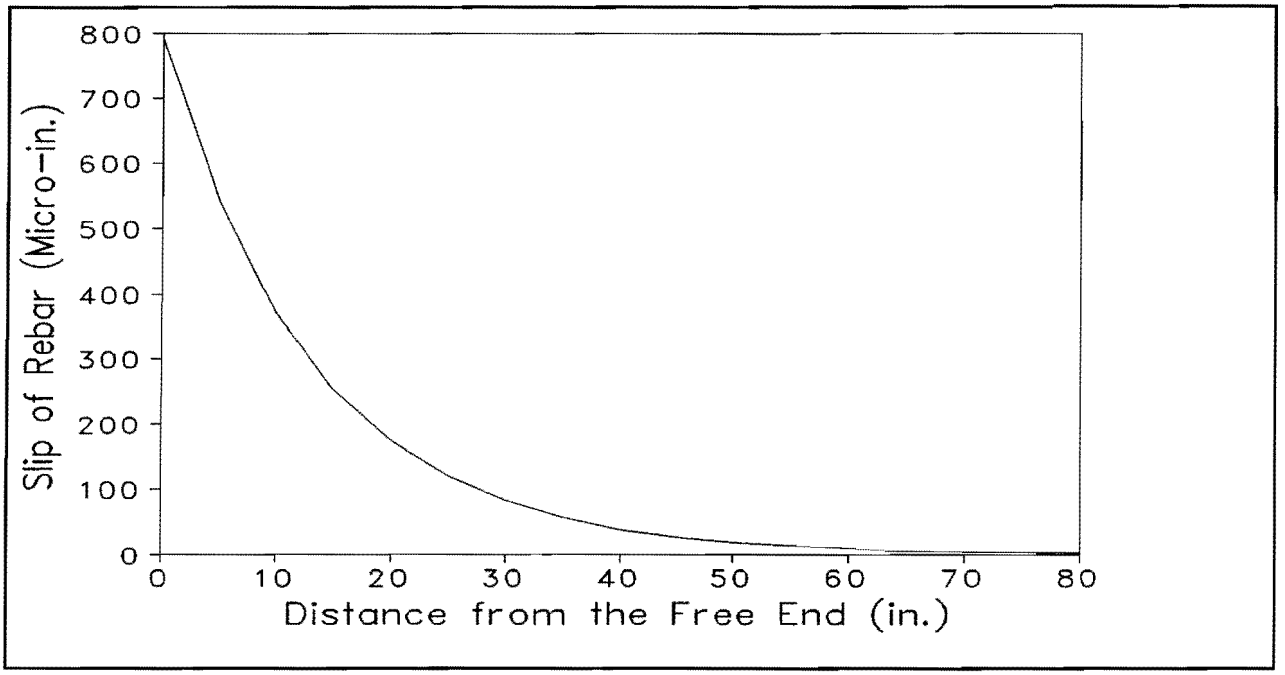

Figure 34.--Slip between Concrete and Steel.

length of the pavement near the free end is small, and it can be assumed that the no-slip model is appropriate to model the effect of the lugs on the movement of the slab. The boundary condition at x=0 is:

$$\sigma_s A_s + \sigma_c A_c = -R$$

where R is the portion of the total reaction of the lug system acting on the cross section of the free-body diagram shown in Figure 25, that is the reaction on a section of width equal to the longitudinal bar spacing. The reaction

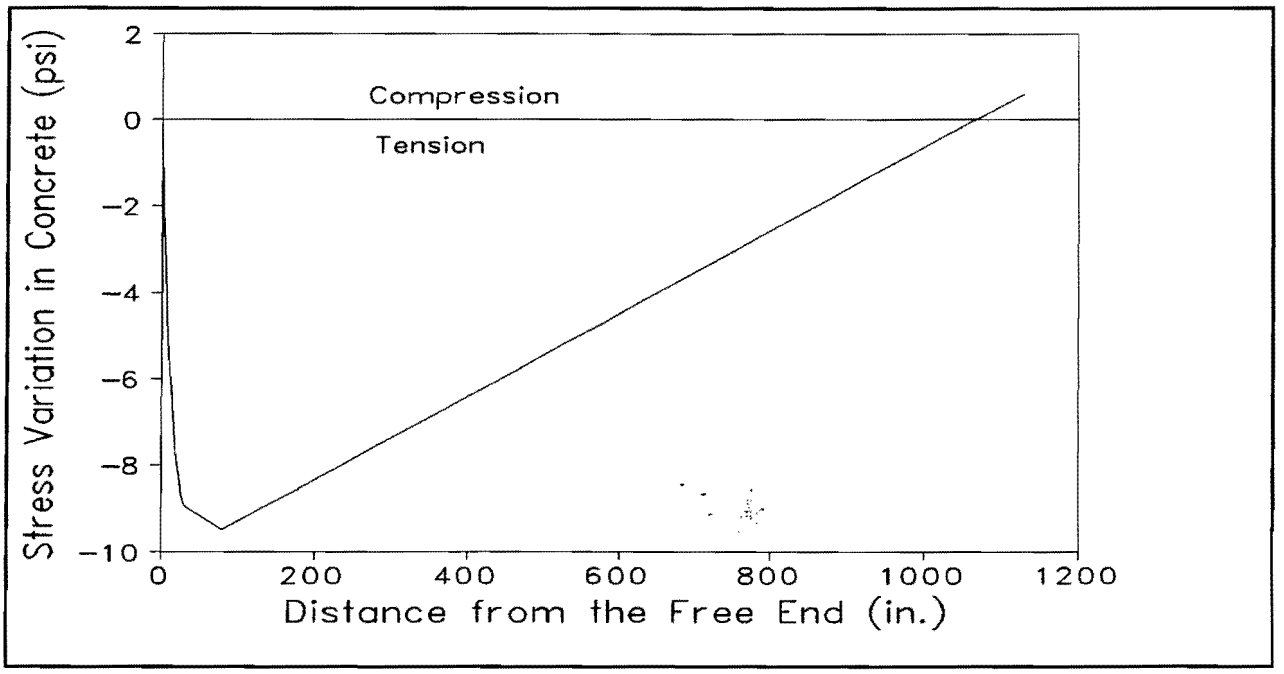

Figure 35.--Concrete Stress near the Free End.

R is determined as a function of the soil resistance using a passive Rankine state of stress based on drained soil strength characteristics. It is assumed that the Rankine approach will provide a reasonable estimate of the longitudinal resistance provided by the backfill material.

$$R = \sigma_p b H$$
$$= \left\{ K_p \sigma_v + 2 \bar{C} \sqrt{K_p} \right\} b H$$

where: σ_p = passive Rankine pressure (psi)

b = Steel bar spacing (in.)

H = lug depth (in.)

$K_p = \tan^2(45+\phi/2)$, the coefficient of passive earth pressure

σ_v = vertical intergranular pressure (psi)

$\bar{C}$ = soil cohesion, drained, (psi)

The effect of a temperature increase and the reaction of the lugs is considered in the structural response of CRC pavement as illustrated in Figure 36. In this figure K_p varies from less than 2 to a maximum of 7. It is noted that the strain due to ASR can have a more significant effect than a single annual temperature cycle. The full friction stress was assumed to be activated at .010 inches of displacement for this analysis. Figure 37 illustrates the depth of lug required as a function of a range of estimated ASR dilational strains which are less than that expected to cause distress in the concrete matrix. The lug requirements are illustrated for the various

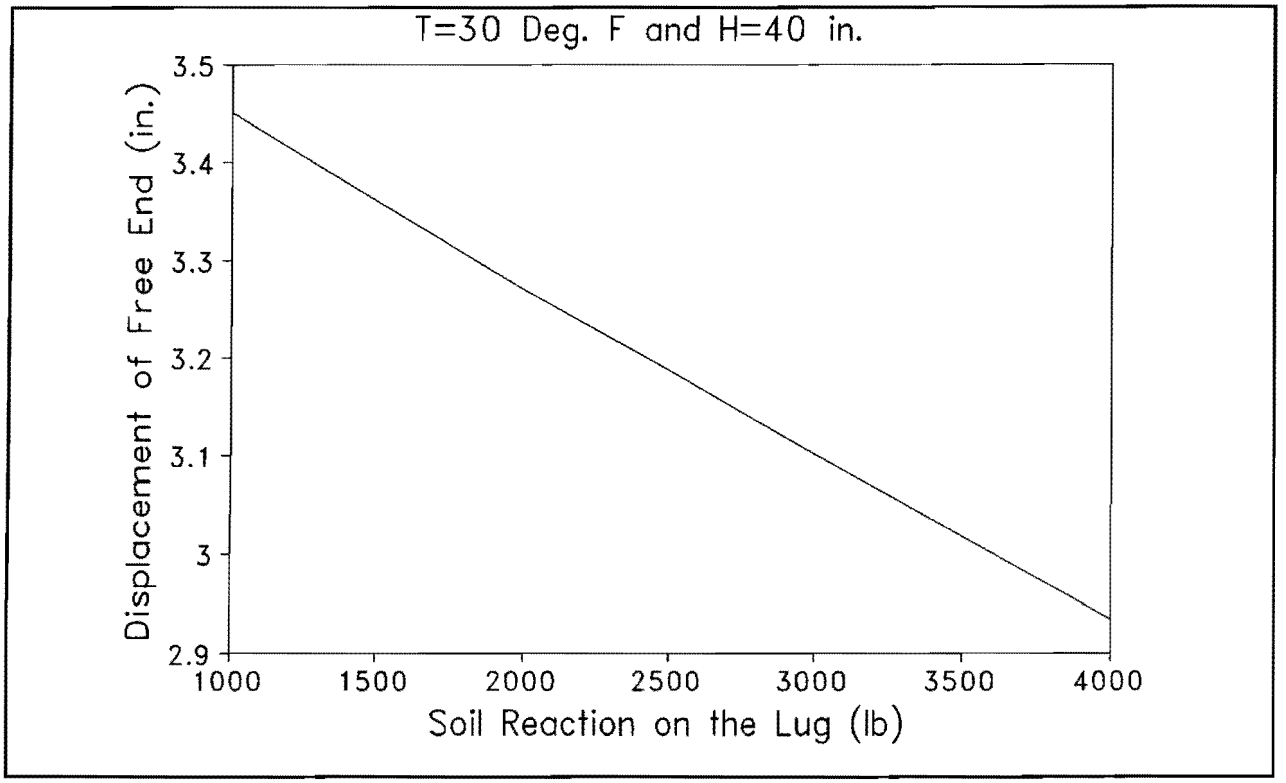

Figure 36.--Displacement of Lugs as a Function of Soil Resistance on Lugs

values of maximum displacement u_0 and coefficient of passive earth pressure K_p. The low value was assumed to represent the degree of restraint provided at the lug due to poor compaction near the lug. These results appear to correlate well with field experience. Greater restraint (greater K_p values) to limit the pavement displacement to tolerable limits (say 1 in.) would require greater lug resistances. Allowable displacement and quality of construction significantly affect the lug wall requirements. Data used in the examples discussed here are presented in Table 10.

It should be pointed out that the assumed lug resistance is perfectly plastic. This feature was incorporated in the model primarily to provide a tool needed to analyze properly working lugs. In reality the lug resistance is mobilized after some elastic displacement, and may drop off after a large displacement. If this occurs in the present lug designs, the results of the free-end model may be more applicable to the analysis of the existing pavement/lug/soils systems. It is important to choose rational and practical coefficients for friction stress functions for different subbase types (Ioannides and Salsilli-Murua 1988) and bond stress functions as well as the strain due to chemical reaction in order to get realistic structural responses of CRC pavement. With realistic inputs this model can provide a useful method to predict structural responses.

Based on the limited experience gained during development and study of this model, the following observations are offered:

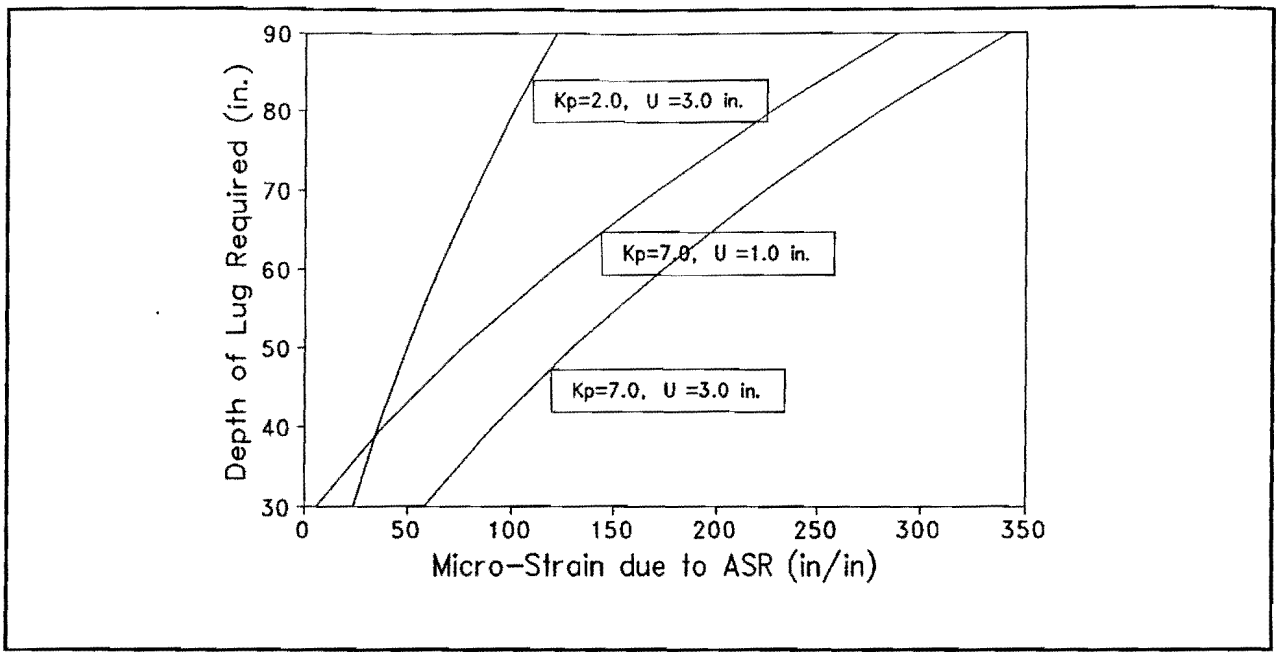

Figure 37.--Variation of Required Lug Depth with Strain due to Alkali-Silica Reaction

1. Alkali-silica reactions may have the potential to cause larger pavement growth than normal annual temperature cycles, depending on the extent of ratcheting which may contribute to the annual cyclic thermally-induced growth. The effect of lugs on the restraining pavement movement is significant, and the present lug designs, while apparently not providing perfect restraint, appear to cause significant restraining forces.
2. The numerical study indicates that the nature (case) of the pavement motion depends not only on the magnitude of temperature change, the coefficients of the stress functions, and the length of slab, but also on other factors such as shrinkage and creep.
3. It is certainly true that the displacement of the free end of a CRCP slab predicted by the simple no-slip model is larger than that predicted by the present model, because of the difference between the thermal expansion coefficients of steel and concrete, and because of the restraining offered by the bond between concrete and reinforcing steel. The steel displacement at the free end of the slab from the simple model is less than that from this model. However, the stresses of the reinforcing bar from the simple model are larger than those from this model, since the elastic modulus of the steel is larger than that of the concrete under the same strain. This model is thought to provide a more rational approximation of the structural response of CRC pavements.

It should be noted that the lugs are modeled in the present study as applying a purely axial resultant to the pavement. The moment created by the actual eccentricity of the soil reaction causes flexural stresses which are not modeled. This simplifying assumption is not thought to have any significant effect on the one-

Table 10. Input Data Used in Examples Discussed

b: Steel Bar Spacing	6.0 inches
d_s: Steel Bar Diameter	0.75 inches
d: Slab Thickness	12.0 inches
E_c: Concrete Modulus of Elasticity	4.0×10^6 psi
E_s: Steel Modulus of Elasticity	29×10^6 psi
K_1: Coeff. for Bond Stress Function	3.0×10^6 pci
K_3: Coeff. for Friction Stress Function	12.0 pci
C_2: Constant in Friction Stress Function	0.12 psi
δ_f: Point of Max. Friction Stress	0.01 inches
α_c: Concrete Thermal Expansion Coeff.	0.4×10^{-5}
α_s: Steel Thermal Expansion Coeff.	0.6×10^{-5}
ΔT: Temperature Change	30 deg F

dimensional prediction; however, cracks observed in practice at the locations of the lugs may be influenced, or even caused, by this neglected moment.

FINITE ELEMENT STUDIES OF MECHANISMS POTENTIALLY CAUSING DAMAGE TO ABUTMENTS

Figure 38 shows a finite element model of this abutment structure. It consists of 8-node solid elements modeling the abutment; and spring elements, not shown in Figure 38, are used to model the soil-structure interaction. A micro-computer version of the finite element software SAP90 was used in this study. All numerical operations are executed in full 64-bit double precision. Assumed concrete material properties are compressive strength f_c' = 4 ksi, unit weight 140 lb/ft^3, elastic modulus E_c= 36,000 ksi, and Poisson's ratio μ = 0.28.

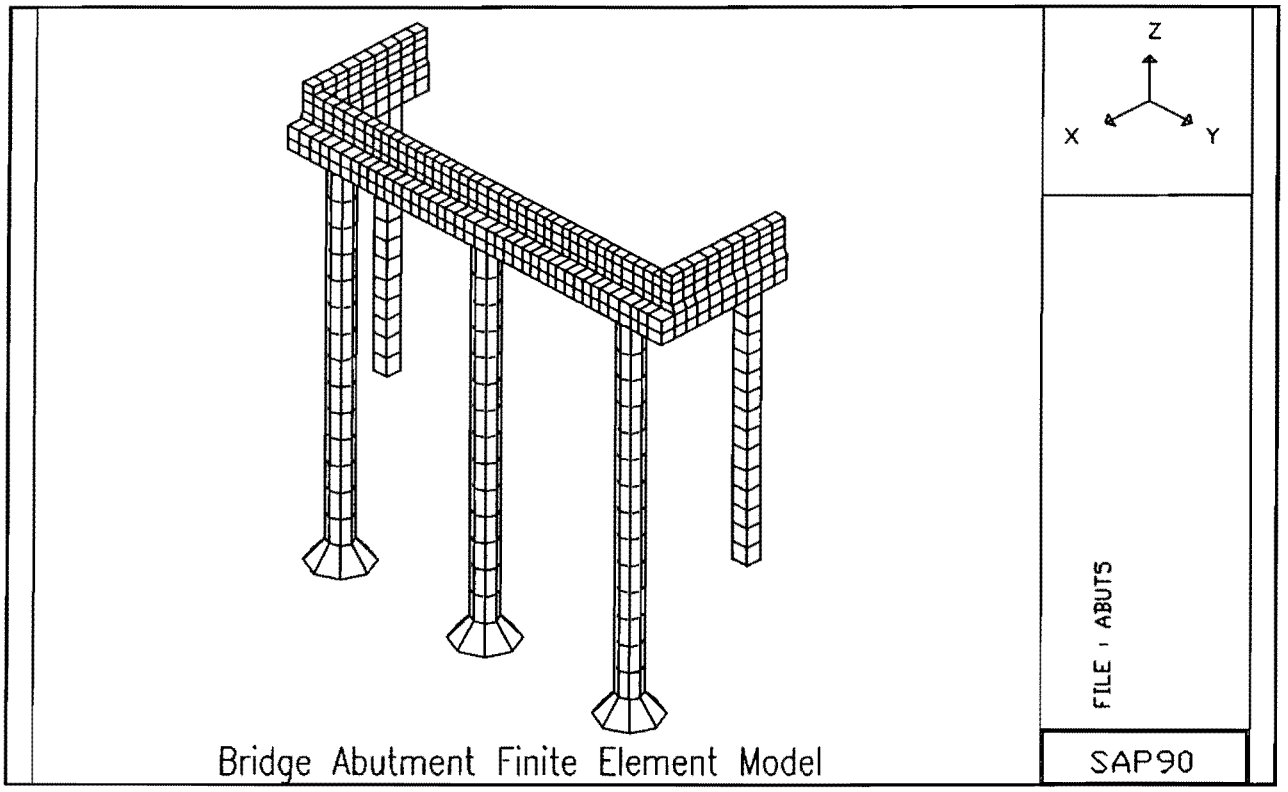

Figure 38.--Finite Element Model of Bridge Abutment

Soil Properties

The soil-structure interaction was simplified by employing a Winkler soil model, as illustrated in Figure 39. The soil surrounding the shaft is represented by a set of elastic springs. Winkler's assumption states that each spring acts independently. Although this assumption does not exactly describe the soil behavior, it has been demonstrated that solutions of beam-on-foundation problems using Winkler's assumption do not differ appreciably from solutions assuming the soil to be an isotropic, elastic continuum. It is convenient to think of the Winkler's model in terms of P-Y curves, also shown in Figure 39. The soil modulus E_s is then taken to be P/Y. Since the P-Y relationship is usually nonlinear, the modulus E_s will not be constant, but it may be linearly

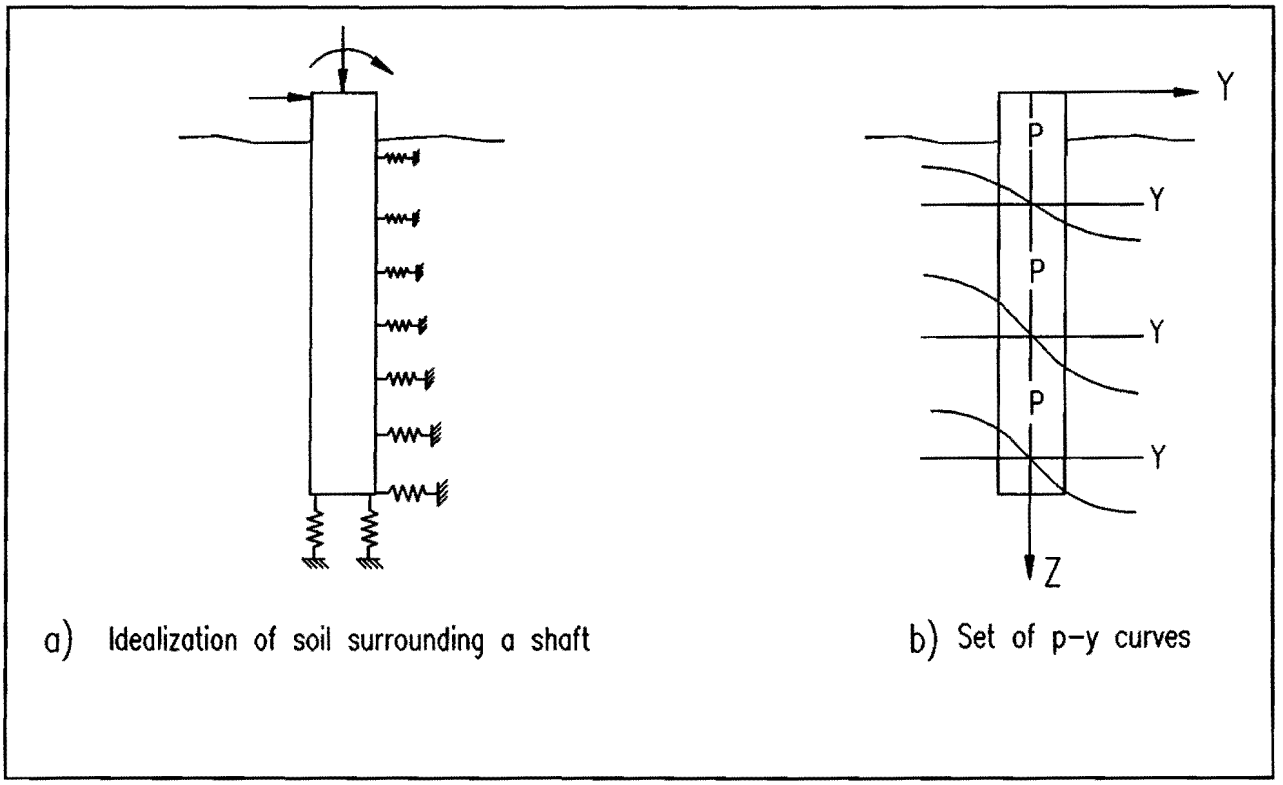

Figure 39.--Representation of Winkler Soil Model and P-Y Curves

approximated for small deflections. A linear approximation was used in this study. Terzaghi (1955) suggested the following formula for stiff clays:

$$k_h = \frac{k_{s1}}{1.5b} \tag{44}$$

where

k_h = coefficient of horizontal subgrade reaction,

k_{s1} = basic value of coefficient of vertical subgrade reaction, and

b = width of pile or drilled shaft.

Then, the soil modulus $E_s = P/Y$ is given by

$$E_s = k_h b \tag{45}$$

The soil strength data obtained from borings at the site modeled is presented in Table 11. The embankment is approximately 20 to 30 ft deep and consists mainly of clay and sandy clay. Dry densities are approximately 100 lb/ft^3. Assuming that the coefficient of subgrade reaction does not depend on depth yields the values for k_{s1} listed in Table 12.

Table 11. Ultimate Strength of the Modeled Soil, q_u (ton/ft^2)

Depth (ft)	Boring No.					
	1	2	3	3A	4	5
1	1.25	4				
3	1.5	1.5			2.0	2.0
5	0.75, 1.75	1.5			2.5	1.0
7	1.5	2.0			0.75	1.0, 2.0
9	2.0	2.0		1.5	2.0, 3.0	3.5
11	2.0	2.5		2.75	2.0	3.5
13	1.5	1.5		2.75	1.75	2.25
15	1.0, 2.5	1.5		1.75	1.75	1.5
17	1.5	2.25		2.0	1.75	2.5
19	2.25	1.5		2.25	1.75	2.0
21	2.25	1.5		2.5	1.75	2.0
23	2.5	2.25		3.0		3.0
25				1.75, 4+		4+
27				4+		2.75
29				4+		
31				1.5		

Table 12. Values of k_{s1} for Calculating Values of Clay Soil Modulus, E_S

	Stiff	Very Stiff	Hard
q_u, ton/ft^2	1-2	2-4	>4
k_{s1}, ton/ft^3	50-100	100-200	>200
Selected k_{s1}, ton/ft^3	75	150	300

The soils surrounding the abutment are modeled as two layers, one representing the embankment fill and one representing natural undisturbed soil. The E_s values used in the model are listed in Table 13. These values were calculated based on the data in Table 11, assuming the average q_u for fill is 1.5 tons/ft^2 and for

natural soil is 2 tons/ft^2, and assuming q_u is about 3-5 tons/ft^2 at 42 ft depth. The spring constants for the Winkler springs are obtained from these values for E_s.

Table 13. Values of E_s Used in the Model

	Horizontal Subgrade	Vertical Subgrade
Filled layer, ton/ft^2	50	75
Natural layer, ton/ft^2	100	150-300

The soil's response to the dynamic loads is known to be significantly different from the response to long-term static loads. To model this, the E_s values used for the live load were taken to be twice the values used for static loads. Using these E_s values, the properties of the soil springs were determined and the finite element model constructed.

Finite Element Analysis

Using the finite element model described above, the following loading cases were simulated:

Case 1: Longitudinal pavement growth

Assuming the end of the approach slab and the top of the abutment backwall are constrained to move together so that the abutment backwall is displaced 1 in. toward the bridge deck

Case 2: Settlement I

Assuming the load capacity of one 30 in. diameter drill shaft on the right side was reduced 50%

i) Dead load only

ii) Live load only (One HS20 truck)

Case 3: Settlement II

Assuming two wingwall piles lose all tip resistance

Case 4: Soil pressure

Assuming 1 kip/ft^2 soil pressure is uniformly distributed on the inside surfaces of the abutment

Case 5: Live load only (One HS20 truck)

Case 6: Dead load only

Case 7: Sensitivity to the soil/structure interaction model

i) Increasing E_s 100% for case 1

ii) Increasing E_s 100% for case 6

iii) Decreasing E_s 50% for case 6

Some simulation results for load case 1 are presented in Figure 40 and Figure 41. In load case 1, the approach slab is forcing the abutment backwall 1.0 in. forward, and the resulting force between the approach slab and the abutment backwall is approximately 228 kip. The wingwall is predicted to rotate approximately 0.37 degree. The abutment vertical settlement is about 0.35 in. From Figure 40 it may be seen that the anticipated damage for this load case is cracking of the backwall or backwall/wingwall intersection, consistent with the observed damage in the field. Similar results from other load cases are not presented here. Case 2 and 5 results indicate highest stress concentrations in the top center of the backwall; and in cases 3 and 4, highest stresses occur at the ends of the backwall. Dead load stresses in case 6 are small as are live load stresses in case 5. Accordingly, it may be concluded that the mechanisms modeled in cases 1, 3 and 4 each acting separately or together could be contributing factors to the damage observed. Because of the other observations implicating pavement growth and because of the low probability of loss of support under the wingwall piles or the development of high lateral earth pressures on the abutment walls, case 1 loading is considered the most likely explanation of the observed damage.

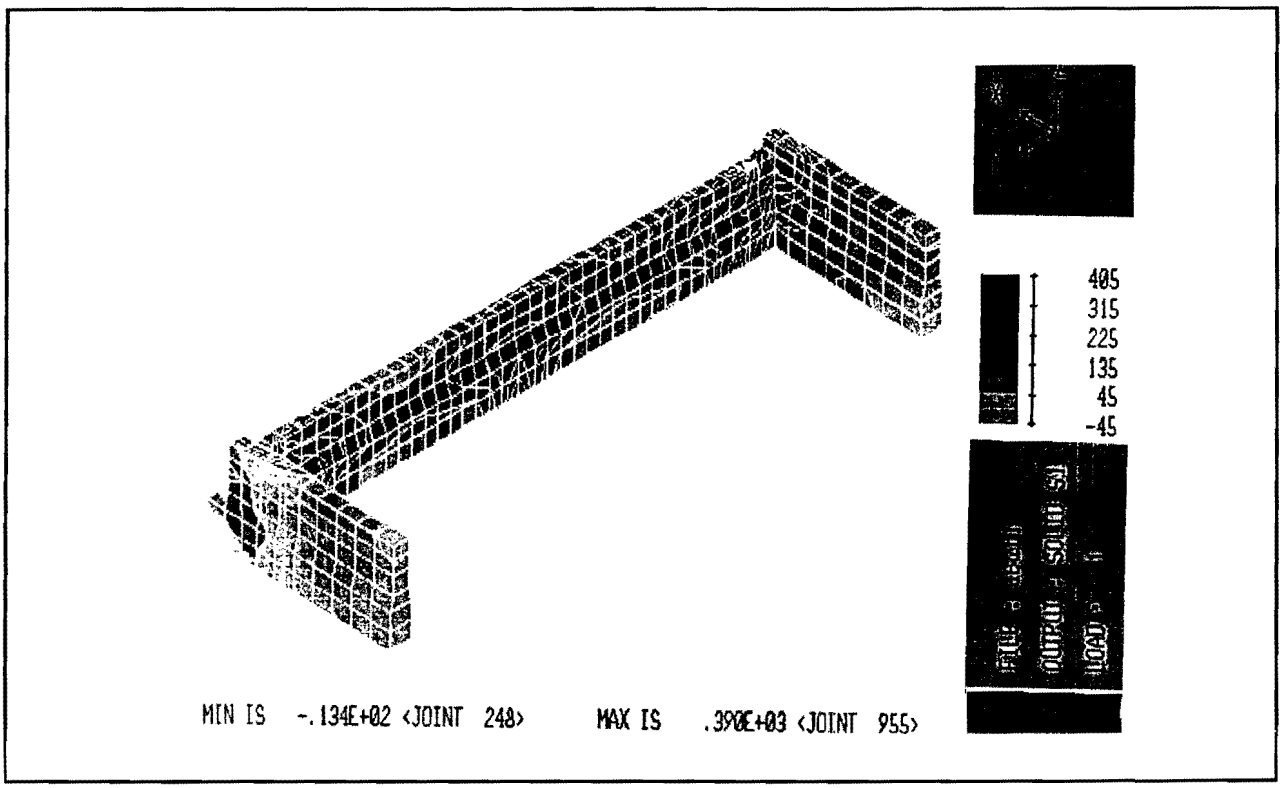

Figure 40.--Predicted Distribution of Maximum Principal Stress For Load Case I (stress units are psi)

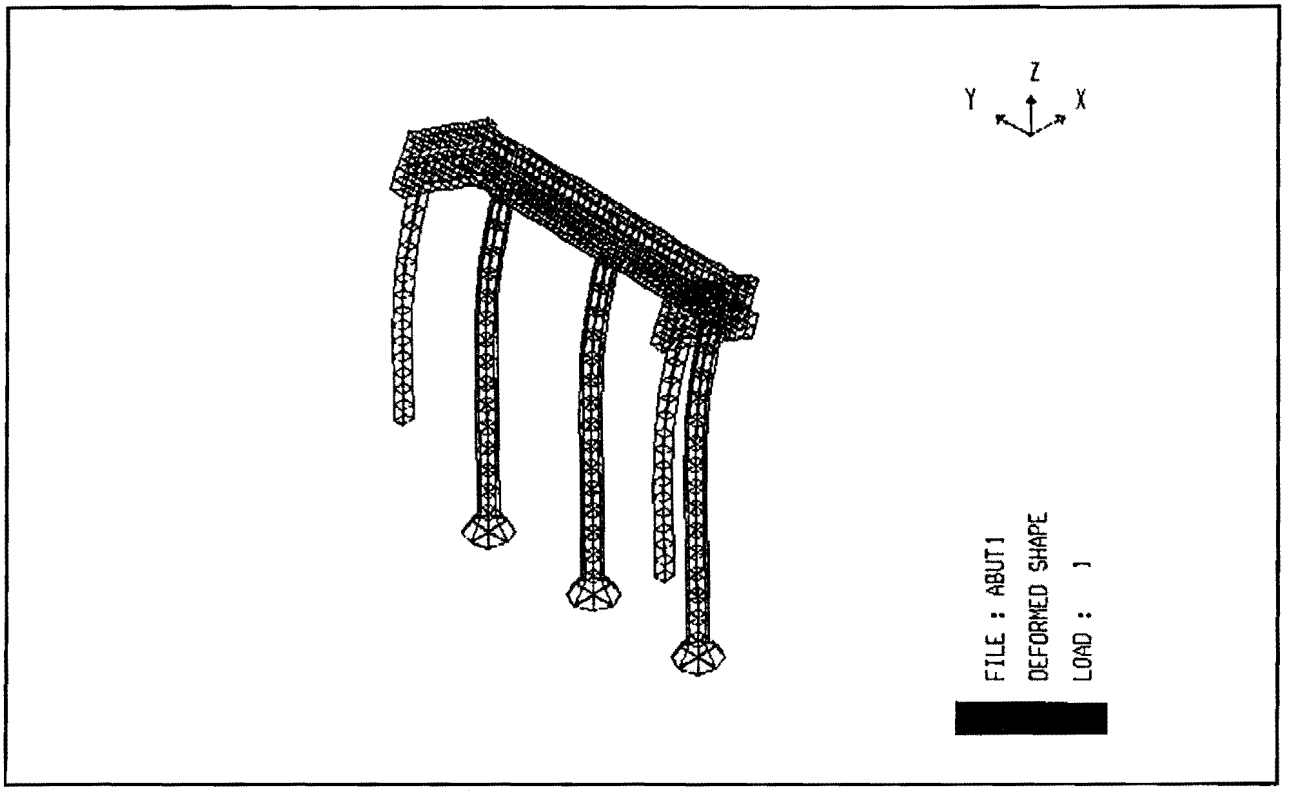

Figure 41.--Predicted Deformed Shape for Load Case I

METHODS TO MITIGATE OR ELIMINATE FUTURE DAMAGE TO ABUTMENTS

The reinforced concrete pavement lugs are intended to anchor the ends of the CRCP. It is apparent that in certain situations, these lugs are not performing their intended function. Two obvious means of mitigating the observed damage are to provide an anchor system that functions reliably or to isolate the CRCP from the approach slab. Strengthening of the abutment backwall sufficiently to resist the expansion of the CRCP is not practical, although it is evident that some redesign of the reinforcement details in the abutment design may be justifiable. The most straightforward way to eliminate future damage to abutments is to provide an isolation or pressure relief joint between the end of the CRCP and the approach slab. An isolation joint consisting of a 36 in. gap filled with ACP has reportedly been used in New York (Kamp 1990, Shirole 1990) and in other states, but efforts to obtain drawings of the detail have been unsuccessful. While the presence of such a joint may increase maintenance by requiring periodic planing or grinding, the increased life of the abutments will easily offset a small increase in maintenance costs. Other methods to isolate the abutment from the approach slab may also prove practical. Mechanical expansion joints have been proposed and studied. Omitting the dowelled connection between the approach slab and abutment backwall prevents damage to the backwall but may be undesirable for other reasons. An unorthodox proposal (Panak 1990) which has not been studied involves a wedge-shaped segment of concrete pavement, sketched in Figure 42, which could possibly be designed to slide transversely in response to the longitudinal pressure created by the growing pavement.

Methods to Mitigate Abutment Rotation

Abutment rotation, in the cases observed, is probably due to post-construction consolidation of poor soils under the embankment. Such rotation is especially likely when the soft soils occur in layers of nonuniform thickness (Wolde-Tinsae, et al. 1987). Based on the few observations of abutment rotation, the direction of rotation away from the bridge is indicative of nonuniform consolidation due to nonuniform loading of the poor soils. This is consistent with the usual case of an embankment of variable depth which decreases away from the bridge. Recommended measures applicable when designing embankments on compressible layers are: (Wolde-Tinsae et al. 1987) the use of surcharge, vertical drains, appropriate waiting periods to preload the compressible layers. Alternatively, removal of unsatisfactory compressible material or use of lightweight embankment fill material may be considered. Such special, non-standarized measures will require site-specific geotechnical engineering efforts.

Methods to Mitigate Pavement Roughness at Approaches

Pavement roughness may be concentrated at bridge approaches causing a more or less discrete bump at the bridge approach. This concentration is believed to be caused by two factors. First, the joint at the pavement/approach slab interface may allow water beneath the pavement resulting in increased soil moisture content and reduced resistance to wheel loads. Maintenance of the seals at joints in the roadway may mitigate

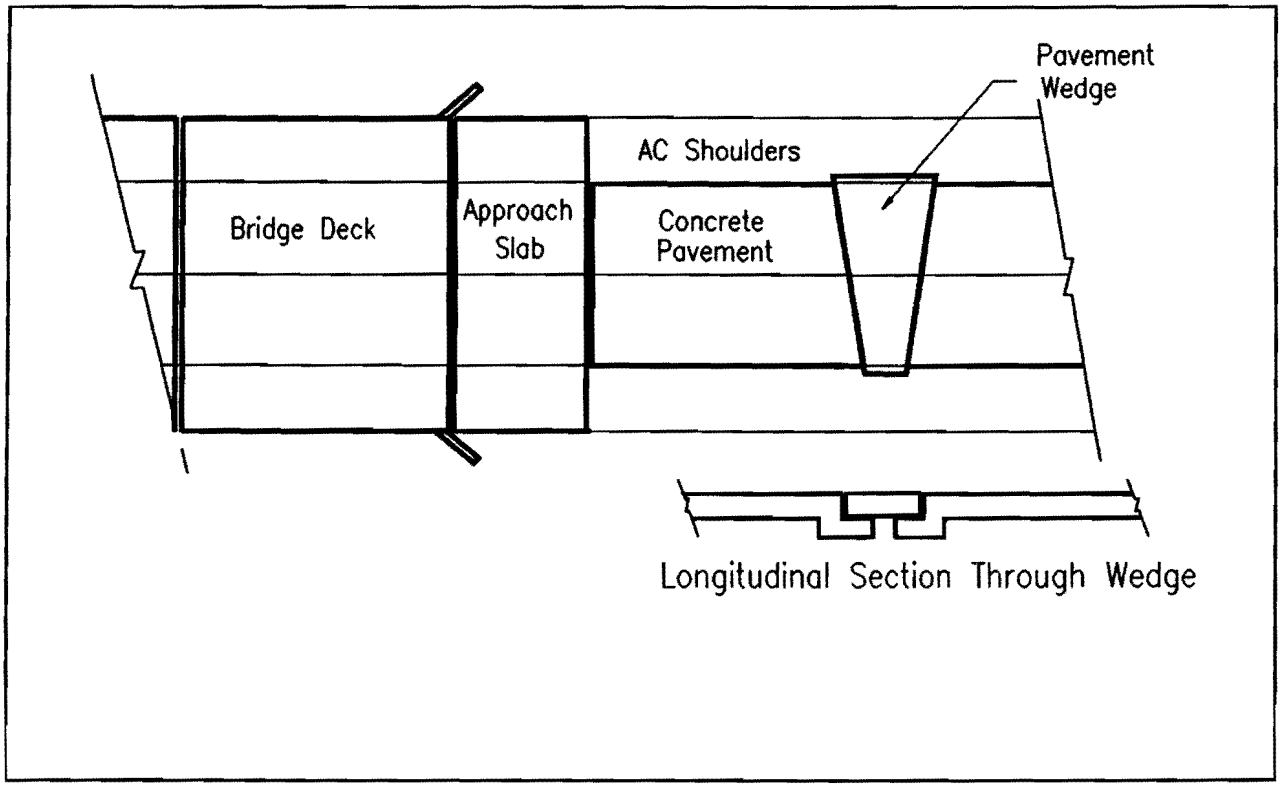

Figure 42.--Proposed Wedge of Concrete Pavement Designed to Relieve Pressure of Pavement Growth (Panak 1990)

damage due to this mechanism. Secondly, depending on the degree of shear transfer between the end of the flexible pavement and roadway and the end of the approach slab, increased wheel load stresses in the pavement may result with subsequent increase in rutting and other wheel-load-induced distress mechanisms. Simple finite element models of the pavement/approach slab interface, neglecting shear interaction between roadway and approach slab, indicate significant, nearly 100 percent increases in local pavement stresses. The degree of interaction actually occurring is not known but will influence such calculations. Improvements in bituminous materials used for pavements near approach slabs by additives or fiber reinforcement could mitigate distress by this second mechanism.

Another, more easily controlled type of pavement roughness at approaches is caused by the feathering of ACP overlays at the approach slab. When ACP overlays are placed continuously across the bridge deck, an extremely smooth ride results. There are significant drawbacks to this practice, however. The additional superimposed dead load on the bridge may be unacceptable, especially in the case of longer spans. Also, the overlay will soon exhibit reflective cracks at the joints at the ends of the approach slab and the deck slabs. With time and traffic, these cracks will ravel and degrade the riding quality. The alternative of feathering the ACP overlay into the approach slab results in a significant bump. Some of the most significant discontinuities observed during the field studies were caused by such feathering. Better feathering practices could reduce the

perceived bump. Practical elimination of the discontinuity would require milling existing flexible pavements before the approach slab for some distance, and it is not known whether a standard exists for such treatment. If no standard exists, then the desired profile should be established by a pavement designer rather than by maintenance personnel. The severity of such discontinuities as were observed in several instances during the field inspections justifies development of a better treatment of ACP overlays at bridge approaches.

Methods to Mitigate Approach Slab Settlement and Cracking

Approach slab settlement and cracking are related. In spite of field measurements which indicate humps in the center of approach slabs studied, many observed cracks in approach slabs appear to be consistent with loss of support from the center of the approach slab. This loss is thought to be caused by erosion of fill materials by water entering through the approach slab or abutment and flowing through or around the fill, usually exiting well down the rip-rap protected slope. In some instances massive failures of rip-rap result, but the more significant structural aspect of this erosion is loss of support under the approach slab. The approach slab designs encountered on this study, shown in the Department's standard drawing BAS-67 (MOD), consists of a 20 ft-long, 9 in.-thick concrete slab reinforced with no. 5 longitudinal bars spaced 18 in. and no. 4 transverse bars on variable spacing (12 to 18 in.) depending on the width of the slab. The basis for this design has not been discovered. Other states imply design philosophies based on the approach slab spanning a portion of its length. Whether the design used in Texas has been designed for such loading is not known. While increased approach slab flexural strength could be used to advantage, it seems more productive to prevent the loss of support which appears to be related to much of the observed damage. In particular, the joints at the approach end of the approach slab and along the sides of the approach slab are usually observed to be inadequately maintained to prevent intrusion of water from the roadway. The frequent placement of a guardrail post in a gutter formed in the edge of the approach slab undoubtedly leads to significant leakage. Such placement should be prohibited in the future. Guardrail posts spacings are determined based on safety considerations, so it is the gutter which must be moved.

SUMMARY AND CONCLUSIONS

The bridge approaches on the roadways traveled by the researchers were generally in good condition. The cost of maintenance required to keep the approaches in this good condition has not been evaluated, however.

Field observations of approaches and abutments indicate that the most serious observed damage is to abutment backwalls. These observations, supported by numerical stress analysis, lead to the conclusion that the observed damage is caused by longitudinal growth of CRCP causing longitudinal pressures on the abutment backwalls. Pressure relief joints have not been used at the sites where damage was observed and are recommended as experimental retrofit solutions at sites where damage has occurred and for prevention at sites where damage has not yet occurred. The use of pressure relief joints may result in increased pavement growth. Whether the longitudinal pavement growth may be attributed to a chemical reaction in the concrete or to a thermal ratcheting mechanism has not yet been determined. This question is suggested as a topic for further study. This observed damage mechanism may or may not strongly influence approach roughness, but it is clearly the cause of some expensive rehabilitation efforts.

One area in which maintenance efforts could be profitably increased is in the sealing of joints around the approach slab. Some of the approach slab damage which contributes to approach roughness is apparently due to loss of support resulting from water leaking through the approach slab and through the embankment.

Also, it is concluded that the reinforced concrete pavement lugs are failing to completely anchor the end of the CRCP, at least at sites where this damage has been observed. A review of the design method for sizing these lugs should be performed as well as a review of several of the failures to determine whether an improved design method for anchor lugs is warranted.

REFERENCES

Carasquillo, R. L., and P. G. Snow (1987). "Effect of Fly Ash on Alkali-Aggregate Reaction in Concrete," **ACI Materials Journal**, Vol. 84, No. 4, American Concrete Institute, Detroit, pp. 299-305.

Cheney, K. (1975). "Bridge Approach Settlement Study," Nebraska Department of Roads.

Chiang, C., B. F. McCullough, and W. R. Hudson. (1975). "A Sensitivity Analysis of Continuously Reinforced Concrete Pavement Model CRCP-1 for Highways." Research Report 177-2, Center for Highway Research, The University of Texas at Austin.

Dunn, K. H., G. H. Anderson, T. H. Rodes, and J. J. Ziehr (1983). "Performance Evaluation of Bridge Approaches," Wisconsin Department of Transportation.

Fabiarz, J., and R. L. Carrasquillo (1986). "Effectiveness of Fly Ash Replacement in the Reduction of Damage Due to Alkali-Aggregate Reaction in Concrete," Report No. CTR 450-1, Center for Transportation Research, The University of Texas, Austin.

Goldbeck, A. J. (1956). Needed Research, STP No. 169, American Society for Testing and Materials, pp. 26-34.

Grover, R. A. (1978). "Movements of Bridge Abutments and Settlements of Approach Pavements in Ohio," **Transportation Research Record**, No. 678, Transportation Research Board, Washington, DC.

Hopkins, T. C. (1969). "Settlement of Highway Bridge Approaches and Embankment Foundations," Kentucky Department of Highways.

Hopkins, T. C., and R. C. Deen (1969). "The Bump at the End of the Bridge," Kentucky Department of Highways.

Hopkins, T. C., and R. C. Deen (1970). "The Bump at the End of the Bridge," **Highway Research Record**, No. 302.

Hopkins, T. C., and G. D. Scott (1970). "Estimated and Observed Settlements of Bridge Approaches," **Highway Research Record**, No. 302.

Hopkins, T. C. (1973). "Settlement of Highway Bridge Approaches and Embankment Foundations," Kentucky Department of Highways.

Hopkins, T. C. (1985). "Long-Term Movements of Highway Bridge Approach Embankments and Pavements," University of Kentucky Transportation Research Program.

IMSL,(1987), User's Manual, Math/Library, FORTRAN Subroutine for Mathematical Application, IMSL, Inc..

Ioannides, A. M., and R. A. Salsilli-Murua (1988). "Interlayer and Subgrade Friction: A Brief Review of the State-of-the-Art," Federal Highway Administration, Publication No. FHWA-RD-88-068, June 1989.

James, R. W., H. Zhang, and D. G. Zollinger (1991). "On Observation of Severe Abutment Backwall Damage," Paper 910623 presentated at the TRB 1991 Annual Meeting, and for publication in the **Transportation Research Record**, Transportation Research Board, Washington, DC.

Kamp, B. (1990). Personal communications.

Kerr, A. D. (1991). "The Assessment of Concrete Pavement Blowups--a User Manual," (Draft) Final Report on FHWA Contract DTFH-90-P00928, University of Delaware, Newark, DE.

Laguros, J. G., D. R. Boyd, M. M. Zaman, I. U. Mahmood (1986). "Evaluation of Causes of Excessive Settlements of Pavement Behind Bridge Abutments and Their Remedies - Phase I," University of Oklahoma.

Laguros, J. G. (1990). Personal communications.

Lytton, R. L., R. L. Bogess, and J. W. Spotts (1976). "Characteristics of Expansive Clay Roughness of Pavements," Transportation Research Record 568, Transportation Research Board, Washington DC, pp 9-23.

Ma, J., and B. F. McCullough. "CRCP-2, An Improved Computer Program for the Analysis of Continuously Reinforced Concrete Pavements." Research Report 177-9, Center for Highway Research, The University of Texas at Austin.

McDowell, C. (1956). "Interrelationships of Load, Volume Change, and Layer Thickness of Soils to the Behavior of Engineering Structures," Proceedings, Highway Research Board, pp. 754 - 772.

Mindess, S., and J. F. Young (1981). Concrete, Prentice-Hall, Inc., Englewood Cliffs, NJ, pp. 671.

Mitchell, R. A. (1963). "End Anchors for Continuously-Reinforced Concrete Pavement." **Highway Research Record**, No. 5, Wash. D.C., pp. 50-82.

Moulton, L. K. (1986). "Tolerable Movement Criteria for Highway Bridges," Report FHWA-TS-85-228, Department of Civil Engineering, West Virginia University, Morgantown, West Virginia, pp. 93.

Neville, A. M. (1981). Properties of Concrete, Third Ed., Pitman Publishing Ltd., London.

O'Neill, M. W., and A. M. Poormoayed (1980). "Methodology for Foundations on Expansive Clays," Journal of the Geotechnical Engineering Division, ASCE Vol. 106 No. GT12 December, pp. 1345 - 1366.

Palmer, R. P., M. P. J. Olsen, and R. L. Lytton (1988). "TTICRCP--A Mechanistic Model for the Prediction of Stresses, Strains, and Displacements in Continuously Reinforced Concrete Pavements," Research Report 371-2F, Texas Transportation Institute, Texas A&M University.

Panak, John J. (1990). Personal communications.

Powers, T. C., and H. H. Steinour (1952). "An interpretation of published researches on the alkali-aggregate reaction," J. Amer. Concr. Inst, 48, p. 513.

Rainville, E. D. (1958). Elementary Differential Equations. The Macmillan Company, NY.

Shirole, A. (1990). Personal communications.

Stanton, T. E. (1940). "Expansion of Concrete Through Reaction Between Cement and Aggregate," **Proceedings**, Vol. 66, No. 10, American Society of Civil Engineers, New York, NY, pp. 1781-1811.

Stewart, C. F. (1985). "Highway Structure Approaches," California Department of Transportation.

Stewart, C. F. (1989). "Evaluation of a New Bridge Approach Slab Concept, Annual Report," California Department of Transportation.

Swami, R. N., and M. M. Al-Asali (1988a). "Engineering Properties of Concrete Affected by Alkali-Silica Reaction," **ACI Materials Journal**, Title No. 85-M41, American Concrete Institute, Detroit, pp. 367-374.

Swamy, R. N., and M. M. As-Asali (1988b). "Expansion of Concrete Due to Alkali-Silica Reaction," **ACI Materials Journal**, Jan.-Feb., American Concrete Institute, Detroit, pp. 33-40.

Tadros, M. K., and J. V. Benak (1989). "Bridge Abutment and Approach Slab Settlement--Phase I," University of Nebraska-Lincoln, Center for Infrastructure Research, Final Report.

Technical Memorandum, Study No. 1244, Center for Transportation Research, The University of Texas at Austin, 7 August 1990.

Tena-Colunga, J. A., B. F. McCullough, and N. H. Burns (1989). "Analysis of Curling Movements and Calibration of PCP Program," Research Report 556-3, Center for Transportation Research, The University of Texas at Austin, August.

Terzhagi, K. (1955). "Evaluation of Coefficients of Subgrade Reaction," **Geotechnique--The International Journal of Soil Mechanics**, Vol. 5, No. 4, The Institute of Civil Engineers, London, pp. 297-326.

Thompson, L. J., and J. P. Thomas (1965). "Optimization of Clay Subgrade Compaction in Arid Regions," Proceedings, Highway Research Board, pp. 36-47.

Vetter, C. P. (1933). "Stresses in Reinforced Concrete Due to Volume Changes," **Transactions**, ASCE, Vol. 98, pp. 1039-1052.

Vivian, H. E. (1950). "Studies in Cement-Aggregate Reaction: X. The Effect on Mortar Expansion of Amount of Reactive Component," Bul. No. 256, Commonwealth Scientific and Industrial Research Organization, Melbourne, Australia, pp. 13-20.

Wolde-Tinsae, A. M., M. S. Aggour, and S. A. Chini (1987). "Structural and Soil Provisions for Approaches to Bridges," Report No. FHWA/MD-89/04, Department of Civil Engineering, University of Maryland, College Park, MD, pp. 105.

APPENDIX A.
TABULATED SUMMARY OF FIELD NOTES FROM INSPECTION OF BRIDGES IDENTIFIED BY DISTRICT PERSONNEL

Site No.	Site Description	Description of Structure	Observed Distress	Probable Causes
9-1	IH35 over US77 and US81 Northbound Str.	Rt-fwd Skew 4-span cont CIP arch gird	Damage to 3-4 in. rt offset at south end Heave (few in.) of north end	Lateral motion (to rt) of embankment Swelling of fill
9-2	IH35 Sbound over Brazos R. South end	4-lames ?RCP	Bad bump reported, not observed AC overlay--good cond Some settlement of embankment 150 ft AC overlay reflecting crack	Construction probs Bridge built before embankment
	North End	?RCP	Open joint Cracks in app.slab Slight settl. app slab	Possible settlement under N. app. slab
9-3	Loop 484 (SH6) over MoPac RR E-bound	Arch girder CIP 7-spans 2 simple,5 cont R-fwd skew 65-70 deg ACP	Left lane, part of rt lane overlaid (multiple repairs) Reflected cracks at ends of ss spans Joints closed, filled w/ gravel Cr refl from end of App slab	
9-4	W-bound	ACP	Similar overlays Ref Crk through olay at end app slab Ref Crk at ea end of ss spans No lat misalign No vert misalign Joints blocked by AC and gravel	Settlement of embankment E of str
9-5	FM940 over MPRR	PS arch slab 5-span left skew,2-lanes recent o'lay ACP	no observed distress in bridge, reflected crack thru A/C pvmt at pvmt-apslab	
9-6	SH6(loop340) over Brazos R.	2-ln, cont arch 3-span; plus 4 PS girder spans overlay	Crk in end of arch slab adj to wingwall	
9-7	FM3400 over Flat Cr.	No App slab, 4-span ACP	heaving in pvmt at N end, rutting in wheel path	

Site No.	Site Description	Description of Structure	Observed Distress	Probable Causes
9-8	US 77 over SH6	PS girders,3-span rt skew,ac pvmt, ACP	small bump at sb end at begin. app slab, open joints in bridge overlayed rutting in AC pvmt some patching	settlement, consolidatio
9-9	SH317 over Middle Bosque R.	Steel Girder Br. 8 SS spans No app. slab	Repaired N end of Br with 3-4 in. AC overlay recently placed	

Site No.	Site Description	Description of Structure	Observed Distress	Probable Causes
12-1	IH10 over Gregg (Eastbound)	CRCP AC overlaid ap slb Built approx 1966	2 in. sag in ap slb Spalled jts Crushed parapet wall 1/2 in. fault ap/br	CRCP growth? Settlement under ap slab
12-2	IH10 over Lathrop (Westbound)	CRCP 4-span continuous 4-lane CIP conc bridge Skewed Replaced portion of app slab Built in winter	Transv. cracks over bents Joints blocked Crack at base of of wing wall	
12-3	IH10 over Kress (Westbound) (West end)	CRCP 4-span continuous 4-lane CIP conc bridge Patched portion of app slab Replaced ap slab Open col abutment	Wing wall base crk 1/2 in. fault at ap slb/bridge Blocked jts Tran crks over bents 2 in. fault Tran crks in app slab	 Neg. Mom LL+DL
12-4	IH10 over Lathrop (Eastbound)	Open col abutment CRCP 4-span continuous 4-lane CIP conc bridge Replaced portion of app slab	Tran crks in ap slb App slab and pvmt higher than bridge Wing wall damage	Heaving under ap slb?
12-5	IH610 over Ship Channel (Eastbound) (West end)	PC girder bridge CRCP AC patch on app slab 18 yr old bridge	Cracked wing wall 1/2 in. longitudinal movement of app slb Closed jt at ap/pvmt Crack parapet wall Rotation of ap slab	 Rotation of ap slab?
12-6	FM270 at Clear Cr. (South end)	PC Gird Br. ACP AC overlay on pvmt	2.4 deg Rotation of abut. 1 in fault at br/ap 2 in open jt at br/ap Blocked armor jt	Settlement of embankment?

Site No.	Site Description	Description of Structure	Observed Distress	Probable Causes
13-1	US59 over FM102	?RCP	Broken Backwall	Pavement growth
13-2	US 59 at SH71	?RCP	Broken Backwall	Pavement Growth
13-3	US59 at LP525	?RCP	Broken Backwall	Pavement Growth
13-4	US 59 at FM444	Conc. Girder AC overlay ?RCP	Broken Backwall	Pavement Growth
13-5	US59 at 822 near Edna			
13-6	US59 over 111 near Edna		Cracked Ap Slab Epoxy repairs to bwall	Settlement under slab
13-7	US 77 over 91 S. of Victoria	CRCP	Broken backwall	Pvmt. Growth
13-8	SH77 over Coleto Cr. So. Victoria	Pan girder 1-span? CRCP	Cavities under crcp overlay on apslab broken off backwall buckled & milled app.slab Rotation of S. Abut	Pvmt Growth Settlement Pvmt. Growth Pvmt Growth/heave Settlement

Site No.	Site Description	Description of Structure	Observed Distress	Probable Causes
17-1	SH6 over SH30 (Northbound)	2-lane, 3-span, 15 skew, PC gird br BAS-67(MOD) ap slab Open abutment CRCP Replaced ap slab	Developing blow up at ap slab/pvmt Trans cracks in new ap slab Trans cracks in CRCP Br joints closed	Settlement under slab Embankment settlement CRCP growth Support loss under slab Heaving under slab Heave under slab Embankment heave
17-2	SH6 at Burton Cr. (Northbound) (South end)	Mud-jacked, o'laid ap slab CRCP	Rel settlement of ap slab, > 1.5 in. prior to maint. No distress now	Settlement under ap slab?
17-3	SH6 at Burton Cr. (Southbound) (South end)	Recent mud-jacking ap slab, CRCP	1 in. low spot in ap slab prior to maint, Pavement cracks at lugs	Settlement under ap slab?
17-4	SH6 at Burton Cr. (Southbound) (North end)	CRCP	Diagonal cracking pattern in ap slab Visible low spot in center of ap slab	Settlement under ap slab? Loss of support under ap slab?
17-5	SH6 over Tabor Rd. Bryan, TX Sbound	CRCP 2-lane, simple span PS conc girders	Cracking in App slab Ruptured backwall	Pavement growth Settlement beneath app. slab
17-6	SH6 over SH105 S. of Navasota	ACP	Sig. Bumps at ends Closed joints Extruded seals No sig. damage to bridge or abutment	AC overlay on pvmt, but not on b. deck results in vert. discontinuity

Site No.	Site Description	Description of Structure	Observed Distress	Probable Causes
20-1			not inspected, need traffic control	
20-2	US69 at Lucas Dr.	steel I beam 2-lane, 3-span ?RCP 20 ft app slab	sag in ap slab, transv. cr in apslb patching in both lanes armor jt open 0.5 in. closed jt at pvmt/apslab spalled backwall rockers tilted mud-jacked ap slab app slab above pvmt 0.5 in.	 settlement in pvmt
20-3	US69 at Fannet Opass SH124	6-span conc girder 2-lanes, 8 ft sho. left skew mud-jacked apslab CRCP	settl N end SB apslab heave S end SB apslab AC patch both lanes deck cracking in app slab sag in app slab	
20-4	SH87 over Intercoastal	2-lane conc. girder No approach slabs	settlement shoul. N end (6 in at br rail) 2-ft drop from shoulder to guardrail	
20-5	SH73 at Main B Canal	8-span waffle slab 4-lanes, 3-ft. med. Overlaid apslab	sagging apslabs refl crs thru overlay 4 in. bumps in overlay 4-in hor. open jt and 1-in vert. disc at app slab/deck jt. rutting ac should. below deck	
20-7	IH10 at US69	s-span steel I bm 2 lane 45 deg skew,1ft fwd ?RCP	repairs to riprap	
20-8	US69 at 4th St	5-span conc girders 10 deg rt skew	sag in app slab and sag in pvmt at S end of SB bridge spalled backwall corner long. crks in app slab reg. trans crks in pvmt	
20-9	SH73 at Savannah Overpass spur 215	4-span arch slab 4-lane divided JRCP	settle under app slab numerous overlays patches at app slab/pvmt pvmt higher than app slab	

APPENDIX B.
CORING LOGS

Buchanan/Soil Mechanics, Inc.

Consulting Engineers

Geotechnical • Materials • Civil Design • Surveying

Bryan, Texas

206 North Sims, 77803/P.O. Box 672, 77806/(409) 822-3767

Rec'd 9/7/89 RJ

LETTER OF TRANSMITTAL

TO: Dr. Ray James
TEXAS TRANSPORTATION INSTITUTE
TAMU-CE-TTI-EDG-BLDG.
Spence Street, Room 802
College Station, Texas 77843-3135

PROJECT: Approach Slab Investigation, Project 1213 B/SMI PROJECT NO. 891082

We are sending you 1 copies of the following:

Pages	Dated	Item	Pages	Dated	Item
		CONCRETE COMPRESSIVE STRENGTH			MECHANICAL ANALYSIS CHART
		FIELD CONCRETE REPORT			OPTIMUM MOISTURE/DENSITY RELATIONSHIP
		IN-PLACE DENSITY TEST RESULTS	5	8/28	SUMMARY OF LABORATORY TEST DATA
		INVOICE			
		FIELD REPORT			
5	8/21 8/24	LOG OF BORING			

Signed: Terena Alonzo
Terena Alonzo

Date: September 7, 1989

REMARKS:

SUMMARY OF LABORATORY TEST DATA

PROJECT: TEXAS TRANSPORTATION INSTITUTE
Approach Slab Investigation, Project No. 1213, Beaumont Site

PROJECT NO: 891082 DATE: August 28, 1989

BORING NO.	DEPTH IN FEET	SAMPLE NO.	TYPE OF MATERIAL	MOISTURE CONTENT %	DRY DENSITY pcf	ATTERBERG LIMITS LL	PL	PI	COMPRESSION TEST: COMPRESSION tsf	STRAIN %	LATERAL PRESSURE psi	TYPE FAILURE	OTHER TESTS: PERCENT PASSING THE NO..200 SIEVE
CB-1	0-2	1672	Tan and gray fat clay with sand (CH)	24	100	51	15	36					76% finer
	2-4	1673	Tan and gray lean clay with sand (CL)	24	99	49	15	34					81% finer
	4-6	1674	Tan and gray lean clay with sand (CL)	22	106	48	13	35					85% finer
	6-8	1675	Tan and dark gray lean clay with sand (CL)	19	104	42	15	27					76% finer
	8-10	1676	Tan and dark gray lean clay (CL)	21	104	40	17	23					86% finer
	10-12	1677	Tan and dark gray lean clay (CL)	20	106	43	16	27					87% finer
	12-14	1678	Tan and dark gray lean clay (CL)	24	99	40	18	22					93% finer
	14-16	1679	Tan lean clay (CL)	19	108	38	16	22					87% finer
	16-18	1680	Tan and gray lean clay with sand and shells (CL)	19	106	38	18	20					85% finer
	18-20	1681	Tan and gray sandy lean clay (CL)	19	107	34	15	19					69% finer
	20-22	1682	Tan and gray lean clay (CL)	30	93	46	17	29					96% finer
	22-24	1683	Tan and gray lean clay (CL)	20	106	47	17	30					97% finer

SUMMARY OF LABORATORY TEST DATA

PROJECT: TEXAS TRANSPORTATION INSTITUTE
Approach Slab Investigation, Project No. 1213, Beaumont Site

PROJECT NO: 891082 DATE: August 28, 1989

BORING NO.	DEPTH IN FEET	SAMPLE NO.	TYPE OF MATERIAL	MOISTURE CONTENT %	DRY DENSITY pcf	ATTERBERG LIMITS LL	PL	PI	COMPRESSION TEST: COMPRESSION tsf	STRAIN %	LATERAL PRESSURE psi	TYPE FAILURE	OTHER TESTS: PERCENT PASSING THE NO. 200 SIEVE
CB-2	0-2	1684	Tan and gray lean clay with sand (CL)	24	98	47	17	30					77% finer
	2-4	1685	Tan and gray lean clay with sand and shells (CL)	21	104	44	16	28					75% finer
	4-6	1686	Tan and gray sandy lean clay (CL)	24	96	41	17	24					65% finer
	6-8	1687	Tan and gray sandy lean clay with shells (CL)	18	110	27	14	13					57% finer
	8-10	1688	Tan and dark gray lean clay (CL)	21	103	37	15	22					91% finer
	10-12	1689	Tan and dark gray lean clay with sand (CL)	15	111	25	14	11					84% finer
	12-14	1690	Tan lean clay (CL)	20	102	37	13	24					86% finer
	14-16	1691	Tan and dark gray lean clay with sand (CL)	17	107	27	14	13					80% finer
	16-18	1692	Tan and gray lean clay (CL)	18	108	36	16	20					87% finer
	18-20	1693	Tan and gray lean clay (CL)	22	101	36	16	20					86% finer
	20-22	1694	Tan and gray fat clay (CH)	22	103	50	17	33					92% finer
	22-24	1695	Tan and gray fat clay (CH)	21	106	51	19	32					96% finer

SUMMARY OF LABORATORY TEST DATA

PROJECT: TEXAS TRANSPORTATION INSTITUTE
Approach Slab Investigation, Project No. 1213, Houston Site

PROJECT NO: 891082 DATE: August 28, 1989

BORING NO.	DEPTH IN FEET	SAMPLE NO.	TYPE OF MATERIAL	MOISTURE CONTENT %	DRY DENSITY pcf	ATTERBERG LIMITS LL	PL	PI	COMPRESSION TEST: COMPRESSION 1sf	STRAIN %	LATERAL PRESSURE psi	TYPE FAILURE	OTHER TESTS: PERCENT PASSING THE NO. 200 SIEVE
8-3	6½-8	1705	Dark gray lean clay with sand and shells (CL)	22		39	13	26					75% finer
	8-10	1706	Tan and gray sandy lean clay with shells (CL)	16	113	32	15	17					68% finer
	10-12	1707	Tan and gray lean clay (CL)	21	105	49	19	30					86% finer
	12-14	1708	Tan and dark gray lean clay with sand and shells (CL)	21	104	48	15	33					77% finer
	14-16	1709	Tan and dark gray lean clay with sand (CL)	26	96	46	15	31					76% finer
	16-18	1710	Tan and dark gray lean clay with brick and sand (CL)	26	98	36	13	23					74% finer
	18-20	1711	Tan and dark gray lean clay with shells and sand (CL)	21	102	42	14	28					80% finer
	20-22	1712	Tan and gray lean clay with sand (CL)	19	109	40	15	25					73% finer
	22-24	1713	Tan and gray sandy lean clay (CL)	18	109	45	17	28					64% finer
	24-26	1714	Dark gray lean clay with shells, sand and nodules (CL)	20	109	39	13	26					73% finer
	26-28	1715	Dark gray fat clay with shells (CH)	22	101	53	16	37					82% finer
	28-30	1716	Dark gray sandy lean clay with shells and brick (CL)	19	107	40	14	26					64% finer
	30-32	1717	Tan and dark gray fat clay (CH)	25	98	55	23	32					94% finer

SUMMARY OF LABORATORY TEST DATA

PROJECT: TEXAS TRANSPORTATION INSTITUTE
Approach Slab Investigation, Project No. 1213, League City Site

PROJECT NO: 891082 DATE: August 28, 1989

BORING NO.	DEPTH IN FEET	SAMPLE NO.	TYPE OF MATERIAL	MOISTURE CONTENT %	DRY DENSITY pcf	ATTERBERG LIMITS LL	PL	PI	COMPRESSION TEST: COMPRESSION tsf	STRAIN %	LATERAL PRESSURE psi	TYPE FAILURE	OTHER TESTS: PERCENT PASSING THE NO. 200 SIEVE
CB-4	3½-4	1719	Tan and gray lean clay with sand (CL)	17	113	36	15	21					78% finer
	4-6	1720	Tan and gray lean clay with sand (CL)	17	113	35	15	20					73% finer
	6-8	1721	Tan and gray lean clay with sand (CL)	19	109	41	15	26					84% finer
	8-10	1722	Tan and gray lean clay (CL)	20	108	43	15	28					87% finer
	10-12	1723	Tan and gray lean clay (CL)	19	104	46	18	28					86% finer
	12-14	1724	Tan and gray lean clay with sand and nodules (CL)	16	114	35	17	18					76% finer
	14-16	1725	Tan and gray lean clay with sand (CL)	20	107	45	17	28					82% finer
	16-18	1726	Tan and gray fat clay (CH)	24	99	54	19	35					89% finer
	18-20	1727	Tan and gray lean clay with sand (CL)	20	108	48	15	33					80% finer
	20-22	1728	Tan and gray fat clay with sand (CH)	26	98	61	18	43					83% finer
	22-23½	1729	Tan silty fine sand (SM)	23		Non-Plastic							
	24-25½	1730	Gray sandy silt (ML)	23		20	18	2					57% finer
	28½-30	1731	Gray silty, clayey sand (SC-SM)	24		18	14	4					39% finer
	33½-35	1732	Gray sandy, silty clay (CL-ML)	28		24	17	7					66% finer

SUMMARY OF LABORATORY TEST DATA

PROJECT: TEXAS TRANSPORTATION INSTITUTE
Approach Slab Investigation, Project No. 1213, Bryan Site

PROJECT NO: 891082 DATE: August 28, 1989

ING NO.	DEPTH IN FEET	SAMPLE NO.	TYPE OF MATERIAL	MOISTURE CONTENT %	DRY DENSITY pcf	ATTERBERG LIMITS LL	PL	PI	COMPRESSION TEST: COMPRESSION tsf	STRAIN %	LATERAL PRESSURE psi	TYPE FAILURE	OTHER TESTS: PERCENT PASSING THE NO. 200 SIEVE
-5	2-4	1734	Tan and gray sandy lean clay (CL)	24	100	42	21	21					62% finer
	4-6	1735	Tan fat clay (CH)	30	91	54	24	30					87% finer
	6-8	1736	Gray clayey sand (SC)	21	104	49	17	32					47% finer
	8-10	1737	Dark gray sandy lean clay (CL)	22	104	45	18	27					64% finer
	10-12	1738	Tan and dark gray sandy lean clay (CL)	23	103	48	17	31					63% finer
	12-14	1739	Dark gray fat clay with sand (CH)	24	101	54	18	36					73% finer
	14-16	1740	Dark gray fat clay with sand (CH)	25	102	51	18	33					75% finer
	16-18	1741	Gray fat clay (CH)	27	92	60	19	41					93% finer
	18-20	1742	Dark gray lean clay with sand (CL)	25	100	33	16	17					83% finer
	20-22	1743	Gray fat clay with sand (CH)	22	105	54	17	37					76% finer
	22-24	1744	Gray sandy lean clay (CL)	23	103	35	19	16					51% finer
	24-26	1745	Gray clayey sand (SC)	23	105	33	17	16					49% finer
	26-28	1746	Tan and gray lean clay with sand (CL)	25	101	39	20	19					78% finer

BORING LOG

PROJECT: Approach Slab Investigation, Project No. 1213
BORING NO: CB-1
LOCATION: Beaumont Site, US 69 and Lucas Drive
CLIENT: TEXAS TRANSPORTATION INSTITUTE
DATE: 8/21/89
PROJECT NO: 891082
BORING TYPE: 4" Auger
DRILLER: Gustavus
SOIL TECHNICIAN: Dean
GROUND ELEV:

■ - Shelby Tube Sample ⊠ - Standard Penetration Test Sample ⊘ - No Recovery J-Jar

Depth in Feet	Sample Type & Sample No.	Penetrometer Reading, tsf	Blows / Foot	DESCRIPTION OF STRATUM
	1672	1.25		Asphalt (1"), grout (12"), then stiff tan and gray clay with sand and organic
	1673	1.5		Stiff tan and gray sandy clay with organic
5	1674	0.75 1.75		Plastic clay (10"), then stiff tan and gray slightly sandy clay
	1675	1.5		Stiff tan and dark gray sandy clay with nodules
	1676	2.0		Stiff tan and dark gray sandy clay with nodules
10	1677	2.0		Stiff tan and dark gray sandy clay with nodules, shells and organic
	1678	1.5		Stiff tan and dark gray sandy clay with nodules, shells and organic
15	1679	1.0 2.5		Plastic to very stiff tan sandy clay with shells and organic
	1680	1.5		Stiff tan and gray sandy clay with small white nodules and shells
	1681	2.25		Very stiff tan and gray sandy clay with small white nodules and shells
20	1682	2.25		Fill clay with organic (4"), then very stiff tan and gray sandy clay (appears to be natural ground)
	1683	2.5		Very stiff tan and gray sandy clay with calcareous nodules, natural ground
25				Bottom at 24'
30				
35				
40				
45				

BORING LOG

PROJECT: Approach Slab Investigation, Project No. 1213 BORING NO: CB-2
LOCATION: Beaumont Site-US 69 and Lucas Drive
CLIENT: TEXAS TRANSPORTATION INSTITUTE
DATE: 8/21/89 PROJECT NO: 891082 BORING TYPE: 4" Auger
DRILLER: Gustavus SOIL TECHNICIAN: Dean GROUND ELEV:

■ - Shelby Tube Sample ⊠ - Standard Penetration Test Sample ☑ - No Recovery J-Jar

Depth in Feet	Sample Type & Sample No.	Penetrometer Reading, tsf	Blows / Foot	DESCRIPTION OF STRATUM
	1684	4+		Asphalt (1"), grout with shells (12"), then stiff to hard tan and gray sandy clay
	1685	1.5		Stiff tan and gray sandy clay with trace of shells
5	1686	1.5		Alternating layers of soft, plastic and stiff tan and gray sandy clay
	1687	2.0		Soft to stiff tan and gray sandy clay with shells
	1688	2.0		Stiff tan and dark gray sandy clay with shells
10	1689	2.5		Very stiff tan and dark gray sandy clay with sand seams, shells and organic
	1690	1.5		Stiff tan sandy clay with shells
15	1691	1.5		Stiff tan and dark gray sandy clay with sand seams
	1692	2.25		Very stift tan and gray sandy clay with small white nodules
	1693	1.5		Stiff tan and gray sandy clay with small white nodules
20	1694	1.5		Stiff tan and gray sandy clay with small white nodules, then tan and gray clay at 21.5' (natural ground)
	1695	2.25		Very stiff tan and gray clay with calcareous nodules, natural ground
25				Bottom at 24'
30				
35				
40				
45				

BORING LOG

PROJECT: Approach Slab Investigation, Project No. 1213 — BORING NO: CB-3

LOCATION: Houston Site, US 610 south end

CLIENT: TEXAS TRANSPORTATION INSTITUTE

DATE: 8/22/89 — PROJECT NO: 891082 — BORING TYPE: 4 1/2" Rotary Wash

DRILLER: Gustavus — SOIL TECHNICIAN: Dean — GROUND ELEV:

■ - Shelby Tube Sample ⊠ - Standard Penetration Test Sample ⊘ - No Recovery J-Jar

Depth in Feet	Sample Type & Sample No.	Penetrometer Reading, tsf	Blows / Foot	DESCRIPTION OF STRATUM
	1703			Concrete (6.5"), then grout (sand and shell)
	1704			Grout
5				Lost circulation at 6.5'
	1705	..	6	Grout (1"), then dark gray sandy clay with shells (4-3-3)
	1706	1.5		Stiff tan and gray sandy clay with shells and small nodules
10	1707	2.75		Very stiff tan and gray sandy clay
	1708	2.75		Very stiff tan and dark gray sandy clay with shells and trace of organic
15	1709	1.75		Very stiff tan and dark gray sandy clay with shells and trace of organic
	1710	2.0		Stiff tan and dark gray sandy clay with red brick
	1711	2.25		Very stiff tan and dark gray sandy clay with shells
20	1712	2.5		Very stiff tan and gray sandy clay with calcareous nodules
	1713	3.0		Very stiff tan and gray sandy clay with calcareous nodules
25	1714	1.75 4+		Stiff to hard dark gray sandy clay with shells
	1715	4+		Hard dark gray clay with shells, trace of organic and gravel
	1716	4+		Hard dark gray sandy clay with shells and red brick
30	1717	1.5		Stiff tan and dark gray clay (natural ground at 30')
35				Bottom at 32'
40				
45				

BORING LOG

PROJECT: Approach Slab Investigation, Project No. 1213
BORING NO: CB-3A
LOCATION: Houston Site, US 610 south end
CLIENT: TEXAS TRANSPORTATION INSTITUTE
DATE: 8/22/89
PROJECT NO: 891082
BORING TYPE 4 1/2" Rotary Wash
DRILLER: Gustavus
SOIL TECHNICIAN: Dean
GROUND ELEV:

Depth in Feet	Sample Type & Sample No.	Penetrometer Reading, tsf	Blows / Foot	■ - Shelby Tube Sample ⊠ - Standard Penetration Test Sample ⊘ - No Recovery J-Jar DESCRIPTION OF STRATUM
				Concrete (12"), shells (12"), then tan clay fill
				Bottom at 2'
5				
10				
15				
20				
25				
30				
35				
40				
45				

BORING LOG

PROJECT: Approach Slab Investigation, Project No. 1213
BORING NO: CB-4
LOCATION: League City Site-FM 27 at Clear Creek
CLIENT: TEXAS TRANSPORTATION INSTITUTE
DATE: 8/23/89
PROJECT NO: 891082
BORING TYPE: 4" Auger
DRILLER: Gustavus
SOIL TECHNICIAN: Dean
GROUND ELEV:

■ - Shelby Tube Sample ⊠ - Standard Penetration Test Sample ⊘ - No Recovery J-Jar

Depth in Feet	Sample Type & Sample No.	Penetrometer Reading, tsf	Blows / Foot	DESCRIPTION OF STRATUM
	1718			Asphalt (11"), then grout with shells
	1719	2.0		Stiff tan and gray sandy clay at 3.5'
5	1720	2.5		Stiff tan and gray sandy clay with shells
	1721	0.75		Plastic gray sandy clay with gravel and tan and gray sandy clay layer
	1722	2.0 3.0		Stiff to very stiff tan and gray sandy clay
10	1723	2.0		Dark gray clay with decayed vegetation (6"), then stiff tan and gray sandy clay
	1724	1.75		Stiff tan and gray sandy clay with nodules
15	1725	1.75		Stiff tan and gray sandy clay with nodules
	1726	1.75		Stiff tan and gray clay with nodules
	1727	1.75		Stiff tan and gray sandy clay with small nodules
20	1728	1.75		Stiff tan and gray clay (8"), then tan silty clay
	1729		12	Firm tan silty fine sand, wet (5-7-5)
25	1730		5	Loose gray sandy silt (1-3-2)
	1731		3	Very loose gray silty, clayey sand with trace of decayed vegetation (2-1-2)
30				
	1732		8	Plastic gray sandy, silty clay (3-4-4)
35				Bottom at 35'
40				
45				

BORING LOG

PROJECT: Approach Slab Investigation, Project No. 1213
BORING NO: CB-5
LOCATION: Bryan Site, SH 6 Bypass and Tabor Road
CLIENT: TEXAS TRANSPORTATION INSTITUTE
DATE: 8/24/89
PROJECT NO: 891082
BORING TYPE: 4 1/2" Rotary Wash
DRILLER: Gustavus
SOIL TECHNICIAN: Dean
GROUND ELEV:

■ - Shelby Tube Sample ⊠ - Standard Penetration Test Sample ▨ - No Recovery J-Jar

Depth in Feet	Sample Type & Sample No.	Penetrometer Reading, tsf	Blows / Foot	DESCRIPTION OF STRATUM
				Asphalt (20"), then clay
	1734	2.0		Stiff tan and gray sandy clay
5	1735	1.0		Plastic tan clay with dark gray clay layer
	1736	1.0 2.0		Plastic gray sandy clay to gray clayey sand with silty fine sand layer
	1737	3.5		Very stiff dark gray sandy clay with organic (wood)
10	1738	3.5		Very stiff tan and dark gray sandy clay
	1739	2.25		Very stiff dark gray clay
15	1740	1.5		Stiff dark gray and olive gray clay
	1741	2.5		Very stiff gray clay with black organic (wood)
	1742	2.0		Stiff dark gray sandy clay
20	1743	2.0		Stiff gray clay (appears to be natural ground)
	1744	3.0		Very stiff gray sandy clay and clayey sand with iron stain
25	1745	4+		Very stiff gray sandy clay and clayey sand with iron stain
	1746	2.75		Very stiff tan and gray sandy clay with sand seams
30				Bottom at 28'
35				
40				
45				

Rec'd 9-15-89
File 1213
RJ

Buchanan/Soil Mechanics, Inc.

Consulting Engineers

Geotechnical • Materials • Civil Design • Surveying

Bryan, Texas

206 North Sims, 77803/P.O. Box 672, 77806/(409) 822-3767

LETTER OF TRANSMITTAL

TO: Dr. Ray James
TEXAS TRANSPORTATION INSTITUTE
TAMU-CE-TTI-EDG-BLDG.
Spence Street
College Station, Texas 77843-3135

PROJECT: Approach Slab Investigation, Project 1213 B/SMI PROJECT NO. 891082

We are sending you 1 copies of the following:

Pages	Dated	Item	Pages	Dated	Item
		CONCRETE COMPRESSIVE STRENGTH			MECHANICAL ANALYSIS CHART
		FIELD CONCRETE REPORT			OPTIMUM MOISTURE/DENSITY RELATIONSHIP
		IN-PLACE DENSITY TEST RESULTS	1	8/28/89	SUMMARY OF LABORATORY TEST DATA
		INVOICE			
		FIELD REPORT			
		LOG OF BORING			

Signed: Nancy E. Wilkinson
Nancy E. Wilkinson

Date: September 13, 1989

REMARKS:

SUMMARY OF LABORATORY TEST DATA

PROJECT: TEXAS TRANSPORTATION INSTITUTE
Approach Slab Investigation, Project No. 1213
PROJECT NO: 891082 DATE: August 28, 1989

ING O.	DEPTH IN FEET	SAMPLE NO.	TYPE OF MATERIAL	MOISTURE CONTENT %	DRY DENSITY pcf	ATTERBERG LIMITS LL	PL	PI	COMPRESSION TEST: COMPRESSION tsf	STRAIN %	LATERAL PRESSURE psi	TYPE FAILURE	OTHER TESTS: SWELL TEST and PERCENT PASSING THE NO. 200 SIEVE
102													
	7		Brown lean clay with sand (CL)	27	96	43	18	25					0.40% consolidation with 0.32 tsf load on sample
													79% finer
102													
	9		Brown fat clay (CH)	33	89	78	28	50					1.29 tsf load required to prevent swell
													98% finer
CAMPO, LOOP		525											
	3		Gray fat clay with sand and calcareous nodules (CH)	25	99	53	19	34					0.64 tsf load required to prevent swell
													83% finer

APPENDIX C.
INTERNAL REPORT OF FIELD OBSERVATIONS OF 83 BRIDGES

This report is written to discuss the observations made on a field study of approach slabs and bridges in ten TxDOT Districts including: 5,6,7,8,9,12,13,14,17 and 23.

Purpose

The purpose of the field trip was:

1. To observe the physical condition of the approach slabs and bridges,
2. To quantify the relative bump at the approach slab, and
3. To identify the causes of the bump, if possible.

Site Selection

The site selection was based on selecting routes to include various classes of roadways and including as many TxDOT Districts as possible. Particular sites were chosen with consideration for safety of the traveling public and safety of the investigator and that the site was representative. Sites with significant bumps were to be investigated but no such cases were found. In order to obtain a more representative sampling of bridges, there was no prior identification of "problem" bridges. This "random" sampling procedure was to determine if observations at problem bridges was typical at all bridges. Also, a verification of conclusions drawn from previous observations and inferences could be made.

Initially almost every bridge along each route was inspected to ensure that no significant data would be overlooked. It soon became apparent that conditions at each site were quite similar, so fewer investigations per route were practical, thus enabling the inspector to cover more routes throughout the state.

General Observations

Approximately 85 sites were fully observed. All bridges crossed were considered for full inspection but were not inspected for one or more of the following reasons:

1. The bridge was typical of those fully observed,
2. There was not enough time to observe all bridges,
3. Safety considerations.

The paving material for the randomly selected routes was almost invariably some form of asphaltic concrete. The last day of the field study concentrated on a route known to be continuously reinforced concrete paving.

The general observation is that Texas roads and bridges are in very good condition. The TxDOT has done an outstanding job of designing, constructing, and maintaining our highways. The bumps at the ends of bridges were minimal; none were severe enough to be considered a hazard to the traveling public. Typically, the bumps at the ends of bridges were no more severe than those occasional bumps along the roadway. The most predictable characteristic of the bumps is that there are bumps at the ends of bridges, the exceptions being for culverts and those drainage structures with more than about one foot of fill over the top and continuous paving.

There were no bridges with significant bumps at the ends. Had the criterion for inspection been to observe bridges with severe bumps, no inspections would have been necessary. Many samples of near perfect conditions could have been obtained.

Particular Observations

Physical Condition

There was minimal structural distress on the 80 bridges observed that had ACP roadways, particularly the type of backwall distress observed on most bridges with CRCP roadways during the earlier phase of the study. There was some structural distress on the deck joints, particularly on bridges with steel beams and on the joints where rocker supports allowed them to expand to the point that the joints were closed causing some spalling of the concrete.

The slab and deck joints typically were open, where observable, on the ACP roadways, although consecutive bridges on the same roadway exhibited different degrees of open joints. Most of the slab and deck joints were covered with patches or pavement overlays making observation difficult. Typically, the slab and deck joints were closed on bridges with CRCP roadways, although the middle deck joints on long, multi-span bridges were often open.

There were erosion problems at some of the sites. A common problem exists where a shallow concrete channel is constructed at the end of the approach slab wingwall to carry water down the embankment. The problem is caused by placing a guardrail post in the middle of this channel--a very common occurrence. The water runs down the post eroding the embankment from under the channel, wingwall and approach slab. Other erosion problems observed include:

1. No concrete channel at the end of the wingwall to protect the earth embankment,
2. Where the riprap covered only a portion of the embankment height, and
3. In a few cases water ran under the riprap.

Relative Bump Evaluation

A subjective bump scale was devised to quantify the relative bumps at the ends of bridges. The scale ranged from 0 = no bump noticed to 5 = threatens loss of control. Certainly, some variation could be expected between individual inspectors, lane of traffic, and the vehicle used in the study. Traveling over some of the same routes in different lanes and in a different vehicle would change some of the ratings. The ratings were accomplished in a 1986 Chevrolet Caprice, a very smooth riding vehicle. The range of assigned ratings varied from 0 to 2 = a slight bump. Unofficial ratings in a different vehicle might increase the range to 3 = a moderate bump, again a testament to the quality of Texas highways. An important observation made when evaluating the bumps is that several senses are activated in recognizing the bump. The first cue is sight. Subconsciously, the initial indicator of an eminent bump was sighting guardrails and/or the bridge structure.

The next cue is sound. The change in materials and construction at the roadway/approach slab/deck interfaces gives a distinct audio cue. The last cue is the feel of the bump. All three have equal weight in recognition of the bump. Bumps along the roadway and at the ends of bridges are approximately equal in magnitude. It is of my opinion that bumps at the ends of bridges are more readily recognized because all three cues are active. On at least one occasion, what was seen, heard and felt turned out to be a bump from a patch about 25 feet from the actual start of the approach slab.

Cause of Bumps

The reason that there are bumps at the ends of the bridges is because of the uneven profile along the roadway, approach slab and bridge decks, particularly the discontinuity at the joints. The cause of the bumps is not due to any single factor but many, somewhat complex interactive factors. In my opinion, there are four basic factors:

1. The difference in the design and construction of the roadway, slab and bridge decks.
2. The difference in materials of and the foundations for the roadway, slab and bridge decks.
3. The difficulty of construction and compaction at the ends of the embankment.
4. The change in the profile along the roadway, slab and bridge deck due to traffic loading, maintenance and changes in geotechnical properties.

The first three items--design, construction and materials--are important but no major changes are likely to be made by TxDOT engineers. Some minor changes could be made to minimize the problem of the bumps by considering how and if this particular design, construction or maintenance will affect the profile. Basically, the performance of the roadways, approach slabs and bridges as individual components and integral parts is very good. Some variation and, therefore, change in profile is almost inevitable with time and use.

This change precipitates the maintenance work that quickly follows. It is my opinion that the majority of the bumps are more severe due to patches and overlays that cause a more pronounced profile change than the problem that they are intended to correct. This is especially true for roadways that are resurfaced or overlaid and the slab and decks are not. The progression of maintenance seems to be:

1. Patches at the roadway-slab joints, almost immediately after construction,
2. Pavement overlay with feathering at the roadway-slab joints,
3. Overlay with feathering at the slab-deck joints, then
4. Continuous overlay across the entire structure.

The most significant bumps on ACP roadways were due to the overlay induced profile changes. When the depth of the continuous overlays exceeded about six inches, the profile changes, material changes and bumps became minimal again.

The primary cause of the uneven profile for two of the bridges investigated could be attributed to differential settlement between the embankment (roadway and approach slab) and the bridge decks. Settlement

probably caused a minor portion of the profile unevenness for the other sites. Some contribution of the uneven profiles is due to loss of material from erosion and pumping, especially the CRCP roadways.

The primary cause for the uneven profiles for routes with CRCP roadways is the observed pavement growth. This action tends to enhance pumping and erosion thereby accentuating the uneven profile. The most significant maintenance problems were observed on CRCP roadways; therefore, the most significant design and construction modification would deal with minimizing pavement growth of CRCP roadways.

APPENDIX D.

CONSULTANT'S REPORT OF PETROGRAPHIC EXAMINATION OF CONCRETE PAVEMENT CORES FROM TWO STUDY SITES

EHA

Erlin, Hime Associates

CONSTRUCTION MATERIAL CONSULTANTS

330 PFINGSTEN ROAD • NORTHBROOK, IL 60062-2095 • (312) 272-7730

TELEX 6713036 WJE UW

FAX (312) 291-5189

AUSTIN BRANCH
8222 JAMESTOWN DR
BLDG A, 113B
AUSTIN TX 78758
(512) 835 0940
FAX (512) 835-6268

W G Hime
J D Connolly

Z T Jugovic
V Kress
T.S. Patty
L Petry
C. Weise

R A. Cechner
P.D. Kofoed
R A Martinek
L L Phelps

August 3, 1990
WJE 908381

Dr. Ray W. James
Structural Research Division
Texas Transportation Institute
Texas A&M University
College Station, Texas 77843-3135

Re: Project No. 12130
PCC Pavement Cores
Brazos (SH6) and Wharton Counties (U559)

Dear Dr. James,

Eighteen concrete cores from the above referenced Texas Highway project, relayed to the EHA-Austin office by Mr. Bob Gallaway - Consultant, have been examined petrographically as requested. The purpose of the study was to establish whether or not evidence of alkali-silica reactivity was present in the concrete. Nine cores from two separate highway projects were received on July 26, 1990. Three cores from three sampling locations within each highway section were taken. One core from each of the three sampling location was selected for detailed examination; the others were only briefly examined for any evidence of alkali-silica reaction. The two highway projects, as referenced, were concrete approach slabs next to bridges. The samples were examined using methods given in ASTM C856, "Petrographic Examination of Hardened Concrete".

Table 1 lists a summary of the findings. Reaction deposits, in the form of alkali-silica gel, were identified in both highway projects. The number of cores with traces of gel were higher for the Wharton County location (6 out of 9 cores) than for the Brazos County site (3 out of 9). The gel deposits were found in voids adjacent to aggregate particles and on aggregate particles in specially cut and polished sections of the concrete after being placed in a moisture chamber for 72 hours.

None of the reaction deposits were found to be associated with recognizable distress features such as cracks. The traces of gel were isolated and not considered significant in comparison to structural concrete known to be undergoing deterioration by alkali-silica attack. The Wharton County samples also exhibited moderate amounts of ettringite (calcium-sulfoaluminate hydrate); however, the presence of this material did not appear associated with any distress and was not considered to be related to sulfate reaction. Ettringite in "normal" concrete is indicative of moisture availability and is a common occurrance.

If we can be of further assistance in this matter, please give us a call.

Sincerely,

Erlin, Hime Associates Division
Wiss, Janney, Elstner Associates, Inc.

Tom S. Patty, Consultant
Manager, Austin Branch Office

TSP:jp

NOTE: Samples will be discarded after one year unless other disposition is requested. Charges may be made for storage after that period.

TABLE 1
TTI PAVEMENT CORES
OPTICAL EXAMINATION

PAVEMENT SECTION	CORE #	GEL DEPOSITS	ETTRINGITE DEPOSITS
Brazos Co. SH6	1*	X	
	2		
	3		
	4		
	5		
	6*	X	
	7*		
	8	X	
	9		
Wharton Co. US59	1*	X	X
	2		
	3		
	4*	X	X
	5	X	
	6		
	7	X	
	8*	X	
	9	X	

*Specially cut and polished section; 72 hours humidity chamber